TEMPERATURE AND HEAT FLOW MODELING OF THREE-DIMENSIONAL BODIES IN A TWO-LAYERED HALF SPACE

by

John A. Dunbar Jr.

Thesis submitted to the Graduate Faculty of the
Virginia Polytechnic Institute and State University
in partial fulfillment of the requirements of the degree of

MASTER OF SCIENCE

in

Geophysics

APPROVED:

J. K. Costain, Chairman	E. S. Robinson
J. A. Snoke	M. C. Gilbert, Department Head

December, 1979

Blacksburg, Virginia

Acknowledgments

I would like to thank Dr. J. K. Costain, Professor, Department of Geological Sciences Virginia Polytechnic Institute and State University for suggesting this thesis topic and providing the opportunity to pursue the topic while employed with the V.P.I. & S.U. Geothermal Program, DOE contract ET-78-C-05-5648. I am also grateful for financial support from V.P.I. & S.U. from August 1978 and August 1979 and for a tuition scholarship for fall 1979, which made the completion of this thesis possible.

I am indebted to the other members of the faculty and staff of V.P.I. & S.U. from whom I received help. Dr. J. A. Snoke helped with the mathematical notation used in the thesis; Dr. A. H. Cogbill gave useful suggestions during the development of the computer programs used; Dr. S. S. Farrar, Dr. J. A. Speer and S. W. Becker provided their geologic insight and Dr. E. S. Robinson read and commented on the text.

I give special thanks to my parents for the moral and financial support they have given me.

Table of Contents

1. Introduction

Steady-state heat flow and temperature anomalies in the earth's crust can be caused by lateral variations in heat production and thermal conductivity. In many respects the problem of interpreting thermal anomalies is identical to the problem of interpreting gravity and magnetic anomalies. Heat production and thermal conductivity vary with rock type, as do density and magnetic susceptibility. As a result, geologic features such as folds, faults, and igneous intrusions can produce thermal anomalies in the same way that they produce gravity and magnetic anomalies. There are also strong mathematical similarities. Temperature fields satisfy the same governing equations as do gravity and magnetic potentials. Solutions to gravity and magnetic problems, then, differ from solutions to analogous temperature field problems only in the nature of the boundary conditions imposed and by constant coefficients. In particular, the heat flow anomaly caused by a body of contrasting heat production is analogous to the gravitional attraction of the same body (Simmons, 1967). Likewise, the heat flow anomaly caused by a body of contrasting thermal conductivity in a uniform heat flow field is mathematically equivalent to the magnetic anomaly caused by a body of

contrasting susceptibility in a uniform inducing field (Carslaw and Jaegar, 1959, p. 425). Temperature anomalies caused by bodies of contrasting heat production and conductivity are respectively analogous tc gravimetric potential and gravitational attraction anomalies.

Because of these similarities it is possible to model heat flow and temperature anomalies using the same techniques used to model gravity and magnetic anomalies. In many cases the same computer programs can be used with only minor modifications. Simmons (1965), for example, suggested a method based on the gravitational attraction of a polygonal lamina (Talwani and Ewing, 1960) for modeling heat flow anomalies due to heat production contrasts in a half space. Thermal modeling techniques of this type are faster computationally and less cumbersome to implement than the numerical techniques such as the methcd of finite differences and the method of finite elements. These advantages become particularly important in situations which require repeated modeling such as in solving inverse problems by trial-and-error methods.

The model proposed by Simmons does not account for the effects of contrasts in thermal conductivity between the anomalous body and the half space. It also dces not account for the effects of a layer of contrasting conductivity

overlying the half space. This more general problem is of current interest in the exploration for low-temperature geothermal resources. The objectives of this exploration are temperature anomalies in low conductivity sediments overlying highly radiogenic lithologies in the crystalline basement (Costain, Glover, and Sinha, 1979). In principle the sedimentary layer would act as an insulator, causing higher temperatures to occur closer to the surface. The problem is also important in the interpretation of heat flow determinations made in sea floor sediments. The latter case was considered by Lee and Henyey (1974) who used the method of finite elements to correct marine heat flow values. An analytical treatment of temperature and heat flow anomalies in a two-layer half space does not exist in the literature.

A more general modeling technique than that proposed by Simmons (1965), based on the gravity and magnetic effects of polygonal prisms (Plouff, 1976), is developed in the following sections. The technique is suitable for modeling temperature and heat flow anomalies associated with three-dimensional bodies of contrasting heat production and conductivity in a two-layered half space.

2. Theoretical Analysis

Units

1.0 heat flow unit (HFU) = 1.0×10^{-6} cal/(cm^2-sec)

1.0 heat production unit (HPU) = 1.0×10^{-13} cal/(cm^3-sec)

1.0 thermal conductivity unit (TCU) = 1.0×10^{-3} cal/(cm-sec-^{o}C)

General Definitions

A = heat production contrast per unit volume between an anomalous body and the surrounding medium;

$a(x,y,z)$ = heat production at the point (x,y,z);

G = the vertical gravitational attraction;

J_Z = the vertical component of the intensity of magnetization vector;

K = the thermal conductivity of a homogenous medium;

M = the vertical component of the induced magnetic field;

q = the vertical heat flow field;

q* = the uniform heat flow from the base of a model region;

q_A = anomalous vertical heat flow field due to a body with a contrasting heat production;

q_K = anomalous vertical heat flow field due to a body with a contrasting thermal conductivity;

q_R= the regional heat flow field which varies only in the vertical direction;

q_S= anomalous vertical heat flow field due to a point source of heat;

s = the heat produced per unit time at a point source;

T = the temperature field;

T_A= anomalous temperature field due to a body of contrasting heat production;

T_K= anomalous temperature field due to a body of contrasting thermal conductivity;

T_R= the regional temperature field which varies linearly with depth;

T_S= anomalous temperature field due to a point source of heat;

(x,y,z)= the coordinates in a right-handed system with z increasing downward, at which the field is to be computed;

(x',y',z')= the coordinates describing the location of points in an anomalous region in space;

γ = the universal gravitational constant;

ρ = density contrast.

Assumptions and Approximations

This study is concerned with the steady-state heat conduction problem for anomalous bodies in a half space overlain by a layer of contrasting conductivity (fig. 1). In general, both the heat production and thermal conductivity of the body differ from that of the surrounding medium. Heat enters the system either as uniform vertical heat flow (q*) from the base of the model region or is generated within the anomalous body and surrounding medium. Heat production in the surrounding medium extends to a finite depth. The surface of the two-layed half space is maintained at a constant temperature. All other factors which influence the terrestrial temperature field are ignored.

In lieu of an exact solution to this problem the temperature and heat flow effects of the body's heat production and conductivity contrasts are calculated seperately and then added. The temperature field is then approximated by the superposition of three independently calculated temperature fields: 1.) the anomalous field due to a body of contrasting heat production in a two-layer half space (T_A), 2.) the anomalous field due to the disturbance in q* by a body of contrasting conductivity in a two-layered half space (T_K), 3.) a regional field which varies only in the vertical direction (T_R).

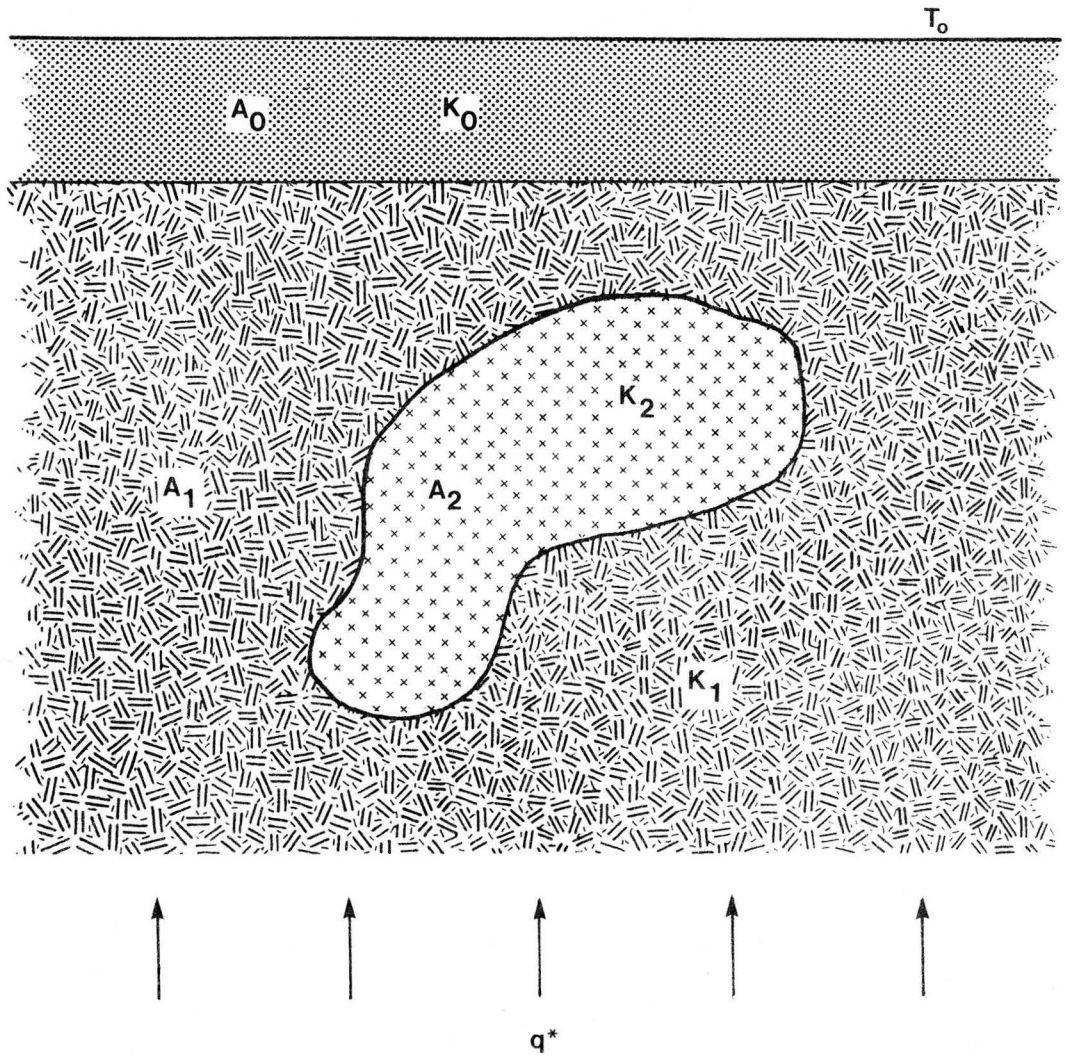

Figure 1 Schematic diagram of an anomalous body of arbitrary shape in a two-layered half space. The vertical heat flow q* enters the system at the base of the model region. The surface is held at a constant temperature T_o.

The effects of arbitrarily shaped three-dimensional bodies are approximated by summing the effects of horizontal polygonal prisms as in Plouff's (1976) gravity modeling method. In the following sections expressions for the temperature and heat-flow anomalies due to anomalous polygonal prisms in a uniform space are developed first. Expressions for the temperature and heat-flow anomalies in a uniform half space and a two-layered half space are then found by the method of images, a standard method in heat conduction (Carslaw and Jaeger, 1957, p. 273) and in electrostatics (Kellogg, 1957, page 207).

Heat Production Contrasts

Steady-state temperature fields in regions of uniform conductivity, like gravity and magnetic potentials, satisfy Poisson's equation

$$\nabla^2 T(x,y,z) = -\frac{1}{K} a(x,y,z) \; . \qquad (1)$$

The solution for a point source in a uniform medium is given by (Carslaw and Jaeger, 1959, p. 422)

$$T_s(x,y,z) = \frac{s}{4\pi RK} \qquad (2)$$

where

$$R^2 = (x-x')^2 + (y-y')^2 + (z-z')^2 .$$

For the case of a uniform heat production A_2 within a region V_0 and a uniform heat production A_1 outside V_0

$$T_A(x,y,z) = \frac{A}{4\pi K}\,\chi(x,y,z,V_0) \tag{3}$$

where

$$\chi(x,y,z,V_0) = \int_{-\infty}^{\infty}\int_{-\infty}^{\infty}\int_{-\infty}^{\infty} V_0(x',y',z')\,\frac{dx'dy'dz'}{R}\quad ;$$

$$V_0(x',y',z') = \begin{cases} 1 \text{ inside the region } V_0 \\ 0 \text{ outside the region } V_0 \end{cases}$$

$$A = A_2 - A_1 .$$

The heat flow field due to the same volume source is found by appling Fourier's law of heat conduction

$$q_A(x,y,z) = -\left(-K\frac{\partial T_A}{\partial z}\right) = \frac{A}{4\pi}\,\psi(x,y,z,V_0) \tag{4}$$

where

$$\psi(x,y,z,V_0) = \int_{-\infty}^{\infty}\int_{-\infty}^{\infty}\int_{-\infty}^{\infty} V_0(x',y',z')\frac{(z-z')dx'dy'dz'}{R^3}\quad ;$$

and where positive heat flow is toward the surface.

The remaining problem is to define χ and ψ for the desired source element. Expressions for χ and ψ exist in the literature for a large number of different source geometries. Of these, polygonal prisms are particularly well suited for representing three-dimensional geologic features. Plouff (1976, eq. (3)) gives the gravitational attraction of an n-sided polygonal prism with vertical edges. Using the current study's notation the expression is

$$G(x,y,z) = \gamma\rho\psi(x,y,z,V_0) \tag{5}$$

where

$$\psi(x,y,z,V_0) = S_m \sum_{i=1}^{n} \left[S_p\theta(Z_2-Z_1)-Z_2(W_{22}-W_{12})+Z_1(W_{21}-W_{11})-PQ \right] ;$$

S_m = -1 if the centroid of the prism is above the fieldpoint and S_m = 1 if the center of mass is below the fieldpoint;

S_p = 1 if P is postive, and -1 if P is negative;

$$\cos\theta = \frac{X_1X_2+Y_1Y_2}{\sqrt{X_1^2+Y_1^2}\sqrt{X_2^2+Y_2^2}} ;$$

$Z_1 = z - z'_1$;

z'_1 = the vertical coordinate of the top of the prism;

$Z_2 = z - z'_2$;

z_2' = the vertical coordinate of the base of the prism;

$$W_{ij} = \tan^{-1} \frac{d_i Z_j}{PR_{ij}} ;$$

$$R_{ij}^2 = X_i^2+Y_i^2+Z_j^2 ;$$

$$d_i = X_i(X_2-X_1)+Y_i(Y_2-Y_1) \Big/ \sqrt{(X_2-X_1)^2+(Y_2-Y_1)^2} ;$$

$(X_1, Y_1) = (x-x_1', y-y_1')$;

(x_1', y_1') = the coordinates of the starting point of an edge;

$(X_2, Y_2) = (x-x_2', y-y_2')$;

(x_2', y_2') = the coordinates of the ending point of an edge;

$$P = (X_1Y_2-X_2Y_1) \Big/ \sqrt{(X_2-X_1)^2+(Y_2-Y_1)^2} ;$$

$$Q = \ln \frac{R_{22}+d_2}{R_{21}+d_2} \cdot \frac{R_{11}+d_1}{R_{12}+d_1} .$$

Because it is known that χ cannot contain terms which are independent of z, χ can be found by integrating ψ with respect to z. All terms included in ψ for a polygonal prism can be written in the forms:

$$S_p \theta Z_j ; \tag{6a}$$

$$Z_j \tan^{-1} \frac{d_i Z_j}{PR_{ij}} ; \tag{6b}$$

$$P \ln(R_{ij}+d_i) . \tag{6c}$$

Term (6a), integrated using the power rule, yields

$$\frac{1}{2}S_p\theta Z_j^2 \ . \tag{7a}$$

Term (6b) is evaluated using integration by parts, Dwight's (1957) integral 200.01 and Plouff's (1976) integral (8a). The result is

$$\frac{1}{2}\left[-(Z_j^2+P^2)\tan^{-1}\frac{d_iZ_j}{PR_{ij}} + Pd_i\ln(R_{ij}+d_i)\right]. \tag{7b}$$

Term (6c) is integrated using the same method and reference integrals as (6b) and yields

$$P^2\tan^{-1}\frac{d_iZ_j}{PR_{ij}} - P(d_i+Z_j)\ln(R_{ij}+Z_j)\ . \tag{7c}$$

Substituting these integrals into ψ for a polygonal prism, χ for the same source volume is given by

$$\begin{aligned}\chi(x,y,z,V_0) = \frac{1}{2}S_m \sum_{i=1}^{n} \Big[&SC\{(Y_2^2-X_2^2)F_2-(Y_1^2-X_1^2)F_1\}+(S^2-C^2)(X_2Y_2F_2-X_1Y_1F_1)\\ &+(X_2^2C^2-2X_2Y_2SC+Y_2^2S^2)(W_{22}-W_{21})-(X_1^2C^2-2X_1Y_1SC+Y_1^2S^2)(W_{12}-W_{11})\\ &+2(Y_2S-X_2C)Q_2-2(Y_1S-X_1C)Q_1+S_p\theta(Z_2^2-Z_1^2)-Z_2^2(W_{22}-W_{12})\\ &+Z_1^2(W_{21}-W_{11})\Big]\end{aligned} \tag{8}$$

where

$$C = (Y_2-Y_1)/\sqrt{(X_2-X_1)^2+(Y_2-Y_1)^2} \ ;$$

$$S = (X_2-X_1)/\sqrt{(X_2-X_1)^2+(Y_2-Y_1)^2} \ ;$$

$$F_j = \ln\left[\frac{R_{j2}+Z_2}{R_{j1}+Z_1}\right] \ ;$$

$$Q_j = Z_2\ln(R_{j2}+d_j) - Z_1\ln(R_{j1}+d_j) \ .$$

For the special case of a rectangular prism centered about the field point, equation (8) reduces to

$$\chi(x,y,z,V_0) = \left[YZ\ln(X+R) - \frac{1}{2}X^2\tan^{-1}\frac{YZ}{XR} + XZ\ln(Y+R) - \frac{1}{2}Y^2\tan^{-1}\frac{XZ}{YR} + XY\ln(Z+R) - \frac{1}{2}Z^2\tan^{-1}\frac{XY}{ZR}\right]\Bigg|_{X_1}^{X_2}\Bigg|_{Y_1}^{Y_2}\Bigg|_{Z_1}^{Z_2} \ . \qquad (9)$$

Equation (9) agrees with the formula for the gravitational potential due to a rectangular prism (Haaz, 1953).

Thermal Conductivity Contrasts

The distortion of a uniform heat flow field by a body of contrasting conductivity is mathematically the same as the distortion of a magnetic field by a body of contrasting magnetic susceptibility. The latter problem has been dealt

with by Talwani (1965) and Plouff (1976). In these studies the contribution to the magnetic field by an infinitismal volume element in the anomalous body is assumed to be the same as a similar volume element alone in free space. The total effect of the anomalous body is then found by integrating the effects of all such volume elements which make up the body. This is not an exact solution because the magnetic field induced in a given volume element will act as an additional inducing field in neighboring volume elements. This interaction between neighboring volume elements is ignored.

The same method can be applied to the analogous heat conduction problem. The temperature effect of a single volume element can be found by considering the temperature anomaly due to a sphere of contrasting conductivity, centered about (x',y',z'), in a uniform heat flow field q* (Carslaw and Jaeger, 1959, p. 426)

$$\Delta T(x,y,z) = \frac{q^* r^3 (K_1 - K_2)(z-z')}{K_1 R^3 (2K_1 + K_2)} \qquad (10)$$

where

r = the radius of the sphere;

K_1 = the conductivity of the surrounding medium;

K_2 = the conductivity of the sphere.

The temperature anomaly due to a spherical volume element ΔV at an arbitrary position in a region V_0 can then be written

$$\Delta T(x,y,z) = \frac{3q^*(K_1-K_2)(z-z')\Delta V}{4\pi K_1 R^3(2K_1+K_2)} . \tag{11}$$

The approximate temperature anomaly associated with a region V_0 of contrasting conductivity is then given by letting ΔV become infinitismal and integrating the effects of all such volume elements in V_0:

$$T_K(x,y,z) = \frac{3q^*(K_1-K_2)}{4\pi K_1(2K_1+K_2)} \int_{-\infty}^{\infty}\int_{-\infty}^{\infty}\int_{-\infty}^{\infty} V_0(x',y',z')\frac{(z-z')}{R^3}\,dx'dy'dz' \tag{12}$$

$$= \frac{3q^*(K_1-K_2)}{4\pi K_1(2K_1+K_2)}\psi(x,y,z,V_0) .$$

Equation (12) is an approximation because, as in the analogous magnetic problem, the interaction between volume elements is ignored. Numerical results from equation (12) are compared with those from exact solutions in section 2.

The vertical heat-flow anomaly associated with a body of contrasting conductivity is given by

$$q_K(x,y,z) = \frac{3q^*(K_1-K_2)}{4\pi(2K_1+K_2)}\omega(x,y,z,V_0) \tag{13}$$

where

$$\omega(x,y,z,V_0) = \int_{-\infty}^{\infty}\int_{-\infty}^{\infty}\int_{-\infty}^{\infty} V_0(x',y',z') \left[\frac{R^2-3(z-z')^2}{R^5}\right] dx'dy'dz' \ .$$

The function ω appears in the expression for the vertical component of the induced magnetic field due to a volume V_0 of contrasting susceptibility in a vertical inducing field. For an n-sided polygonal prism this component of the magnetic anomaly is written (Plouff, 1976. eq. 9)

$$M(x,y,z) = J_z\omega(x,y,z,V_0) \qquad (14)$$

where

$$\omega(x,y,z,V_0) = \sum_{i=1}^{n} (W_{22}-W_{21}-W_{12}+W_{11}) \ .$$

Heat Conduction in One- and Two-Layered Half Spaces

Equations (3), (4), (12) and (13) give temperature and heat-flow anomalies due to anomalous bodies in an otherwise uniform space. For a realistic representation of the terrestrial temperature and heat flow fields, the thermal effects of the earth's surface must be accounted for. This can be done by the method of images if the earth is

represented by a half space with a constant surface temperature. Simply stated, the method of images involves constructing a system of sources and sinks in a medium with uniform material properties in such a way as to duplicate the temperature field in a region with discontinuous material properties. The combined effect of all the sources and sinks is required to satisfy the governing equation throughout the region of interest and to behave in a specified manner at the boundaries of the region.

The geometry of the source-sink system for a point source at (x',y',z') in a half space with a uniform conductivity (one-layered half space) is shown in figure 2. The expression for the temperature anomaly is (Carslaw, and Jaeger, 1959, p. 273)

$$T_s(x,y,z) = \frac{s}{4\pi K}\left[\frac{1}{R} - \frac{1}{\bar{R}}\right] \tag{15}$$

where

$$\bar{R}^2 = (x-x')^2 + (y-y')^2 + (z+z')^2.$$

For a volume source in a one-layered half space

$$T_A(x,y,z) = \frac{A}{4\pi K}\left[\chi(x,y,z,V_0) - \chi(x,y,z,\bar{V}_0)\right] \tag{16}$$

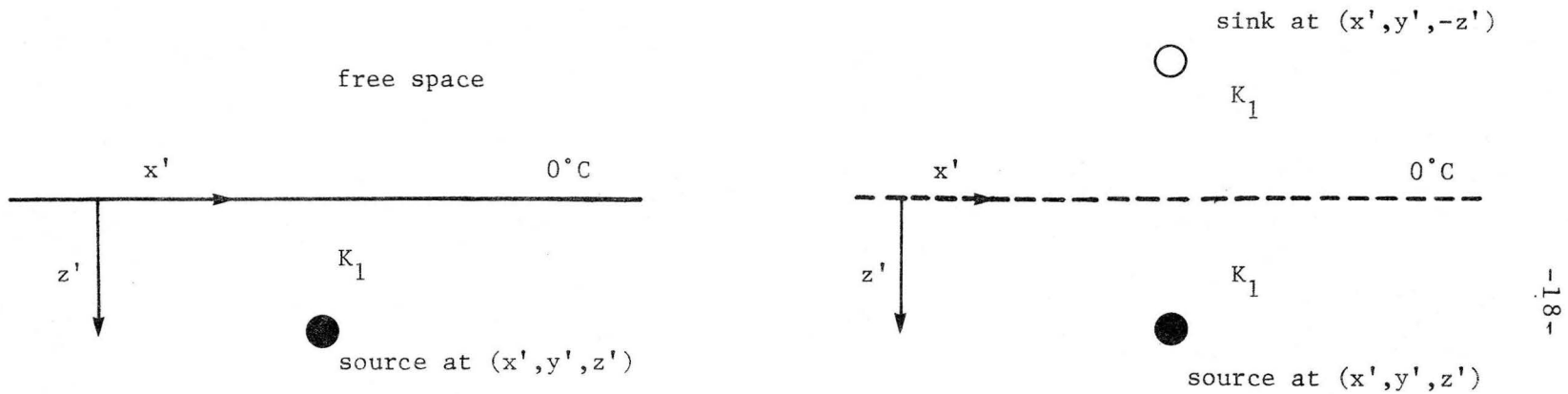

Half Space

Equivalent Image System for $z \geq 0$

Figure 2 Point-source image system for temperature in a uniform half space.

where

$$\bar{V}_0(x',y',z') = V_0(x',y',-z').$$

Likewise, for a one-layered half space

$$q_A(x,y,z) = \frac{A}{4\pi}\left[\psi(x,y,z,V_0) - \psi(x,y,z,\bar{V}_0)\right] ; \quad (17)$$

$$T_K(x,y,z) = \frac{3q^*(K_1-K_2)}{4\pi K_1(2K_1+K_2)}\left[\psi(x,y,z,V_0) + \psi(x,y,z,\bar{V}_0)\right] ; \quad (18)$$

$$q_K(x,y,z) = \frac{3q^*(K_1-K_2)}{4\pi(2K_1+K_2)}\left[\omega(x,y,z,V_0) + \omega(x,y,z,\bar{V}_0)\right] . \quad (19)$$

The uniform half space model of the earth is not applicable where a layer of contrasting conductivity overlies the source region. Such a situation occurs in the Atlantic Coastal Plain, where the conductivity of the basement complex can be twice that of the overlying sediments (Costain, et al, 1979). The effects of the sedimentary layer can be accounted for by placing a layer of thickness h and conductivity K_0 over the uniform half space with conductivity K_1. The boundary conditions for this two-layered earth model are:

1.) $$\lim_{R\to\infty} T_s(R) = 0 ;$$

2.) $$T_s(x,y,0) = 0 \ ;$$

3.) $$-K_0 \frac{\partial T_s}{\partial z}\bigg|_{z=h^-} = -K_1 \frac{\partial T_s}{\partial z}\bigg|_{z=h^+}$$

4.) $$\lim_{z \to h^-} T_s(x,y,z) = \lim_{z \to h^+} T_s(x,y,z) \ .$$

For a source at an arbitrary location in the region of conductivity K_1, an infinite series of images is required to satisfy all four conditions simultaneously (fig. 3).

The temperature at the point (x,y,z) due to a point source at (x',y',z') is given by

$$T_s(x,y,z) = \frac{s}{2\pi}\left[\frac{1}{\beta\sqrt{(x-x')^2+(y-y')^2+(z-z')^2}} + \frac{1}{\alpha}\sum_{i=0}^{\infty}(-1)^{i+1}(\alpha/\beta)^{i+1}\left(\frac{1}{\sqrt{(x-x')^2+(y-y')^2+(z+2ih+z')^2}} + \frac{\alpha}{\beta\sqrt{(x-x')^2+(y-y')^2+(z-2(i+1)h-z')^2}}\right)\right] \qquad 0 \le z < h$$

$$T_s(x,y,z) = \frac{s}{4\pi}\left[\frac{1}{K_1\sqrt{(x-x')^2+(y-y')^2+(z-z')^2}} - \frac{\alpha}{K_1\beta\sqrt{(x-x')^2+(y-y')^2+(z-2h+z')^2}} + \frac{4K_0}{\alpha^2}\sum_{i=0}^{\infty}(-1)^{i+1}(\alpha/\beta)^{i+2}\frac{1}{\sqrt{(x-x')^2+(y-y')^2+(z+2ih+z')^2}}\right] \qquad z > h \qquad (20)$$

where

K_0 = the conductivity of the layer over the half space;

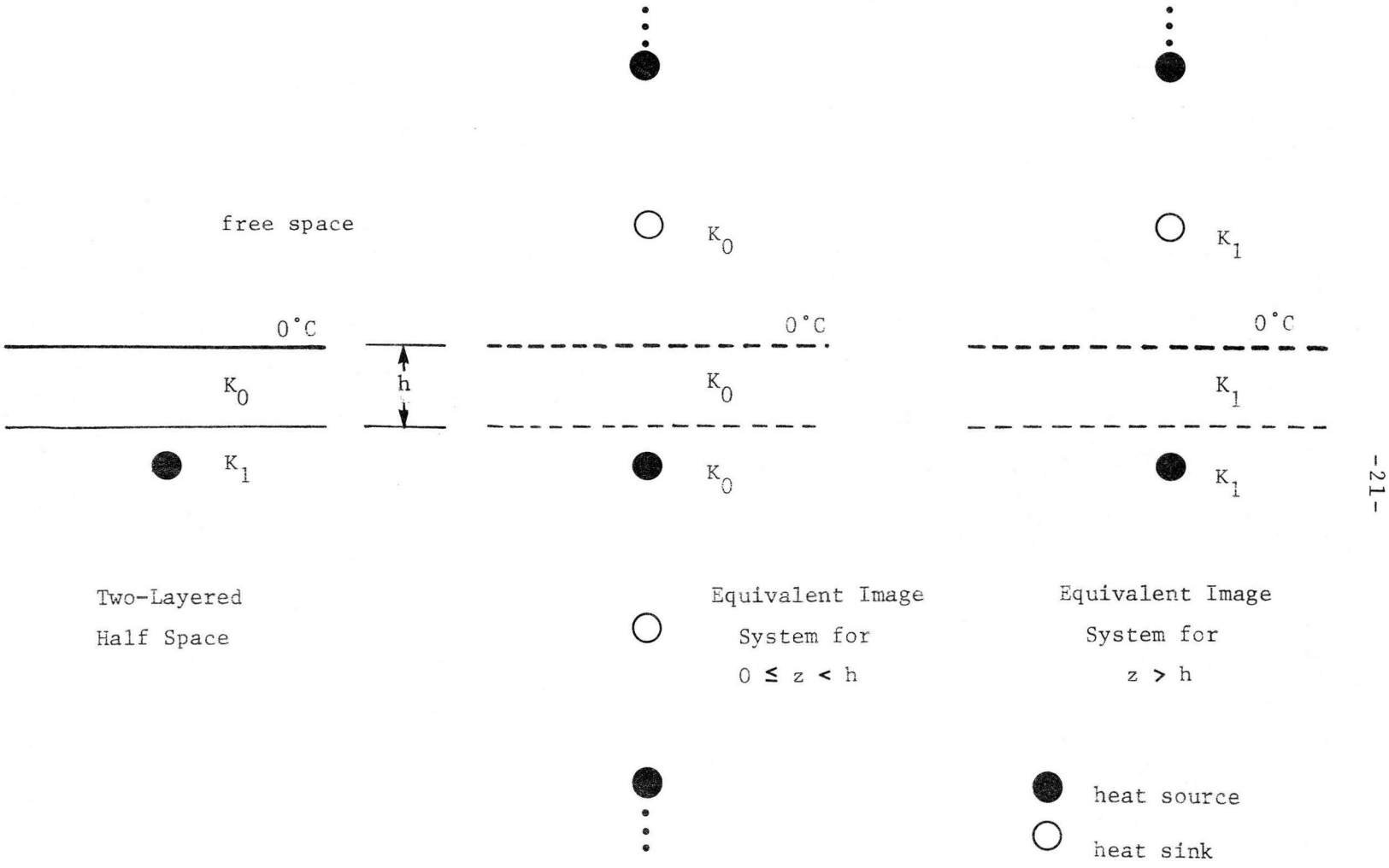

Figure 3 Point-source image system for temperatures in a layer over a half space.

K_1 = the conductivity of the half space;

h = the thickness of the layer over the half space;

$\alpha = K_0 - K_1$

$\beta = K_0 + K_1$.

For an arbitrary volume source the temperature is

$$T_A(x,y,z) = \left[\frac{A}{2\pi}\ \frac{1}{\beta}\,\chi(x,y,z,V_0) + \frac{1}{\alpha}\sum_{i=0}^{\infty}(-1)^{i+1}(\alpha/\beta)^{i+1}\left(\chi(x,y,z,\bar{V}_i) + \frac{\alpha}{\beta}\,\chi(x,y,z,V_{i+1})\right)\right] \qquad 0 \le z < h \tag{21}$$

$$T_A(x,y,z) = \frac{A}{4\pi}\left[\frac{1}{K_1}\chi(x,y,z,V_0) - \frac{\alpha}{\beta K_1}\chi(x,y,z,\tilde{V}_0) + \frac{4K_0}{\alpha^2}\sum_{i=0}^{\infty}(-1)^{i+1}\cdot(\alpha/\beta)^{i+2}\chi(x,y,z,\bar{V}_i)\right] \qquad z > h$$

where

$V_j(x',y',z') = V_0(x',y',2jh+z')$;

$\bar{V}_j(x',y',z') = V_0(x',y',-2jh-z')$;

$\tilde{V}_j(x',y',z') = V_0(x',y',2h-z')$.

Because each term in equation (21) satisfies Poisson's equation, the equation itself must also satisfy Poisson's equation. Both series in the equation can be shown to converge absolutely by the ratio test (Thomas, 1972, p. 805 and 849) for all physically realizable values of thermal conductivity. It can also be seen by inspection that equation (21) satisfies all four of the boundary conditions placed on it.

The errors incurred by truncating the series in equation (21) are easily estimated. For

$$K_0 > K_1$$

both series are alternating. The truncation error can then be no larger in magnitude than the absolute value of the first truncated term. For

$$K_0 < K_1$$

the series are either all positive or all negative. A bound for the error resulting from truncating the series after the nth term is given by

$$\begin{aligned} R_n &\leq \left| \frac{\chi(x,y,z,V_n)}{2\pi\alpha} \int_n^{\infty} \left[(\alpha/\beta)^{j+1} + (\alpha/\beta)^{j+2} \right] dj \right| \\ &\leq \left| \frac{\chi(x,y,z,V_n)}{2\pi\alpha \ln(\alpha/\beta)} \left[(\alpha/\beta)^{n+1} + (\alpha/\beta)^{n+2} \right] \right| \qquad \begin{array}{l} 0 \leq z < h \\ 0 < |\alpha| < \beta \end{array} \end{aligned} \tag{22}$$

$$\begin{aligned} R_n &\leq \left| \frac{\chi(x,y,z,V_n)K_0}{\pi\alpha^2} \int_n^{\infty} (\alpha/\beta)^{j+2} dj \right| \\ &\leq \left| \frac{\chi(x,y,z,V_n)K_0\alpha^{n-2}}{\pi\beta^{n+2}\ln(\alpha/\beta)} \right| \qquad \begin{array}{l} z > h \\ 0 < |\alpha| < \beta \end{array} \end{aligned}$$

where

R_n = the magnitude of the largest possible error caused by truncating the series after n terms;

In at least two special cases the infinite series vanish entirely. For the case in which

$$K = K_0 = K_1$$

equation (21) reduces to equation (16).

The case in which h and z' become large without bound, while the difference

$$2h - z'$$

remains constant, is equivalent to removing the interface at

$$z = 0.$$

Under this condition equation (20) reduces to

$$T_s(x,y,z) = \frac{s}{4\pi}\left[\frac{2}{K_0+K_1}\,\frac{1}{\sqrt{(x-x')^2+(y-y')^2+(z-z')^2}}\right] \qquad z < h$$

$$T_s(x,y,z) = \frac{s}{4\pi}\left[\frac{1}{K_1\sqrt{(x-x')^2+(y-y')^2+(z-z')^2}}\right. \qquad (23)$$

$$\left. + \frac{K_1 - K_0}{K_1(K_0+K_1)}\,\frac{1}{\sqrt{(x-x')^2+(y-y')^2+(z-2h+z')^2}}\right] \qquad z > h.$$

Equation (23) is identical, in form, to the solution to the analogous problem in electrostatics (Kellogg, 1957, p. 209).

Up to this point only the problem of heat production in a two-layered half space has been considered. A similar development for the problem of contrasting conductivities yields

$$T_K(x,y,z) = \frac{3q^*(K_1-K_2)}{2\pi K_1(2K_1+K_2)} \left\{ \frac{1}{\beta}\psi(x,y,z,V_0) \right. \qquad 0 \leq z \leq h$$

$$\left. + \frac{1}{\alpha}\sum_{i=0}^{\infty}\left[(-1)^{i+1}(\alpha/\beta)^{i+1}\left(\frac{\alpha}{\beta}\psi(x,y,z,V_{i+1})-\psi(x,y,z,\bar{V}_i)\right)\right]\right\} \tag{24}$$

$$T_K(x,y,z) = \frac{3q^*(K_1-K_2)}{4\pi K_1(2K_1+K_2)} \left\{ \frac{1}{K_1}\psi(x,y,z,V_0)+\frac{\alpha}{\beta K_1}\psi(x,y,z,\tilde{V}_0) \right.$$

$$\left. - \frac{4K_0}{\alpha^2}\sum_{i=0}^{\infty}(-1)^{i+1}(\alpha/\beta)^{i+2}\psi(x,y,z,\bar{V}_i)\right\} \qquad z > h.$$

Expressions for heat flow in a two layered half space are found by applying Fourier's law of heat conduction to equations (21) and (24).

The Regional Temperature Field

The portion of the temperature field which varies only in the vertical direction will be termed the regional field. Because it does not vary laterally it is governed by Poisson's equation for one-dimensional heat conduction

$$\frac{\partial^2 T_R}{\partial z^2} = -\frac{1}{K}\, a(z).$$

For the case of a two-layered half space the boundary conditions are:

1.) $$T_R(x,y,0) = T_0 \ ;$$

2.) $$-K_0 \frac{\partial T_R}{\partial z}\bigg|_{z=h^-} = -K_1 \frac{\partial T_R}{\partial z}\bigg|_{z=h^+} \ ;$$

3.) $$-K_1 \frac{\partial T_R}{\partial z}\bigg|_{z=D} = q^* \ .$$

The solution is then given by

$$T_R(z) = \frac{1}{K_0}\left[zq_0 - \frac{1}{2} A_0 z^2 \right] + T_0 \qquad 0 \leq z < h$$

(25)

$$T_R(z) = \frac{1}{K_0}\left[hq_0 - \frac{1}{2} A_0 h^2 \right] + \frac{1}{K_1}\left[(z-h)q_0 - \frac{1}{2} A_1 (z-h)^2 \right] + T_0$$

$$D \geq z > h$$

where

q_0= the regional heat flow at the surface;

D= the depth to the base of the heat producing layer.

Equation (25) can be generalized to the case in which heat production in the region

$$z > h$$

varies in a step function manner. If the ith heat producing layer is characterized by a heat production A_i and a depth to the base of the layer D_i then

$$T_R(z) = \frac{1}{K_0}\left[zq_0 - \frac{1}{2} A_0 z^2 \right] + T_0 \qquad 0 \leq z < h$$

$$T_R(z) = \frac{1}{K_0}\left[hq_0 - \frac{1}{2} A_0 h^2 \right] + \frac{1}{K_1}\left[(z-h)\cdot(q_0 - A_0 h) - \frac{1}{2} A_{1m}(z-D_{m-1})^2 \right. \qquad (26)$$

$$\left. - \frac{1}{2} \sum_{i=1}^{m-1} A_{1i}(D_i - D_{i+1})^2 \right] + T_0. \qquad D_m \geq z \geq D_{m-1}$$

For the general case of a body of contrasting heat production and thermal conductivity the approximate total temperature field is given by the algebraic sum of equations (21), (24) and (26)

$$T(x,y,z) \cong T_A(x,y,z) + T_K(x,y,z) + T_R(z). \qquad (27)$$

3. Comparison of Different Solutions

Exact Solutions for Bodies With Simple Shapes

Exact solutions to the problem of determining temperature in a half space are available for anomalous bodies with simple shapes. These solutions provide an independent check on the validity of equation (27) as well as on the accuracy of computer programs based on this equation.

The expression for the temperature about a spherical heat source of radius a and heat production A follows directly from equation (15),

$$T_A(x,y,z) = \frac{a^3 A}{3K}\left[\frac{1}{R} - \frac{1}{\bar{R}}\right]. \qquad R > a \qquad (28)$$

The vertical heat flow at the surface is then given by

$$q_A(x,y,z) = \frac{2a^3 Az'}{3R^3} . \qquad (29)$$

A comparison of values given by equations (28) and (29) with those given by a polygonal prism model based on equation (27) is shown in figure 4. The geometry of the polygonal model is shown in figure 5. Values given by the two sets of equations agree to within 1% throughout the model region.

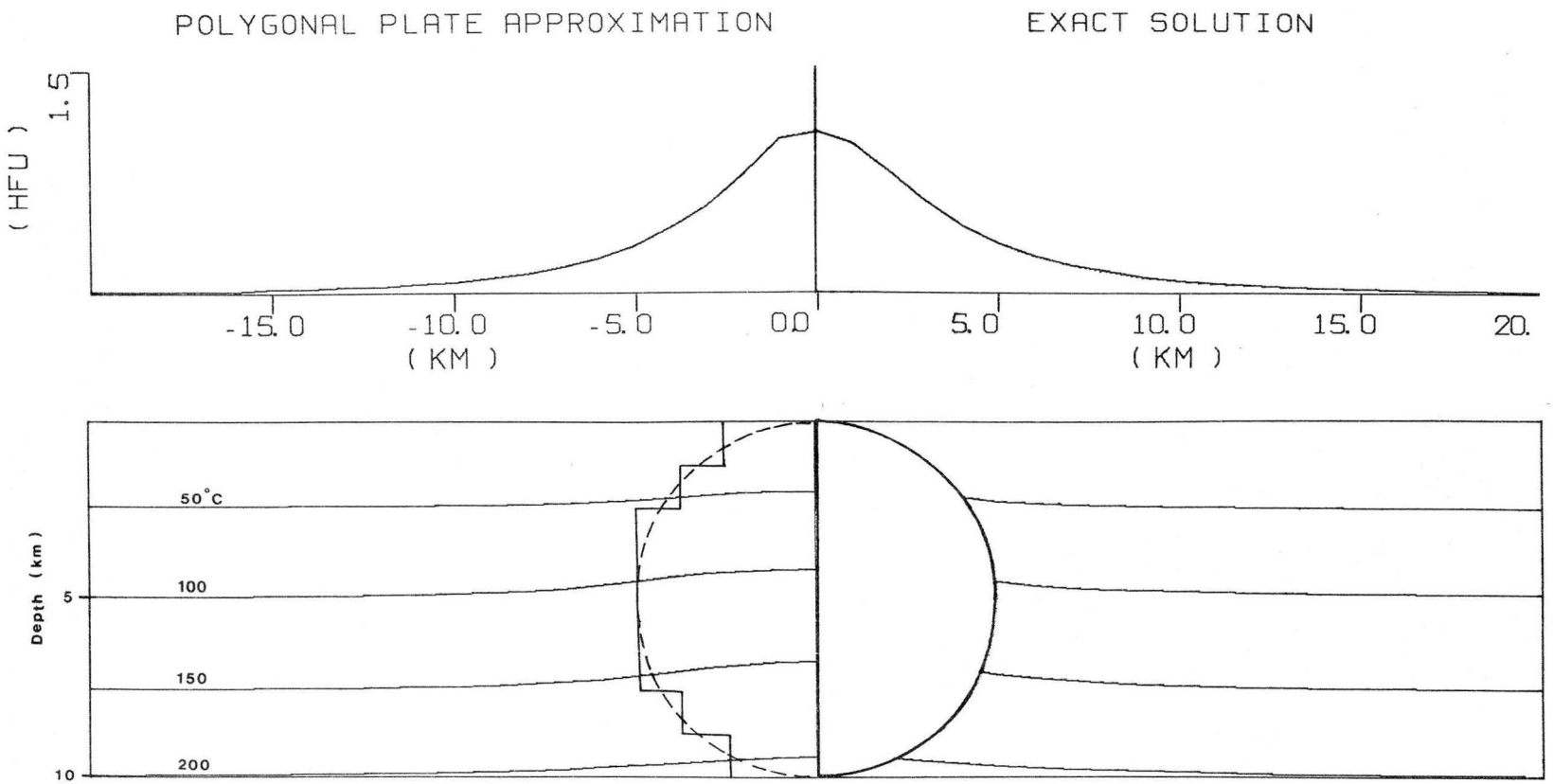

Figure 4 Comparison of the exact solution and polygonal prism approximation for a spherical heat source. Dashed line indicates the shape approximated by the polygonal prism model. The polygonal prism model is shown in figure 5.

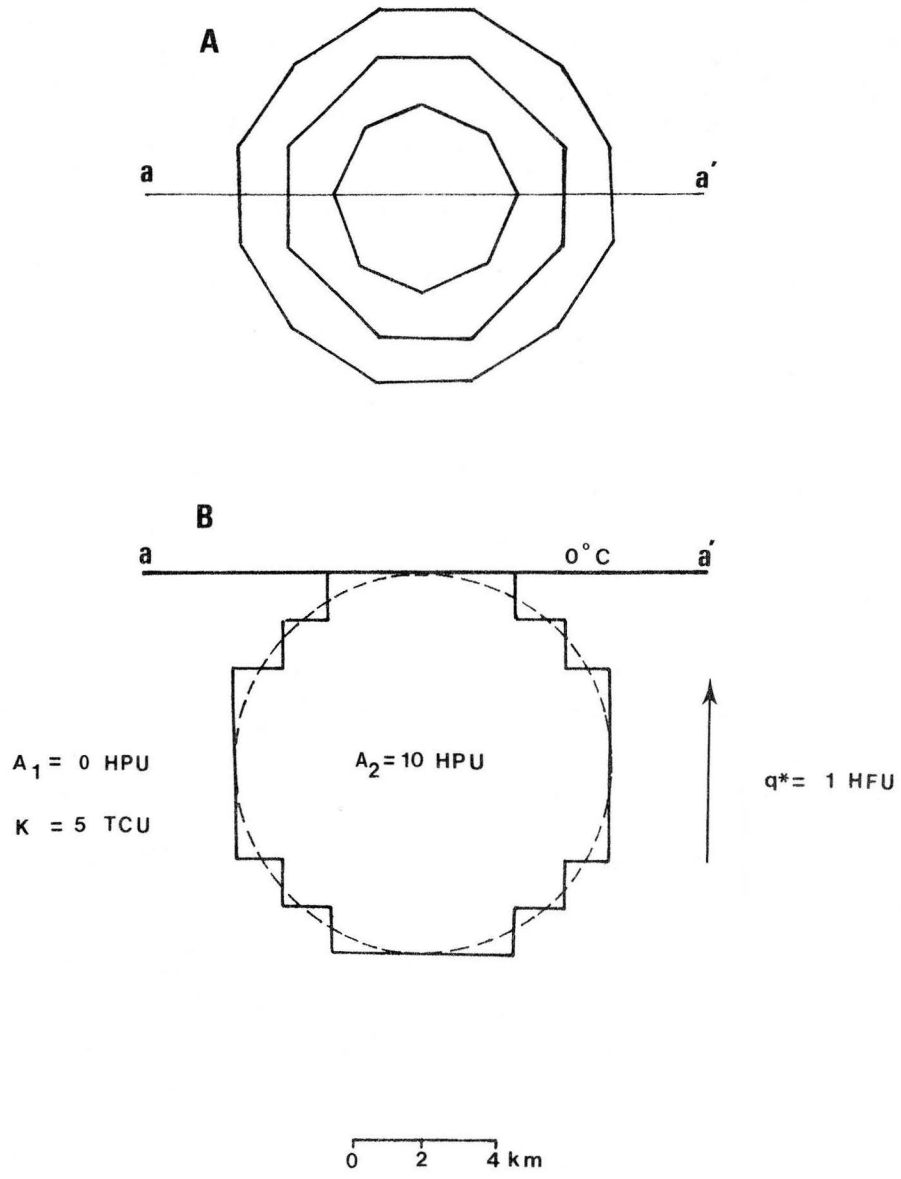

Figure 5 Polygonal prism model of the spherical heat source (fig. 4). Part A shows a map view of the model; Part B shows a cross-sectional view along line a-a'.

This difference can be reduced to an arbitrary level by refining the geometry of the polygonal model and increasing the precision of the arithmetic used to evaluate the equations.

Exact solutions for a hemisphere and a horizontal semi-circular cylinder of contrasting conductivity are given by Carslaw and Jaeger (1957, p. 426). Comparisons between these solutions and polygonal prism approximations based on equation (27) are shown in figures 6 and 8. The corresponding polygonal models are shown in figures 7 and 9, respectively.

In both cases the approximate temperature and heat flow anomalies are of the same sign and general shape as the exact anomalies. The superposition of exact and approximate heat flow profiles in figures 10 and 11 indicate that the approximation is poorest over the edges of the anomalous body and improves with increasing distance from the edges. Heat flow values over the center of the hemisphere in the exact and approximate solutions (fig. 10) agree to with 0.5%. For the semi-circular cylinder (fig. 11) the agreement is within 3.5%. These error levels cannot be improved to an arbitrary level by refining the geometry of the model and arithmetic precision as in the case of heat production contrasts. These error levels vary as a

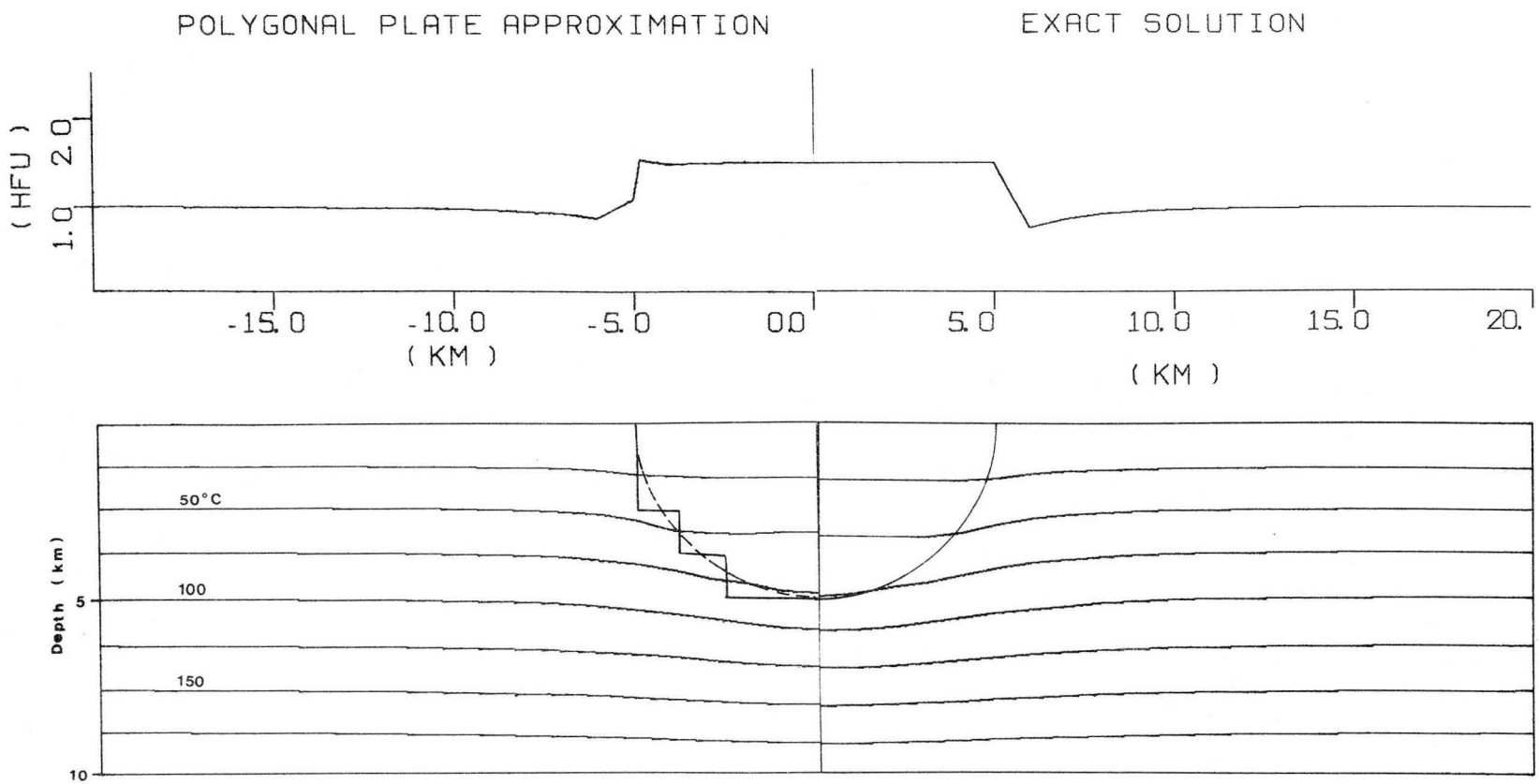

Figure 6 Comparison of the exact solution and the polygonal prism approximation for a semi-spheroid with a 2:1 conductivity contrast. The polygonal prism model is shown in figure 7.

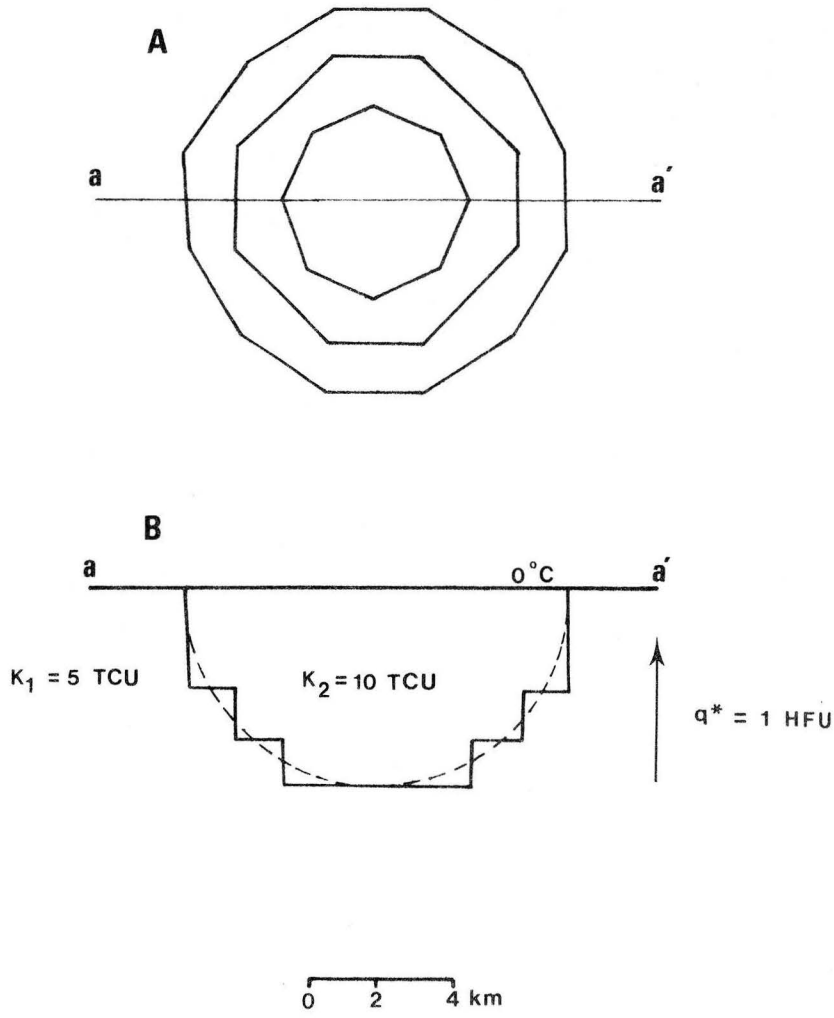

Figure 7 Polygonal prism model of the semi-spheroid of contrasting conductivity (fig. 6).

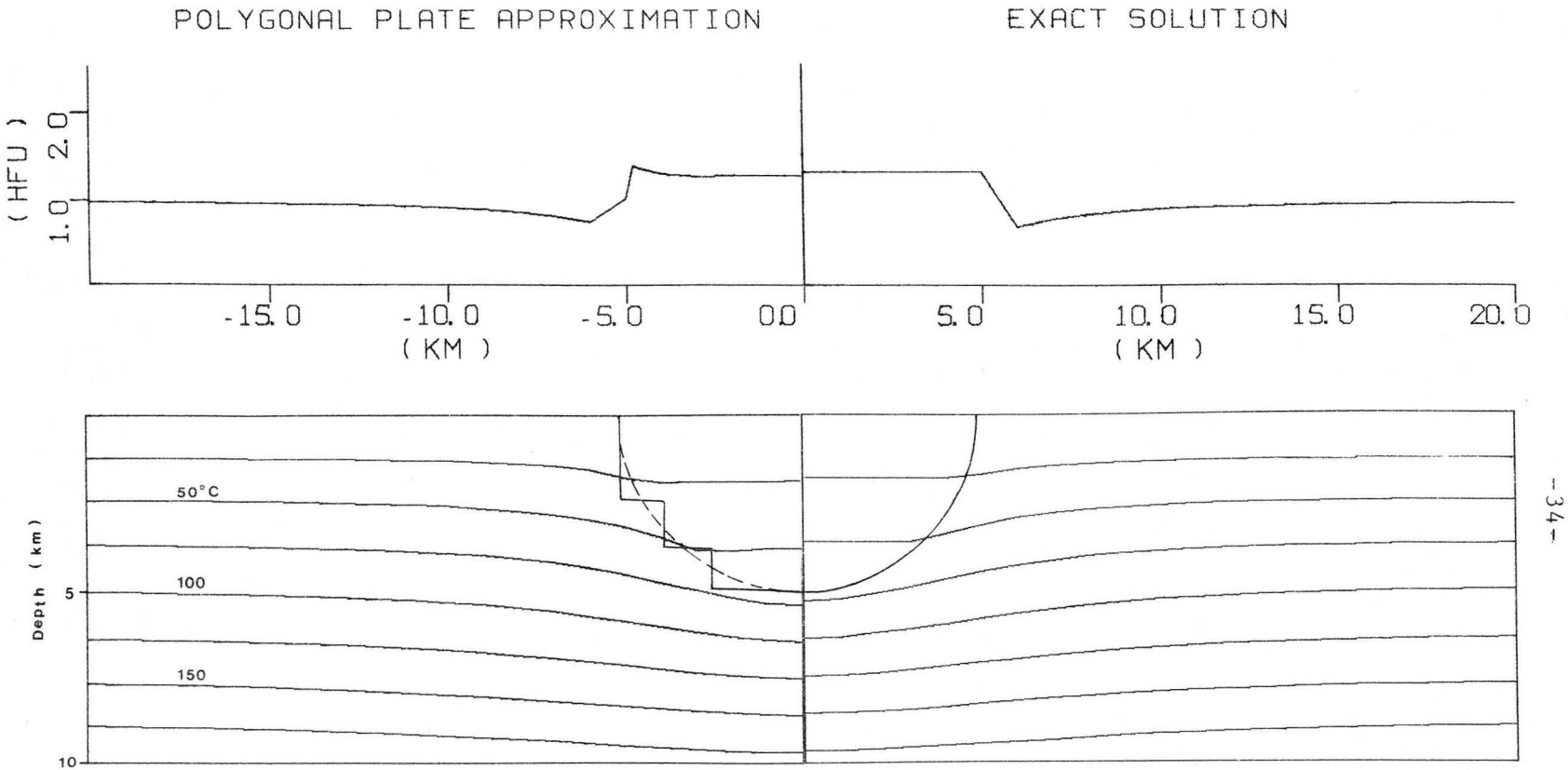

Figure 8 Comparison of the exact solution and polygonal prism approximation for a semi-circular cylinder with a 2:1 conductivity contrast. The polygonal prism model is shown in figure 9.

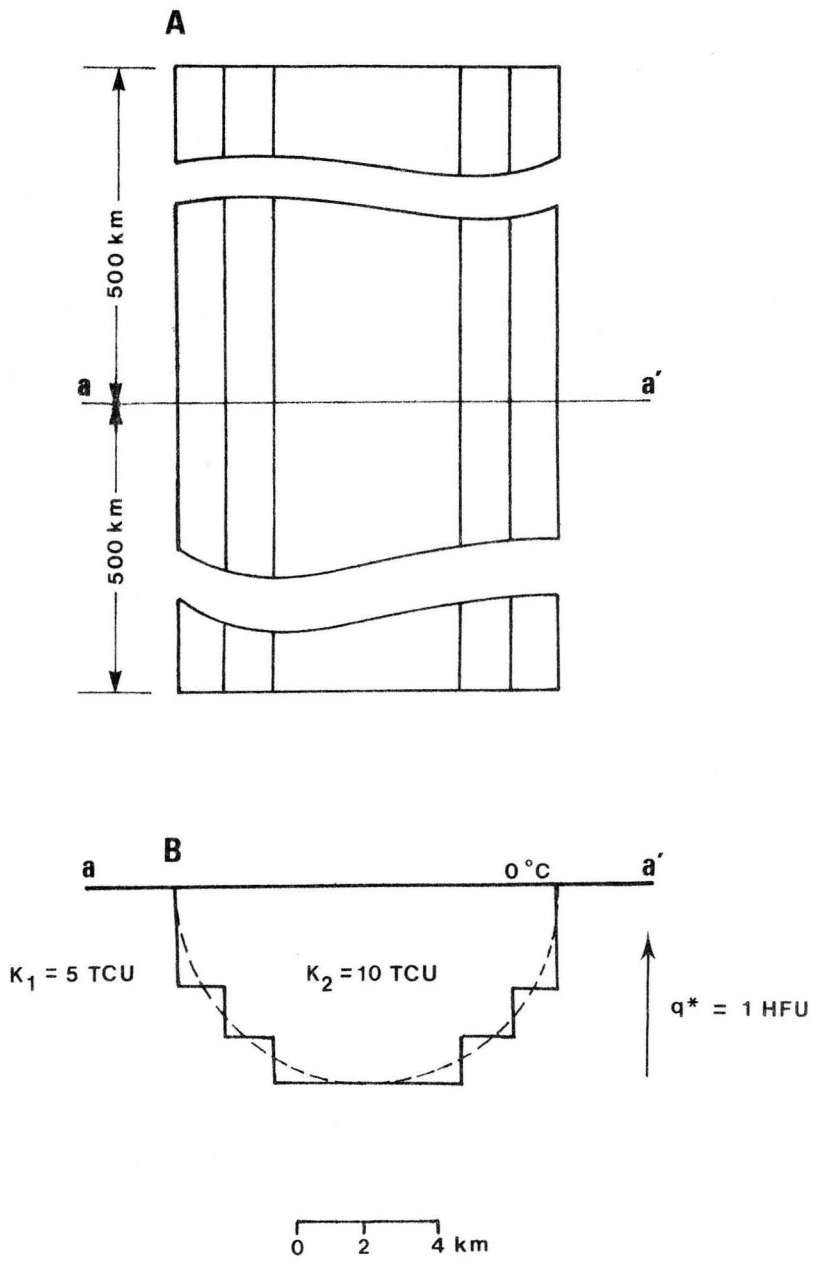

Figure 9 Polygonal prism model of the semi-circular cylinder of contrasting conductivity (fig. 8).

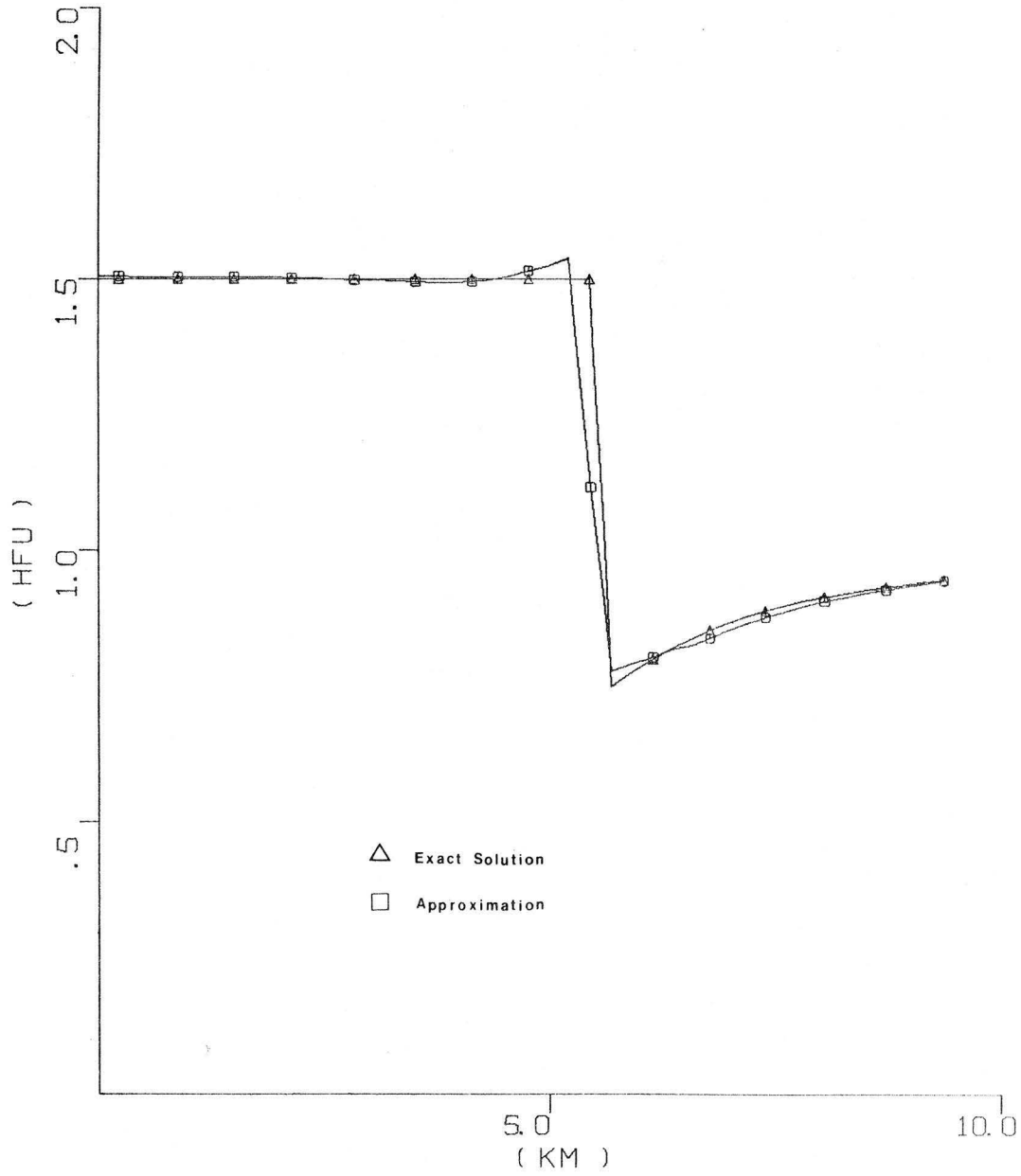

Figure 10 Superposition of exact and approximate heat-flow profiles over a semi-spheroid of contrasting conductivity.

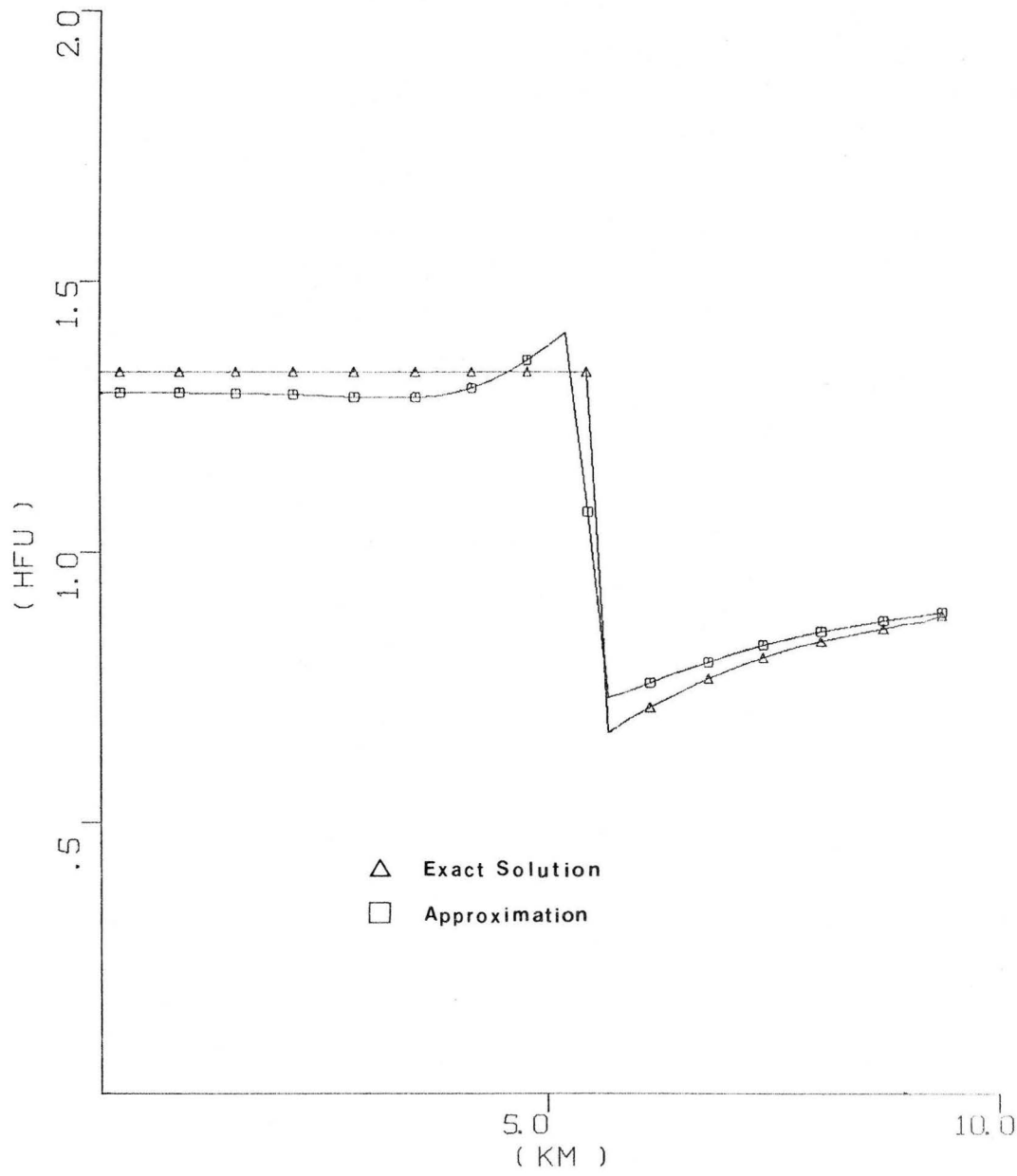

Figure 11 Superposition of exact and approximate heat-flow profiles over a semi-circular cylinder of contrasting conductivity.

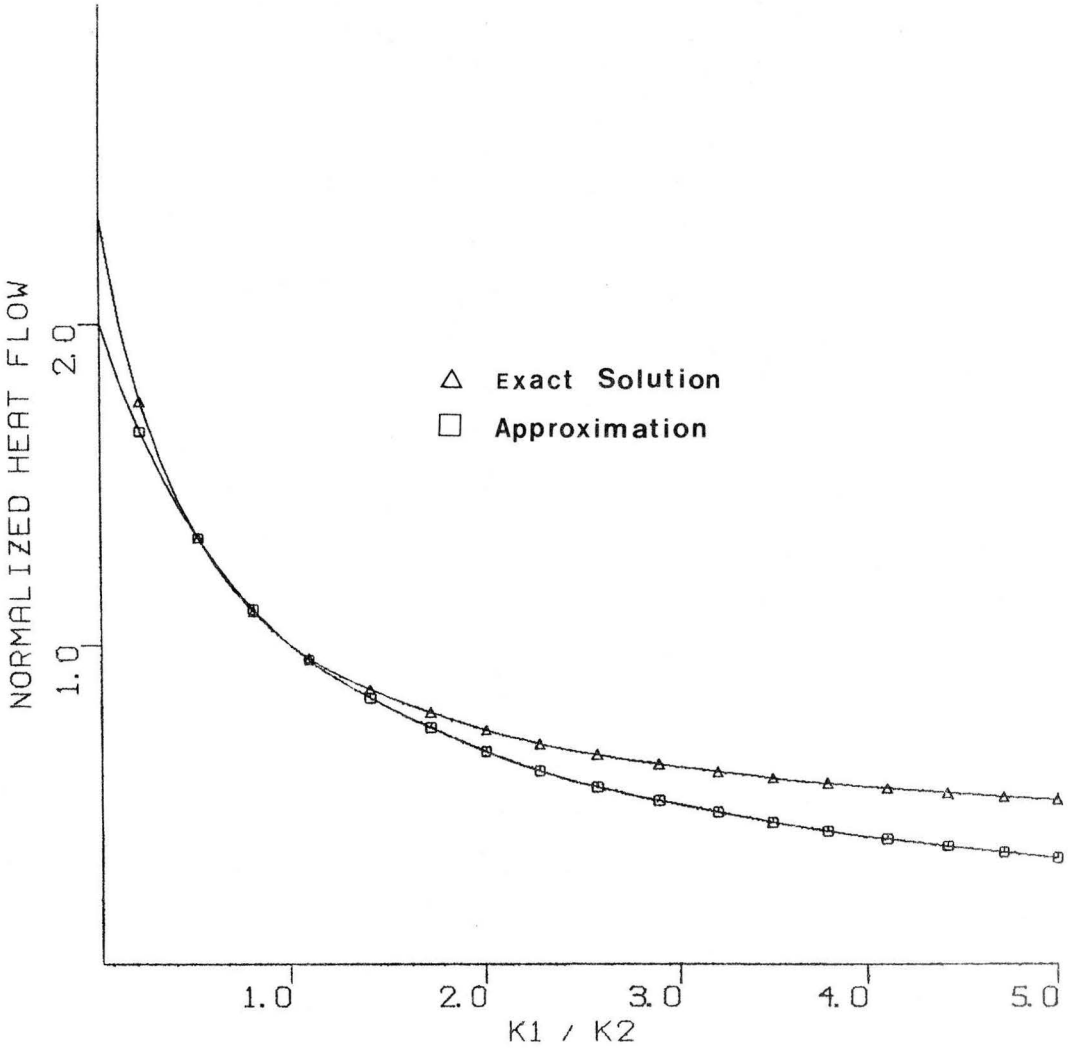

Figure 12 Normalized heat flow as a function of the ratio of the conductivity of the medium surrounding a cylinder and that of the cylinder.

function of the ratio of the conductivities of the media. Figure 12 shows the exact and approximate heat flow over the center of the semi-circular cylinder as a function of the conductivity ratio (K_1/K_2). The two solutions agree to within 5% over the range of conductivity ratios

$$0.25 < K_1/K_2 < 1.5.$$

Although the range of agreement varies with the geometry of the anomalous body, figure 12 clearly demonstrates that the agreement is closest for conductivity ratios near unity. Equation (12) is then a small contrast approximation for the disturbance to a linear temperature field by a body of contrasting conductivity.

Comparison With Numerical Solutions

Fehn et al., (1978) used a two-dimensional finite difference model, which couples heat transport and fluid flow equations, to model the Conway Granite in New Hampshire. For the case of an impermeable region, heat transport becomes purely conductive. The polygonal prism model of the Conway Granite is shown in figure 13; figure 14 shows a comparison of the results of the polygonal prism and finite difference models (Fehn et al., 1978, fig. 2). Fehn et al. report a maximum temperature at the base of the

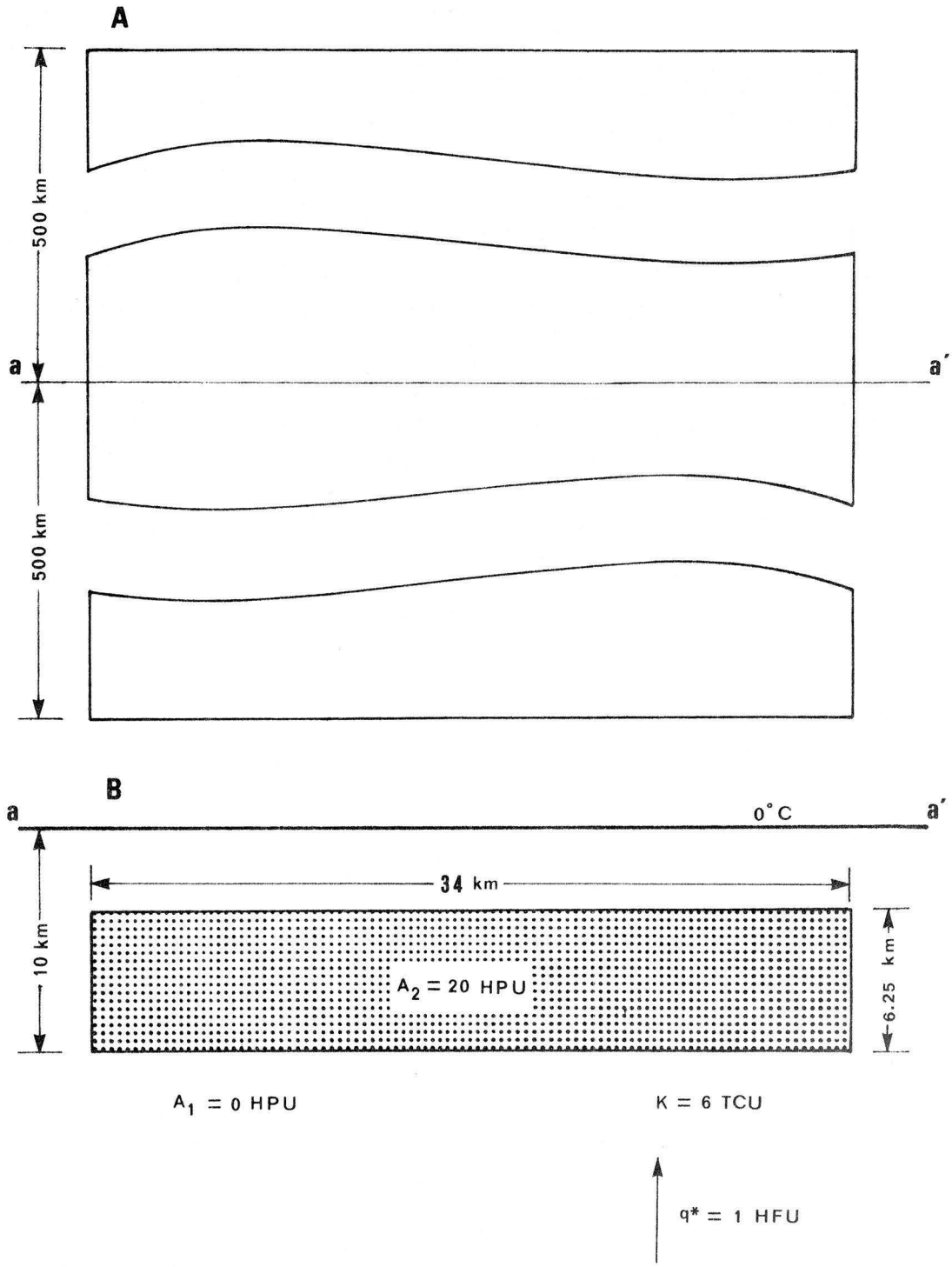

Figure 13 Polygonal prism model the Conway granite in New Hampshire.

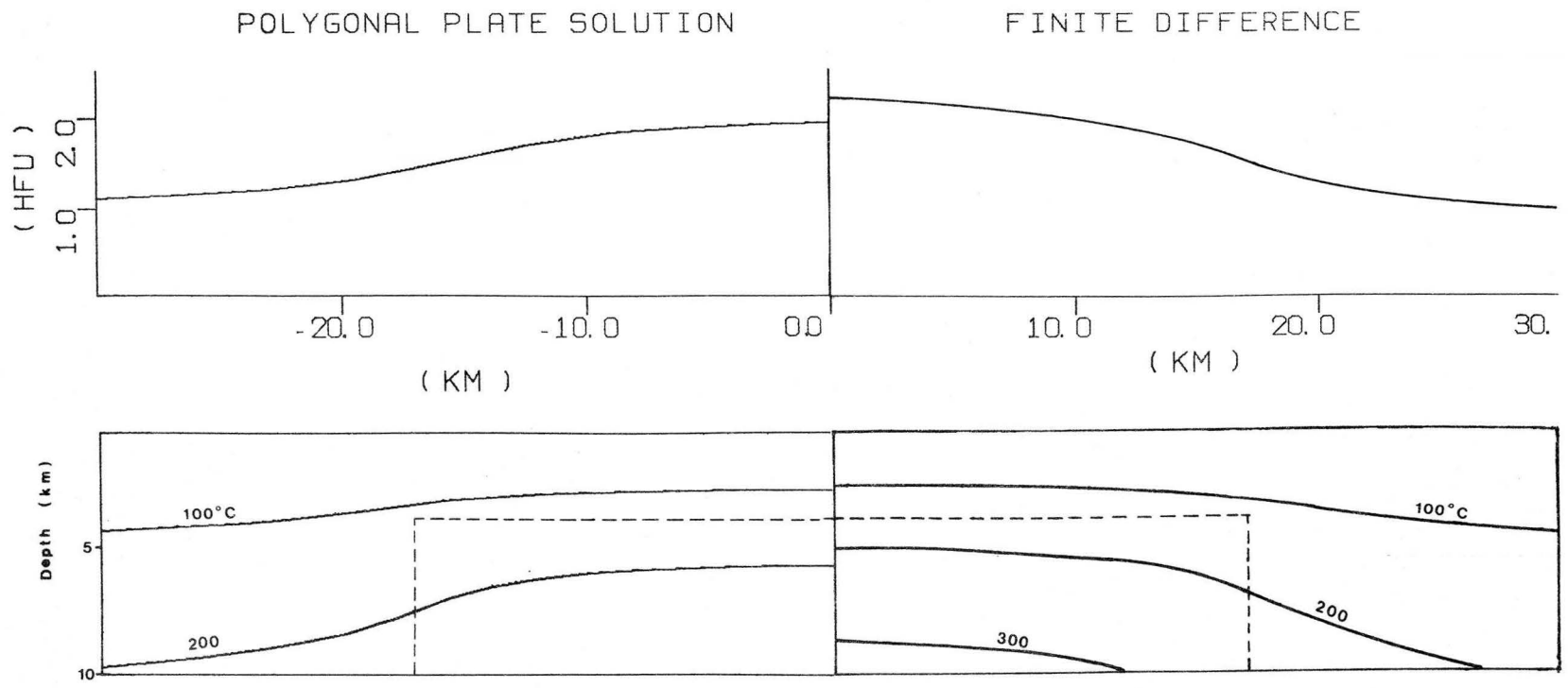

Figure 14 Comparison between polygonal prism and finite difference models of the Conway granite in New Hamshire. The finite difference model is from Fehn et al (1978).

pluton of 326°C and a maximum surface heat flow of 2.2 HFU. The maximum temperature and heat flow anomalies are 140°C and 1.2 HFU. For the same problem the polygonal prism solution gives a maximum temperature of 283°C and a heat flow of 1.9 HFU. The maximum temperature and heat flow anomalies given by the two methods differ by 40% and 33% respectively. The large difference is attributed to the diffences in boundary conditions. The boundary conditions for the finite difference version are:

1.) $$T(x,y,0) = 0 \quad ;$$

2.) $$- K \frac{\partial T}{\partial x}\Big|_{x=0} = 0 \; ;$$

3.) $$- K \frac{\partial T}{\partial z}\Big|_{x=60\ \text{km}} = 0 \quad ;$$

4.) $$- K \frac{\partial T}{\partial z}\Big|_{z=10\ \text{km}} = 1.0\ \text{HFU}.$$

The boundary conditions for the the polygonal prism solution are:

1.) $$T(x,y,0) = 0 \; ;$$

2.) $$- K \frac{\partial T}{\partial x}\Big|_{x \to \infty} = 0 \; ;$$

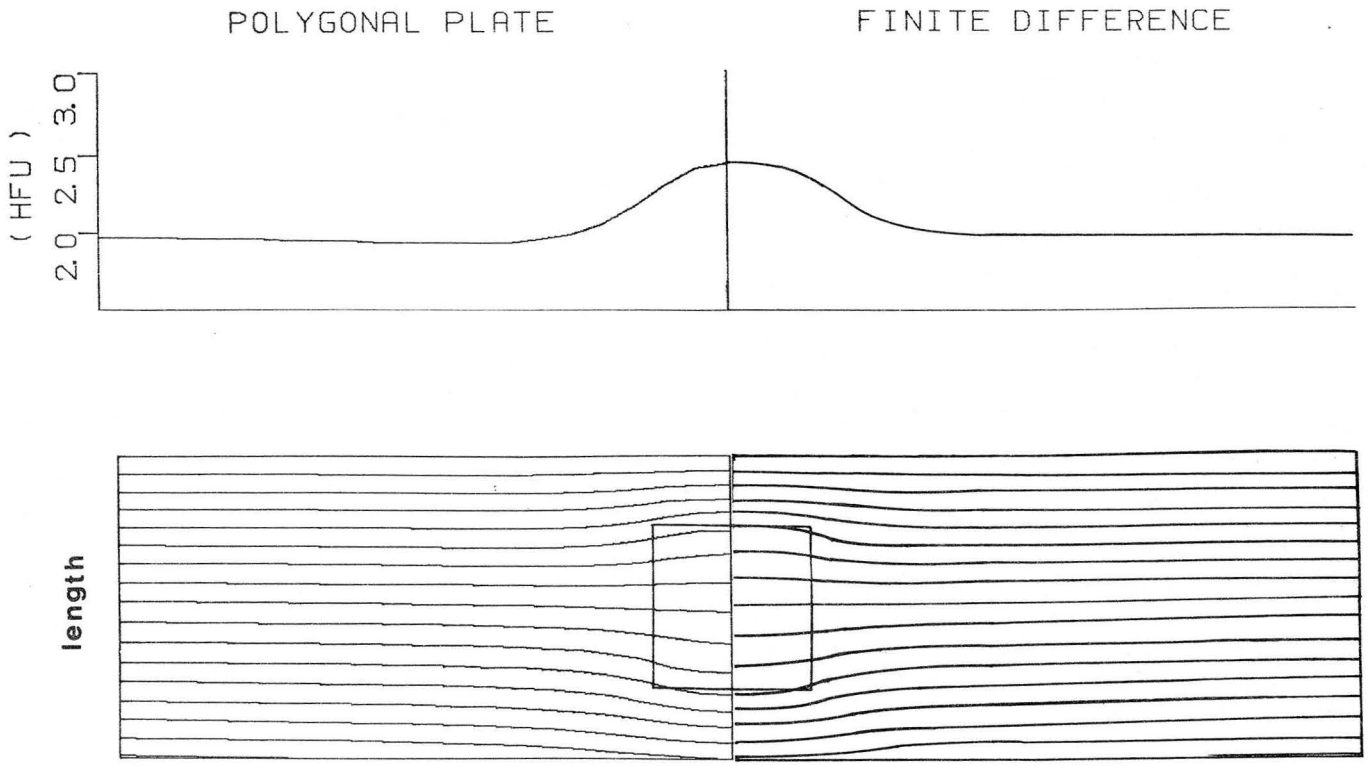

Figure 15 Comparison of the polygonal prism and finite difference approximations for a buried two-dimensional body with a 2:1 conductivity contrast. The length scale and contour interval are arbitrary. The polygonal prism model is shown in figure 16. The finite difference model is from MacKenzie (1965).

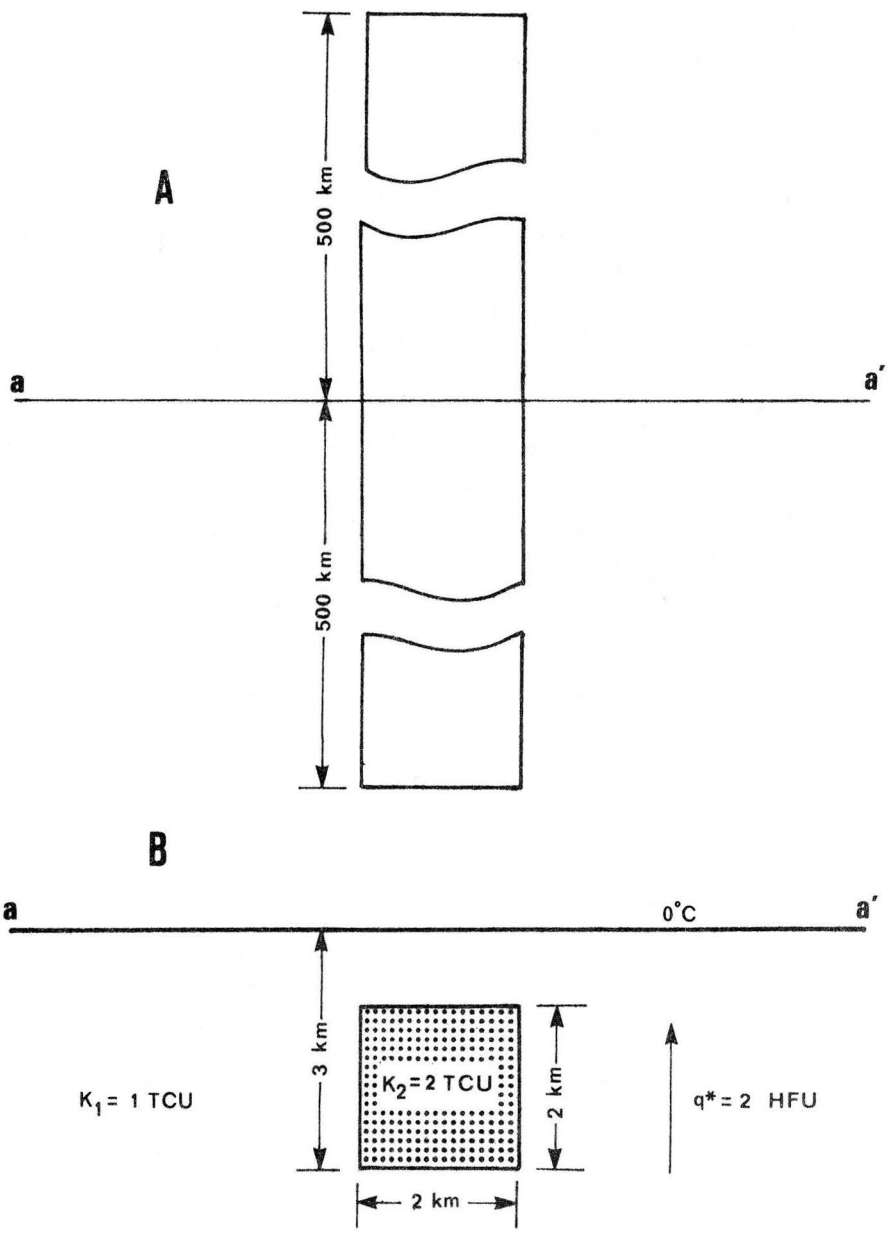

Figure 16 Polygonal prism model of the two-dimensional body of contrasting conductivity (fig. 15).

3.) $$- K \frac{\partial T}{\partial z}\Bigg|_{z \to \infty} = 1.0 \text{ HFU.}$$

The uniform flow condition that is placed at the base of the pluton in the finite difference model forces heat that would normally flow out the base of the pluton to flow toward the surface. This is unrealistic; it would be more accurate to place the uniform flow condition at a depth at which the isotherms are nearly horizontal.

MacKenzie (1965) used the finite difference method to compute temperature and heat flow in regions with two-dimensional variations in conductivity. Figure 15 shows the comparison between the finite difference method (MacKenzie, 1965, fig. 12 and 14) and the polygonal prism model shown in figure 16. As in the comparison with the exact solutions to the conductivity problem, the difference between the two approximate solutions is greatest at the boundary beteen the two media and improves with distance from the boundary.

Comparison With One-Dimensional Heat Conduction

Steady-state heat flow from an infinite slab of thickness D and heat production A is given by

$$q = A_2 D \qquad (30)$$

Surface heat flow on the axis of a vertical circular cylinder of thickness D, radius r, and heat production A is given by

$$q = (A_2-A_1)\left[(r^2+D^2)^{1/2} - (r+D)\right] + A_1D \tag{31}$$

The ratio of the heat flow from the cylinder and from the slab can be described by the dimensionless function $\sigma(\tau)$,

$$\sigma = \frac{A_2-A_1}{A_1D}\left[(r^2+D^2)^{1/2} - (r+D)\right] + \frac{A_1}{A_2}$$

$$\tau = \frac{2r}{D}. \tag{32}$$

This function provides a useful measure of the degree to which a tabular body of finite lateral extent can be considered an infinite slab. It can be used to estimate the error introduced by applying one-dimensional theory and as an approximate geometric correction factor. Figure 17 shows the variation of $\sigma(\tau)$ for 4 different heat production ratios. The aspect ratio required to attain less than 10% error with one-dimensional theory varies between 0 for a ratio of unity to 10 for a vanishing ratio. A similar relationship between heat flow from two-dimensional sources and slabs has been defined numerically for the special case

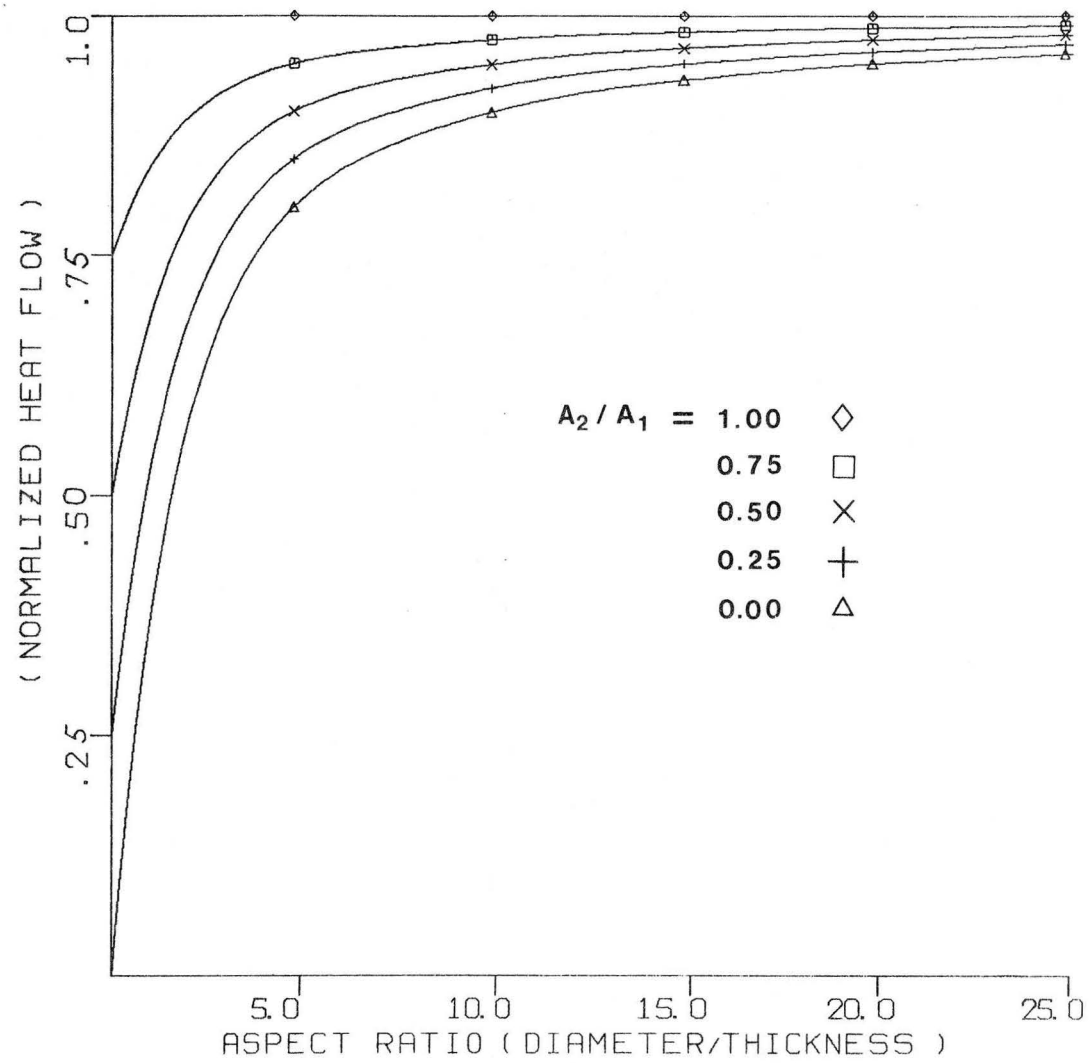

Figure 17 Normalized heat flow as a function of aspect ration for vertical cylinders with different heat production ratios. A1= heat production of the surrounding medium; A2= heat production of the cylinder.

of a country rock without heat production (Fehn et al., 1978).

A similar development can be used to describe the error in one-dimensional models resulting from lateral variations in conductivity. One-dimensional heat flow is not affected by vertical contrasts in conductivity. Hence, for the case of heat flow q* entering a layer of thickness D from beneath,

$$q = q^*. \tag{33}$$

The approximate surface heat flow on the axis of a cylinder of contrasting conductivity follows from equation (21),

$$q = q^* - \frac{3q^*(K_1-K_2)}{2K_2 + K_1} \left[\frac{D}{(r^2+D^2)^{1/2}} \right] \tag{34}$$

where

K = the conductivity of the half space;

K = the conductivity of the cylinder.

The ratio of equations (34) and (33) defines a function $\phi(\tau)$ which describes the error in one-dimensional models as a function of aspect ratio,

$$\phi = 1 - \frac{3(K_1-K_2)}{2K_1+K_2} \left[\frac{D}{(r^2+D^2)^{1/2}} \right], \qquad \tau = \frac{2r}{D}. \tag{35}$$

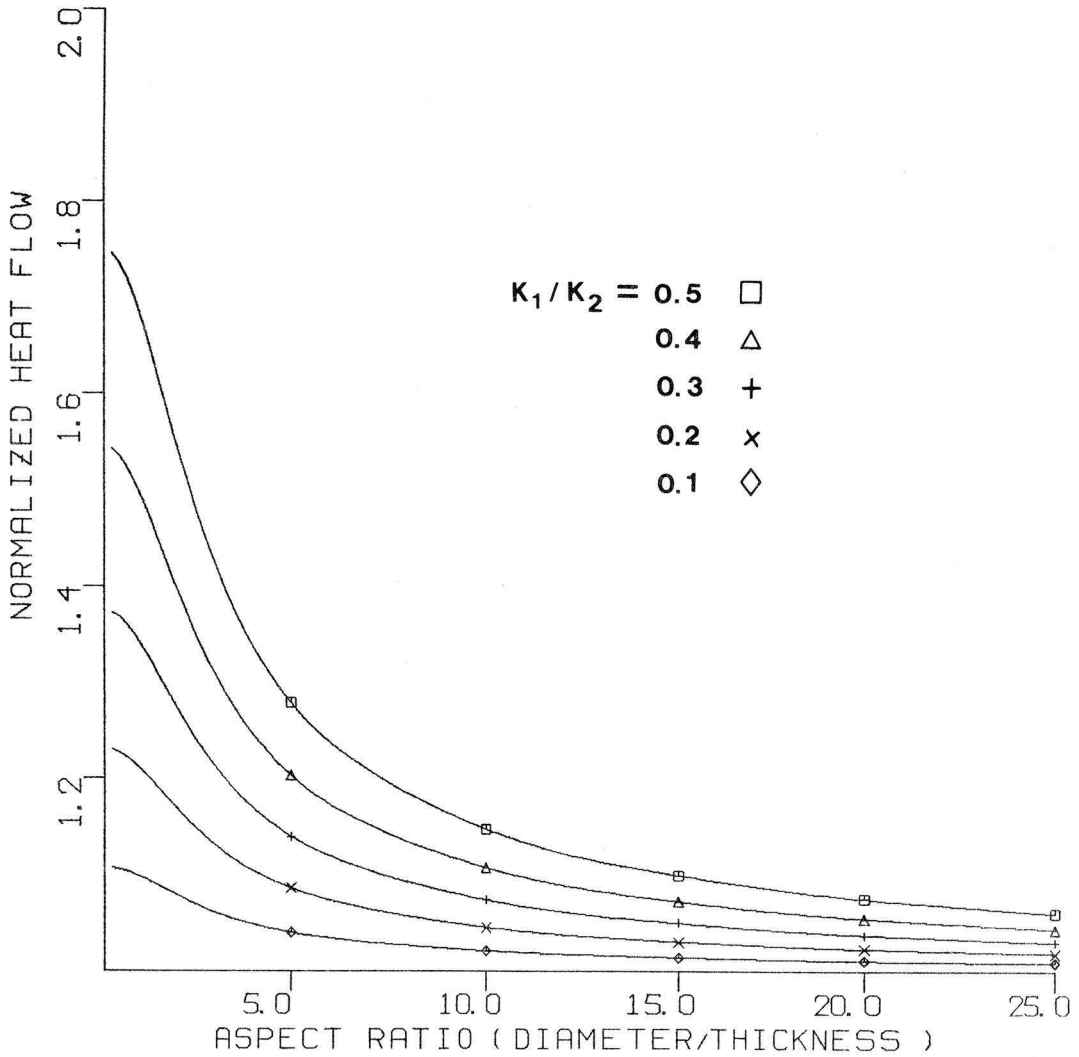

Figure 18 Normalized heat flow as a function of aspect ratio for vertical cylinders with different conductivity ratios. K1= conductivity of the surrounding medium; k2= conductivity of the cylinder.

The function $\phi(\tau)$ is graphed in figure 18 for 5 different conductivity ratios. The maximum aspect ratio that yields 10% error or less ranges from 2 for a conductivity ratio of 0.9 to 18 for a conductivity ratio of 0.5.

Figures 17 and 18 indicate that applicability of one-dimensional theory to three-dimensional sources is governed by the aspect ratio of the source and by the heat production and conductivity of both the source and the surrounding medium. For irregularly shaped bodies polygonal prism models can be used to generate sets of curves analogous to those in figures 17 and 18.

Half Space and Two-Layered Half Space Solutions

The temperature and heat flow fields associated with a cube in a half space and a cube in a two-layered half space are shown in figure 19. Differences can be seen in both temperature and surface heat flow fields. The maximum temperature at the depth of 2 km in the two-layered model is 96.7°C, which is 30°C higher than the regional field at 2 km. For the half space model, the maximum temperature at 2 km is 52.3°C, which is 19°C higher than the regional field at that depth.

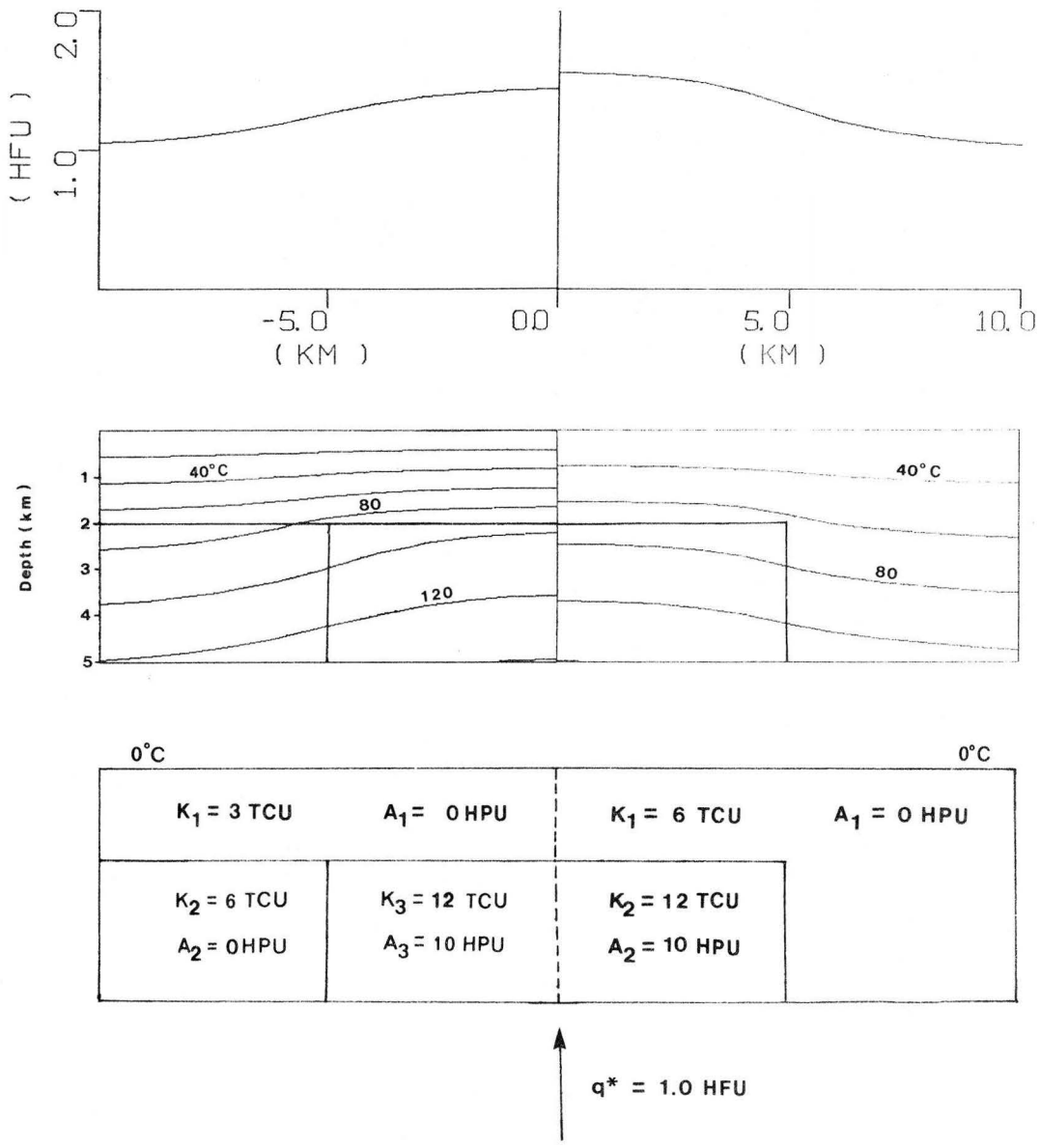

Figure 19 Comparison of half space and two-layered half space solutions for a buried cube.

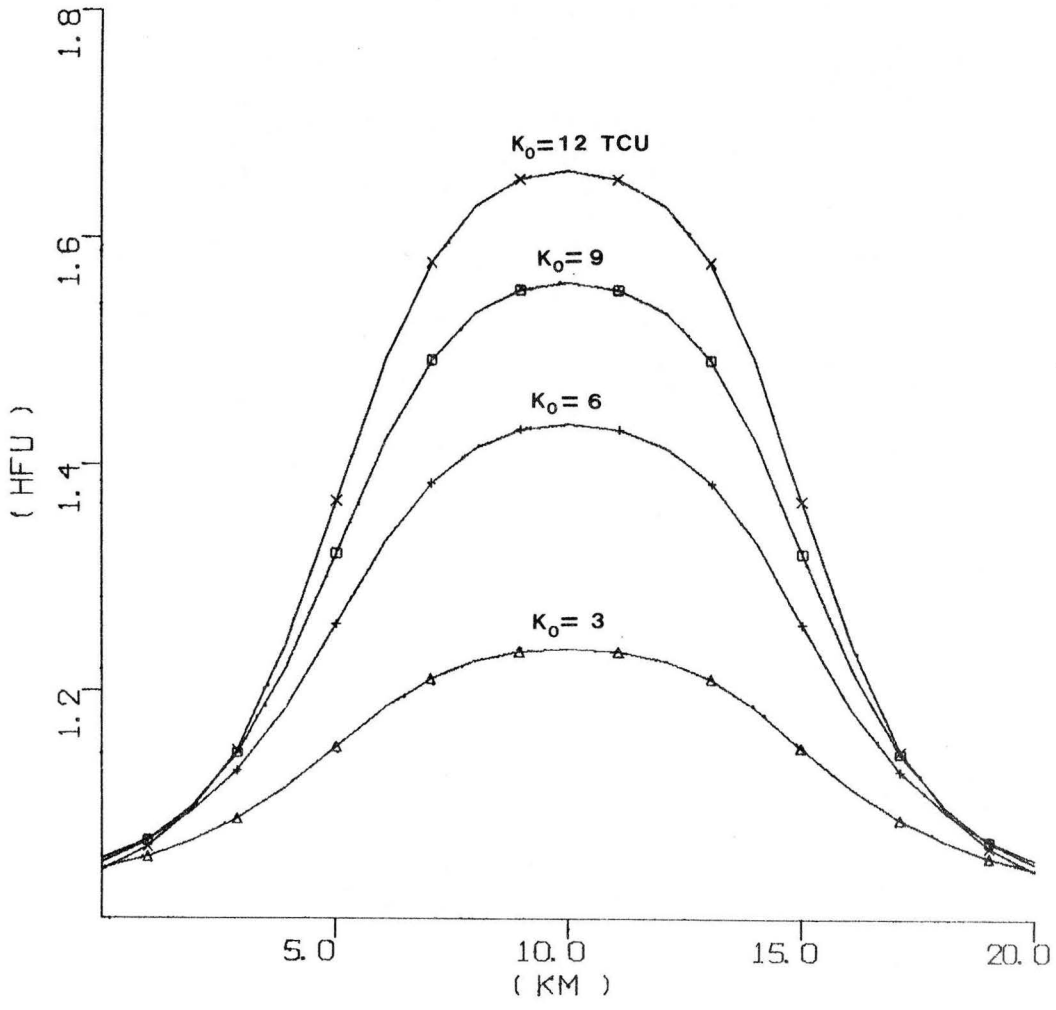

Figure 20 Heat flow anomalies over the two-layered half space model (fig. 19) for different first layer conductivities.

The surface heat flow anomaly over the two-layered model, shown in figure 19, is lower in amplitude than the anomaly over the half space model by as much as 28%. The rate at which heat is produced in the model region and the rate at which it flows in from below are the same in both models. More heat must flow laterally and downward in the two-layered model because of the insulating effect of the low conductivity layer. If the layer has a higher conductivity than the underlying material more heat flows toward the surface than in the half space model. This produces a larger heat flow anomaly over the same anomalous body. An example of this phenomenon is shown in figure 20 in which heat flow anomalies over the same anomalous body are given for different layer conductivities.

4. Interpretation of a Heat-Flow Anomaly

Heat flow anomalies can be modeled by using a trial-and-error method similar to that used in gravity and magnetic modeling. The heat production and conductivity of the body and surrounding medium and the regional heat flow field are normally estimated first. The geometry of the body is then varied until a satisfactory agreement between the observed field and theoretical field is reached. As in gravity and magnetic modeling the resulting solution is not unique, but is a member of a family of possible solutions.

To illustrate the modeling process a family of heat flow models has been prepared for the Rolesville batholith and adjacent Castalia pluton, in Franklin and Nash Counties North Carolina. Both bodies are coarse-grained granitic intrusions emplaced in metamorphic rocks of the Raleigh belt (fig. 21). The Raleigh belt has been interpreted as a south-plunging antiform and has a trend of increasing metamorphic grade from south to north (Farrar, 1980). Both characteristics suggest differential uplift and erosion between the southern and northern portions of the belt. The location of 5 heat flow stations in the area are shown in figure 22. The heat production, thermal conductivity, and heat flow at these sites are given in table 1 (Costain et

Table 1 Data from heat flow sites in the vicinity of the Rolesville batholith and Castalia pluton, from Costain et al, 1979).

Hole	Heat Production	Conductivity	Heat Flow
CS1	5.6 HPU	7.64 TCU	1.44 HFU
RL2	6.0	7.22	1.30
RL3	---	8.03	1.13
RL4	6.7	6.84	1.05
SB1	3.3	8.03	0.94

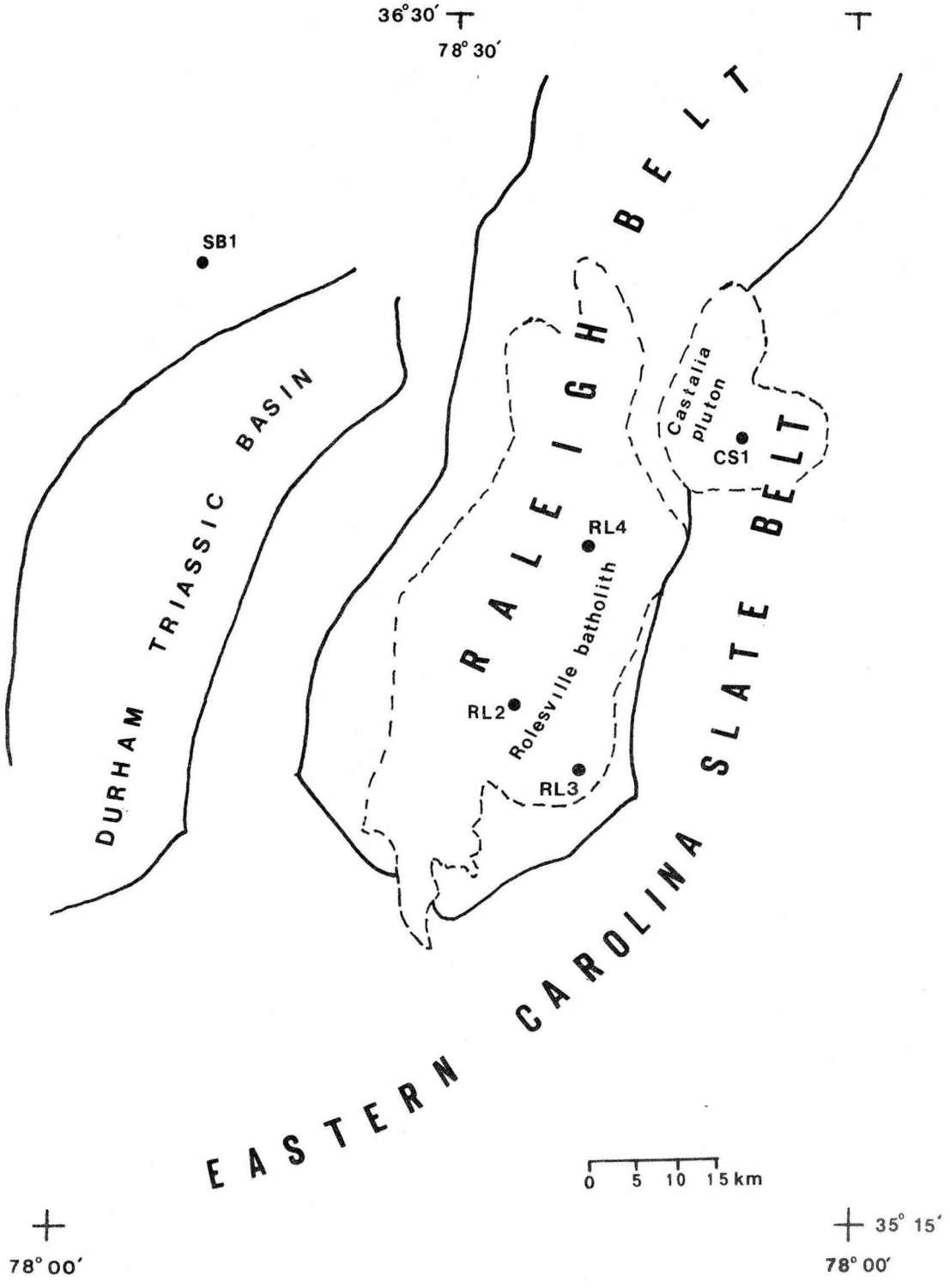

Figure 21 Geologic map of the Rolesville batholith and vicinity (simplified from Farrar, 1980). Dots indicate locations of heat-flow stations.

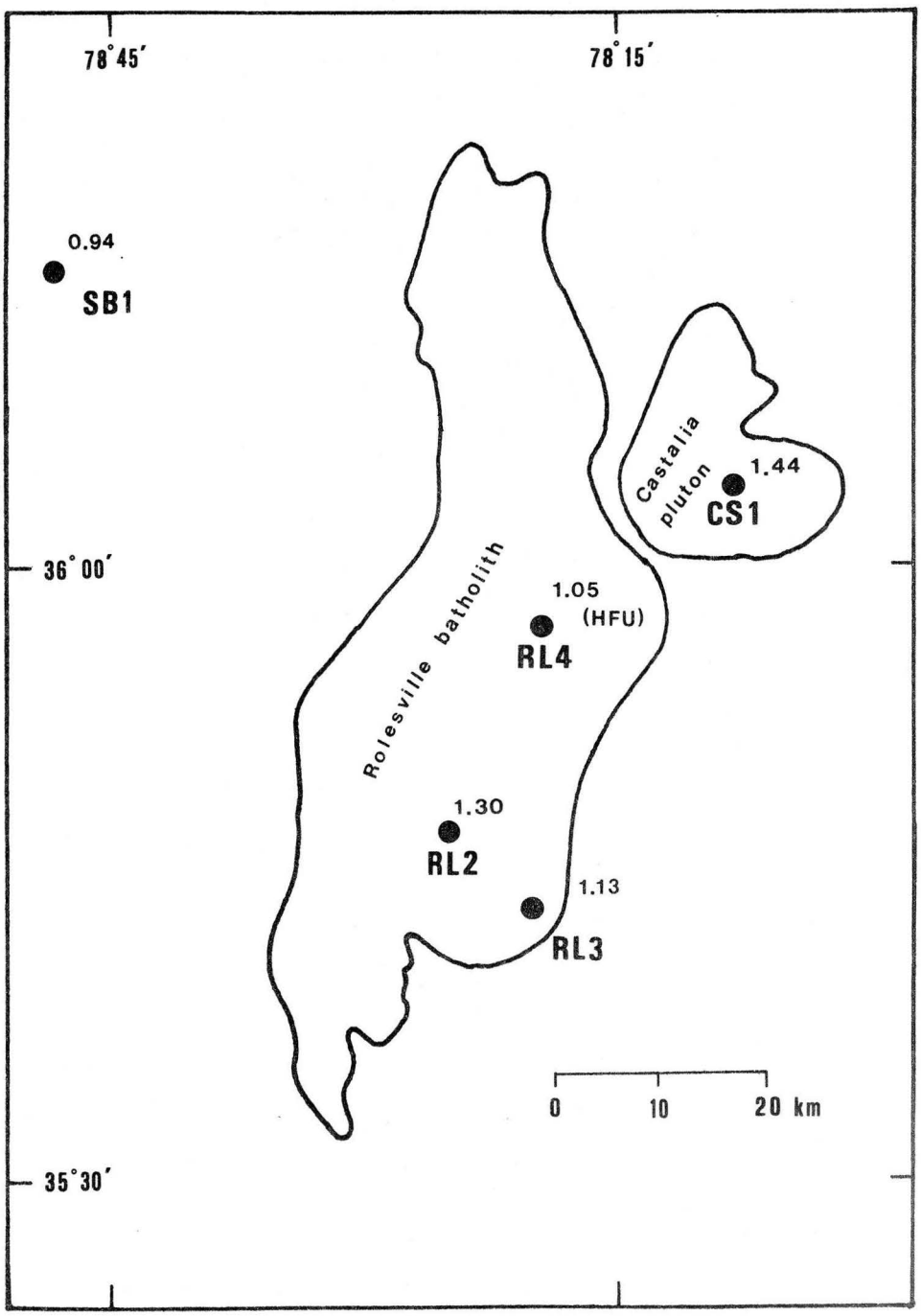

Figure 22 Heat flow in the vicinity of the Rolesville batholith (Costain et al, 1979).

al, 1979). Because there is no sedimentary layer in the region the problem was treated as a one-layered half space problem. At the time of this writing data for a two-layered case are not available.

The data in table 1 were collected as part of a study of heat flow and heat production for plutonic rocks. As a result heat production and thermal conductivity are relatively well determined for the granites but almost unknown for the country rock. In the current study a range of hypothetical country rock models was considered in order to determine if one-dimensional heat conduction theory applies to the region or if the three-dimensional aspects of the granitic bodies (so called edge effects) must be considered.

If the Rolesville batholith was emplaced before or during the deformation period, as Farrar (1980) suggests, erosion following the differential uplift would cause the body to be thickest down plunge. The lack of variation of heat production and conductivity at the surface of the batholith, despite the proposed differential erosion, suggests that these two parameters are nearly uniform throughout the body. In the heat-flow models both granites have a uniform heat production of 6.0 HPU and conductivity of 7.5 TCU.

The heat flow (0.94 HFU) at station SB1 in the volcanics of the adjacent Carolina Slate Belt is typical of background (country rock) heat flow in the southeastern United States (Costain et al, 1979). The heat flow from the lower crust and upper mantle in the southeastern United States is approximately 0.65 HFU (Costain and Perry, 1979). The regional heat flow field was then assumed to be made up of a 0.65 HFU component from the lower crust and upper mantle and a 0.29 HFU component derived from heat production in the upper crust. The heat production of non-granitic surface samples in the southeastern United States range from near 1.0 HPU to near 6.0 HPU (personal communication L. D. Perry, 1978). The average country rock heat production was assumed to fall in this range. The thermal conductivity if the country rock was assumed to be 6.5 TCU; this is a representative value for schist, gneiss, and volcanics (Clark, 1966) which are the dominant rock types of the Raleigh belt country rocks.

Four heat-flow models were developed which are consistent with the surface geology (fig. 21) and Farrar's structural interpretation and based on the 4 country rock heat production models shown in figure 23. Each of the country rock models produces the required 0.29 HFU contribution to the regional heat flow. The horizontal

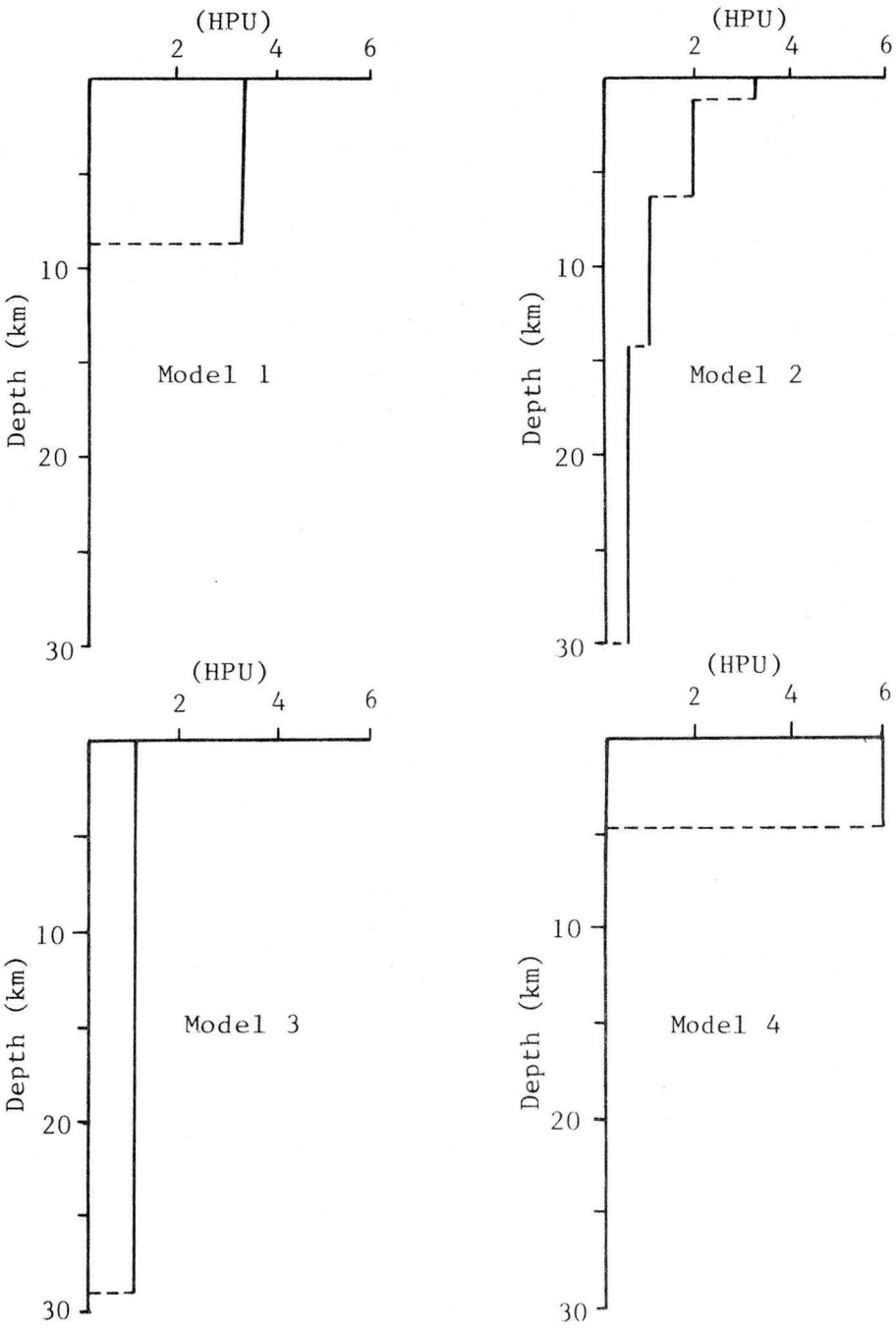

Figure 23 Vertical country rock heat production distributions for the four heat-flow models of the Rolesville batholith and Castalia pluton.

outlines of the prisms which make up the 4 heat-flow models are the same for each model (fig. 24). Only the vertical dimensions of the prisms were changed from model to model. Vertical dimensions for the prisms in models 1, 2, 3, and 4 are given in tables 2, 3, 4, and 5, respectively. The theoretical heat flow fields produced by the 4 models agree with the observed heat flow to within 2.5% at the 5 heat flow stations. The theoretical heat-flow fields for models 1 and 2 are shown in figures 25 and 26, respectively. Theoretical heat flow profiles and temperature cross-sections along lines A-A' and B-B' in the second model are shown in figure 27.

A comparison between the thicknesses of the polygonal prism models and granite thickness estimates based on one-dimensional heat conduction (Costain and Perry, 1979) is given in table 6. The model thicknesses are highly dependent on the lateral heat production contrast between the granite and the country rock. Heat conduction is then three-dimensional in the region and edge effects must be considered.

Model thicknesses are also expected to depend on the conductivity contrast between the granite and the country rock. The maximum heat-flow anomaly due to the conductivity contrast of 6.5 TCU to 7.5 TCU, for the 4 models considered

Table 2 Vertical dimensions of the polygonal prisms which make up heat flow model 1, of the Rolesville batholith and Castalia pluton.

Prism	Depth to Top	Depth to Base
1	0 km	1 km
2	1	10
3	10	20
4	0	2
5	2	8
6	8	22

Table 3 Vertical dimensions of the polygonal prisms which make up heat flow model 2, of the Rolesville batholith and Castalia pluton.

Prism	Depth to Top	Depth to Base
1	0 km	1 km
2	1	10
3	10	14
4	0	2
5	2	6
6	6	18

Table 4 Vertical dimensions of the polygonal prisms which make up heat flow Model 3, of the Rolesville batholith and Castalia pluton.

Prism	Depth to Top	Depth to Base
1	0 km	1 km
2	1	8
3	8	12
4	0	2
5	2	6
6	6	15

Table 5 Vertical dimensions of the polygonal prisms which make up heat flow Model 4, of the Rolesville batholith and Castalia pluton.

Prism	Depth to Top	Depth to Base
1	--	--
2	4.8 km	20 km
3	20	30
4	--	--
5	4.8	15
6	15	30

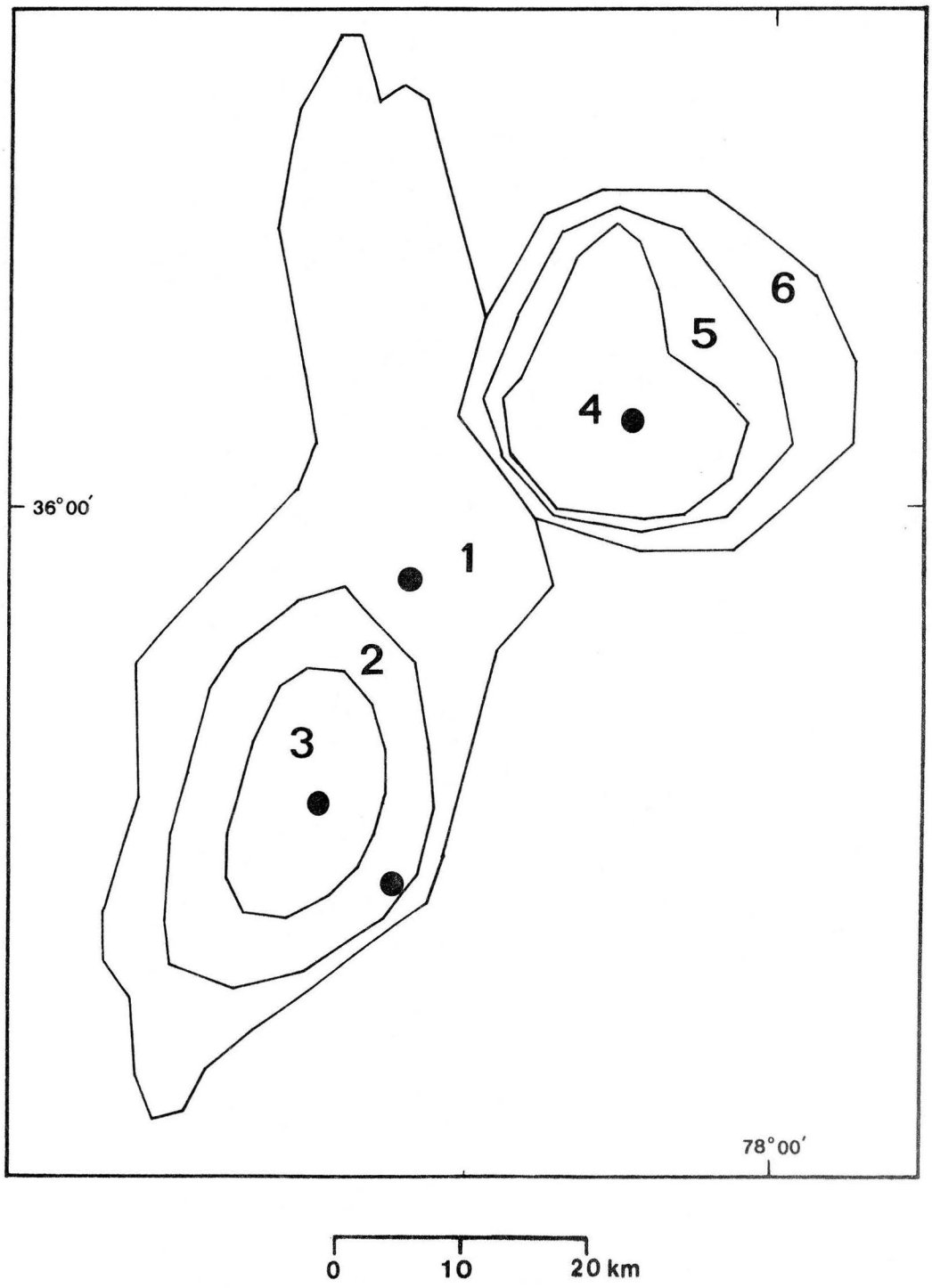

Figure 24 Outlines of the 6 prisms used to represent the Rolesville batholith and Castalia pluton in all four heat-flow models.

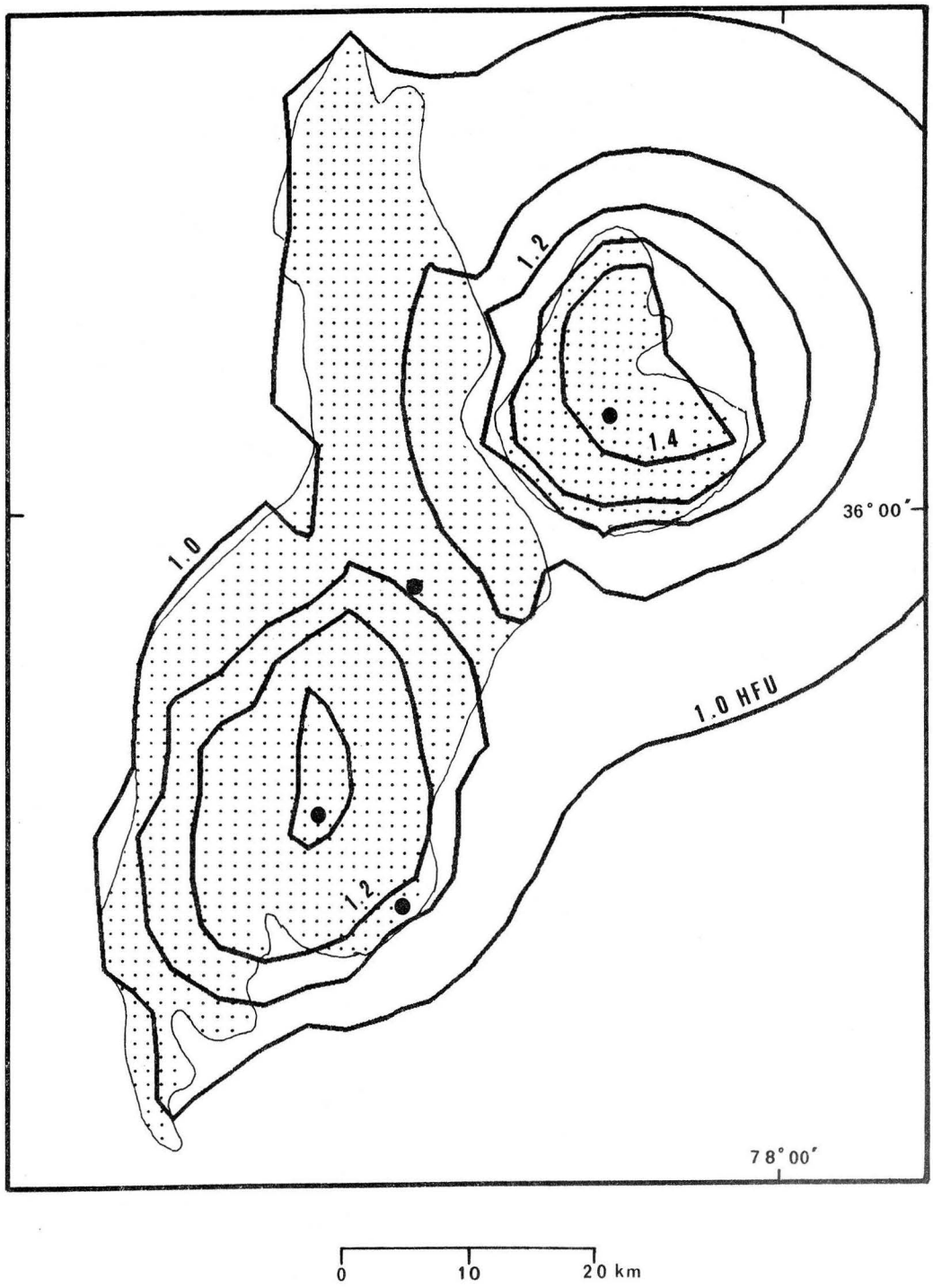

Figure 25 Theoretical heat flow map for Model 1 of the Rolesville batholith and Castalia pluton. The vertical country rock heat production distribution for Model 1 is given in figure 23. The polygonal prism model is shown in figure 24.

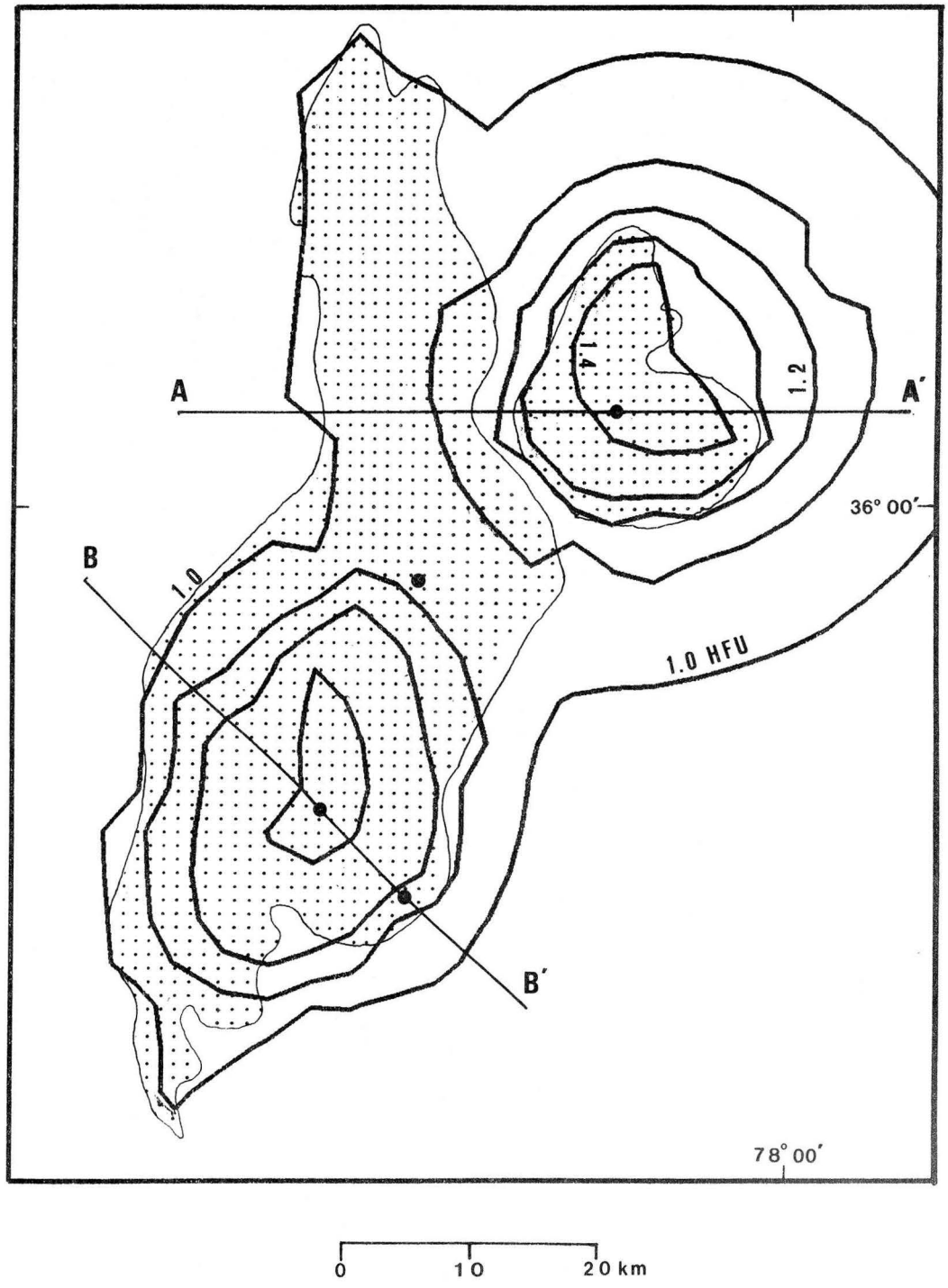

Figure 26 Theoretical heat flow map for Model 2 of the Rolesville batholith and Castalia pluton. The vertical country rock heat production distribution for Model 2 is shown in figure 23. The polygonal prism model is shown in figure 24.

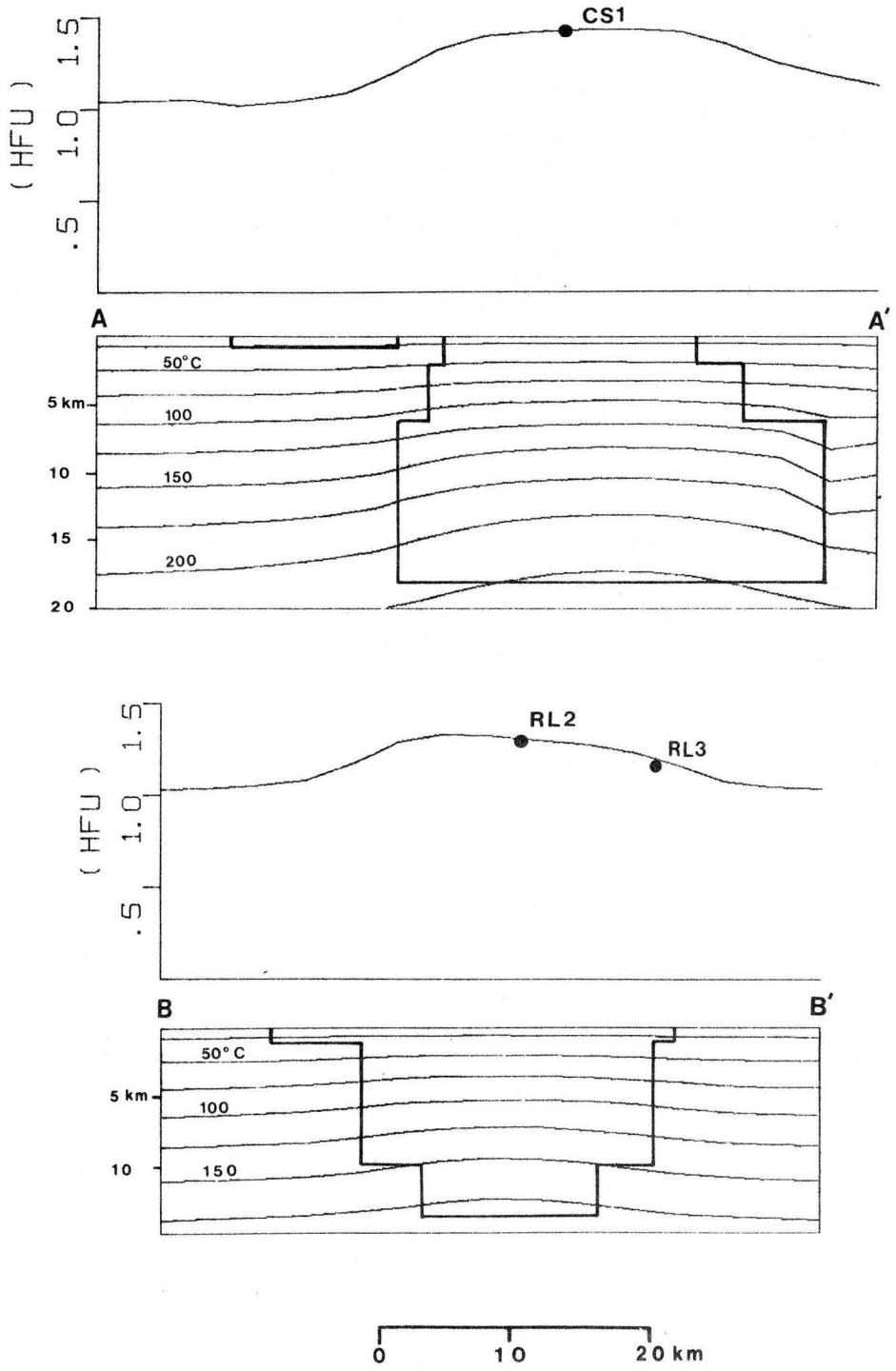

Figure 27 Theoretical heat flow profiles and temperature cross-sections for Model 2, along lines A-A and B-B (fig. 22 and 23).

is 0.11 HFU. If the average conductivity of the country rock is greater than 6.5 the model thicknesses (table 6) would have to be increased to explain the observed heat flow. If the average conductivity is less than 6.5 thiner models could be used to explain the observed heat flow.

In all 4 polygonal prism models the Rolesville batholith is thickest in the south and thins northward. This northward thinning is consistent with the structural interpretation given by Farrar (1980). The large difference in the thicknesses of the Castalia pluton and the northern part of the Rolesville batholith is not supported by the gravity expression of the two bodies, however. The Bouguer gravity map of the model region (Cogbill, 1978) (fig. 28) shows a -30 mgal anomaly at the site of RL4, where the heat flow is 1.05 HFU and the models are all 1 km thick. There is also a -30 mgal anomaly at the site of CS1, where the heat flow is 1.44 HFU and the models are 15 km to 30 km thick. Simmons (1967) gives the relationship between the vertical heat flow and gravity anomalies at the surface, caused by volume sources with both contrasting density ρ and heat production A

$$q = GA/2\pi\gamma\rho.$$

Table 6 Thicknesses of one- and three-dimensional models of the Rolesville batholith and Castalia pluton at 3 heat flow stations. The thicknesses given by one-dimensoional analysis are from Costain and Perry (1979).

Model	Model Thickness at Stations CS1	RL2	RL4
Model 1	22 km	20 km	1 km
Model 2	18	14	1
Model 3	15	12	1
Model 4	30	30	1
1-D Model	14	11	6

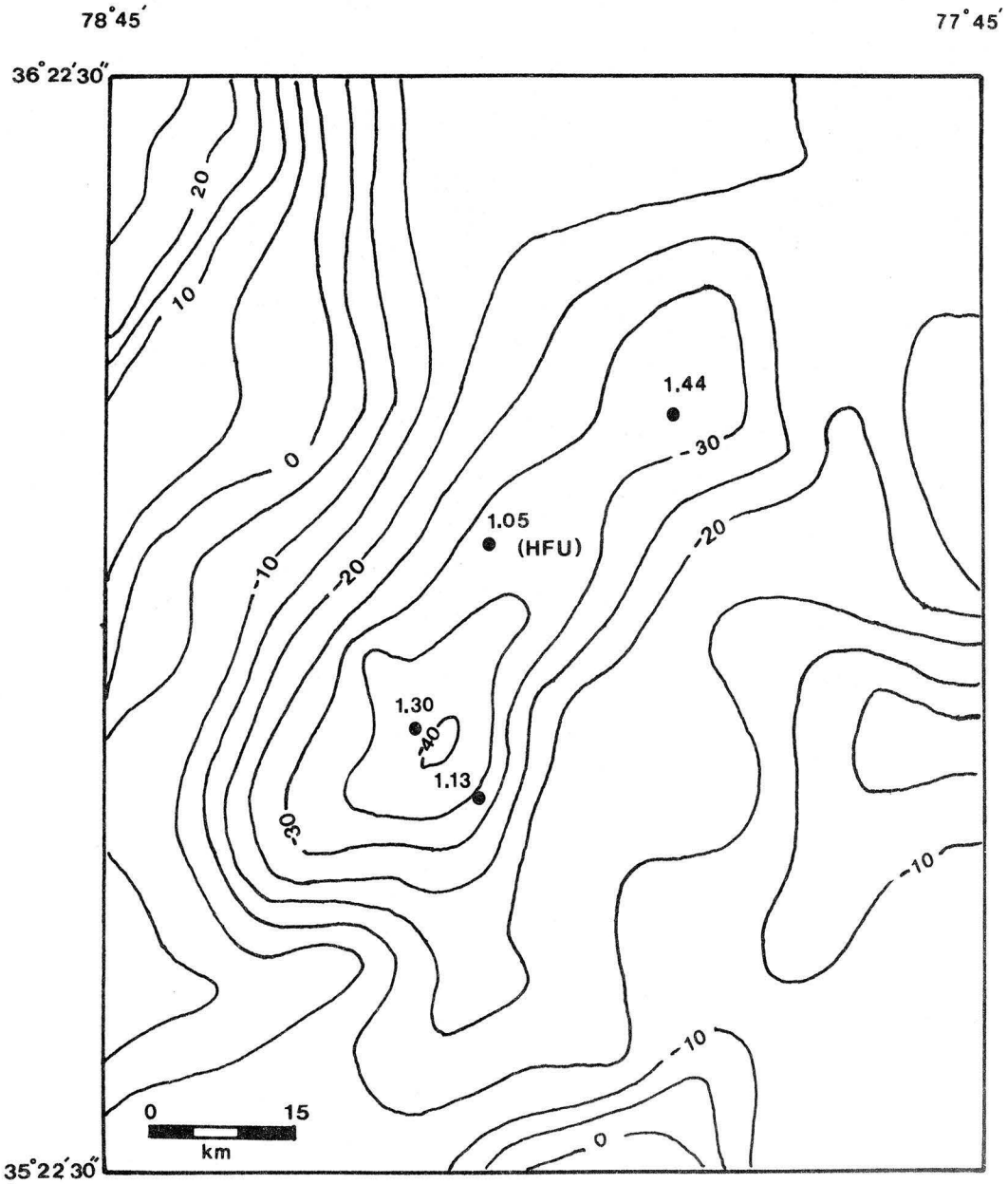

Figure 28 Bouguer gravity field (contoured in mgal) (from Cogbill, 1979) and heat flow (HFU) (from Costain and Perry, 1979) in the vicinity of the Rolesville batholith; dots indicate locations of heat-flow stations.

Heat flow varies significantly between stations RL3 and CS1 but the gravity field does not. It can be concluded that variations in gravity and heat flow over the model region cannot be explained by sources with the same shapes. A possible explanation can be found in the low density country rock in which the batholith was emplaced. In hand specimen, the densities of the dominant metamorphic rock types in the Raleigh belt are not significantly different from the density of the main phase of the Rolesville granite. The gravity field is then indicative of the thickness of the entire Raleigh belt rather than the thickness of the granite alone. The heat flow field would reflect only the thickness of the granite.

5. Discussion

New analytical solutions have been developed for temperature and heat-flow anamolies caused by a polygonal prism source in a two-layered half space. An approximate solution to the problem of a polygonal prism with contrasting conductivity in a two-layered half space was also given. In section 3 a comparison was made between the exact and approximate heat flow over an infinte semi-circular cylinder of contrasting conductivity. The two heat flow fields agree to within 5% for conductivity ratios between 0.25 and 1.5. Comparing this error range with that for a semi-spheroid of contrasting conductivity indicates that the error level does not change rapidly with changes in the shape of the anomalous body. A survey of thermal conductivities of different rocks types (Clark, 1966) suggests that this range of conductivity ratios is sufficient for modeling many geologic problems. The uncertainty in the 5 heat flow values (table 1) used in section 4 is about 0.05 HPU or approximately 10% of the total heat flow anomaly in this region. This error level is typical of other heat flow determinations made in crystalline rocks (Costain and Perry, 1979). The 5% error level in the component of heat flow due to contrasts in thermal conductivity is then not excessive.

In section 4 the modeling technique based on these solutions was used to interpret a localized heat flow anomaly. The interpretation was carried out in the same way a gravity anomaly would be analyzed using Plouff's method (1976). Temperature on cross-sections through the model region was estimated by computing the temperature field associated with the heat-flow model. This method of estimating the amplitude and spacial extent of temperature anomalies could be useful in the exploration for low-temperature geothermal resources.

The modeling technique is also applicable to regional heat flow studies. In many regional studies (see for example Roy et al, (1968), Lachenbruch (1970), and Costain and Perry (1979)), one-dimension heat conduction is assumed. Lateral variations in heat production and conductivity cause deviations from one-dimensional conduction. The modeling technique presented in this study can be used to estimate the heat flow effects of variations in heat production and conductivity in the vicinity of a heat flow station. The heat flow value can then be adjusted accordingly.

These problems can also be solved with numerical techniques such as the method of finite differences. The disadvantage of these methods is that temperatures must be

found everywhere in the model region simultaneously. As a result computer storage requirements of detailed three-dimensional models can exceed the space available at most computer installations. As an example, the maximum available storage on the IBM 370/158 at V.P.I. & S.U. is 3 megabytes under normal operating conditions. This limits the maximum number of nodes that can be considered while using the finite difference heat conduction program TRUMP (Edwards, 1969) to approximately 4000. The largest three-dimensional mesh that can be considered is then 20 by 20 by 10 nodes. Computation time requirements can also become prohibitive, particularly when trial-and-error fitting methods are used. In the modeling technique presented in this study unknowns are calculated at points of interest only. Storage requirements are therefore not a problem. The modeling technique is also computationally efficient; the heat flow models of the Rolesville batholith and Castalia pluton in section 4 required 0.26 msec computation time per field point per polygonal edge on an IBM 370/158 computer.

References Cited

Carslaw, H. S., and Jaeger, J. C., 1959, Conduction of heat in solids: Oxford, Clarence Press, 510 p.

Clark, S. P., 1966, Thermal Conductivity: The Geological Society of America Memoir 97, section 21, p. 459-482.

Cogbill, A. H., 1978, Gravity data in the southeast United States: Progress report VPI&SU-5648-3 J. K. Costain, L. Glover III and A. K. Sinha, DOE contract no. ET-78-C-05-5648, p. c65-c110.

Costain, J. K., Glover II, l., and Sinha, A. K., 1979, Research objectives: Progress report VPI&SU-5648-5, DOE contract no. ET-78-C05-5648, p. 10-11.

Costain, J. K., Perry, L. D., Dashevsky, S., Mclung, W. S., and Higgins, S. P., 1979, Heat flow and heat generation: Progress report VPI&SU-5648-5 J. K. Costain, L. Glover III, A. K. Sinha, DOE contract no. ET-78-C-05-5648, p. c139-c153.

Costain, J. K., and Perry L. D., 1979, Linear relationship between heat flow and heat generation: Progress report VPI&SU-5648-5 J. K. Costain, L. Glover and A. H. Sinha, DOE contract no. ET-78-C-05-5648, p. c154-c157.

Dwight H. B., 1957, Tables of intergrals and other mathematical data: New York, New York, Macmillan Publishing Co. Inc., 336 p.

Edwards A. L., (1969), TRUMP: a computer program for transient and steady-state temperature distributions in multidimensional systems; NTIS publication UCRL-14754 Rev. II, 257 p.

Farrar S. S., 1980, The Raleigh block: a preliminary interpretation of the northeastern piedmont of North Carolina (in preparation) : Progress report VPI&SU-5648-6 J. K. Costain, L. Glover and A. H. Sinha, Doe contract no. ET-78-C-05-5648.

Fehn, U., Cathles, L. M., and Holland, H. D., 1978, Hydrothermal convection and uranium deposits in abnormally radioactive plutons: Economic Geology, v. 73, p. 1556-1566.

Haaz, I. B., 1953, Relations between the potential of the attraction of the mass contained in a finite retangular prism and its first and second derivatives (in Hungarian): Geofizikai Kozlemeyek, v. 2, no. 7, p. 57-66.

Kellogg, O. D., 1929, Foundations of potential theory: Berlin, Julius Springer, 384 p.

Lachenbruch, A. H., 1968, Preliminary geothermal model of the Sierra Nevada: Journal of Geophysical Reseach, v. 73, no. 22, p. 6977-6989.

---------, 1970, Crustal temperature and heat production: implications of the linear heat-flow relation: Journal of Geophysical Reseach, v. 75, no. 17, p. 3291-3300.

Lee, T., and Henyey, T., 1974, Heat flow refraction across dissimilar media, Geophysical Journal, v. 39, no. 2, p. 319-333.

MacKenzie, M. V., 1967, A digital computer model of terrestrial heat flow refraction: Unpublished masters thesis, University of Utah.

Plouff, D., 1976, Gravity and magnetic fields of polygonal prisms and applications to magnetic terrain corrections: Geophysics, v. 41, no. 4, p. 727-741.

Roy, R. F., Blackwell, D. D., and Birch, F., 1968, Heat generation of plutonic rocks and continental heat flow provinces: Earth and planetary science letter, v. 5, p. 1-12.

Simmons, G., 1967, Interpretation of heat flow anomalies 1. contrasts in heat production: Reviews of Geophysics, v. 5, no. 1, p. 43-52.

Talwani, M., 1965, Computation with the help of a digital computer of magnetic anomalies caused by bodies of arbitrary shape: Geophysics, v. 30, p. 797-817.

Talwani, M., and Ewing M., 1960, Rapid compution of gravitation attraction of three-dimensional bodies of arbitrary shape, Geophysics, v. 25, no. 1, p. 203-225.

Thomas, B. G., 1972, Calculus and analytic geometry, Philippines, Addison-Wesley Publishing Co. Inc., 1034 p.

```
C-----------------------------------------------------------------C
      SUBROUTINE TIMAGE(L,N,FX,FY,FZ,ZOBS,M,BX,BY,TOP,BASE,
     &H,HPC,QSTAR,K0,K1,K2,NT,RI,T,W1,W2,W3)
C-----------------------------------------------------------------C
C
C     SUBROUTINE TO COMPUTE THE TEMPERATURE ANOMALY CAUSED
C     BY A POLYGONAL PRISM  OF CONTRASTING HEAT PRODUCTION
C     AND THERMAL CONDUCTIVITY IN A TWO-LAYERED HALF SPACE.
C     THE PROGRAM IS BASED ON EQUATIONS (21) AND (24).
C
C
C     COORDINATE SYSTEM
C
C     A LEFT HANDED COORDINATE SYSTEM IS USED WITH THE ORIGIN
C     AT THE SURFACE AND THE Z AXIS POSITIVE DOWN.
C
C                          *
C                        Y *
C                        *
C                      * * * * *
C                      *   X
C                    Z *
C                      *
C                      *
C
C
C     UNITS
C
C     THE UNITS OF ALL ARGUMENTS ARE ASSUMED TO BE CONSISTENT IN
C     THE DIMENSIONS OF ENERGY, LENGTH, TIME, AND TEMPERATURE.
C     FOR EXAMPLE IF ENERGY IS IN CALORIES, LENGTH IS IN KILOMETERS,
C     TIME IS IN SECONDS, AND TEMPERATURE IN DEGREES CENTIGRADE
C     THEN THERMAL CONDUCTIVITY MUST BE GIVEN IN
C     CAL/KM-SEC-DEGREE C.
C
C
C     ARGUMENTS
C
C     L=THE NUMBER OF CONDUCTIVITY LAYERS IN THE MODEL, (1 OR 2).
C     N= THE NUMBER OF FIELD POINTS AT WHICH THE TEMPERATURE WILL
C     BE COMPUTED.
C     FX,FY= ARRAYS OF LENGTH N CONTANING THE X,Y COORDINATES
C     OF THE FIELD POINTS.  ALL FIELD POINTS ARE ASSUMED TO BE
C     AT A COMMON DEPTH = ZOBS.
C     FZ= A WORK ARRAY OF LENGTH N.
C     BX,BY= ARRAYS OF LENGHT M CONTAINING THE X,Y COORDINATES
```

```
C      OF THE CORNER POINTS IN CLOCKWISE ORDER AROUND THE PRISM.
C      NOTE:  THE LAST CORNER POINT MUST COINCIDE WITH THE FIRST;
C      THAT IS, BX(M)=BX(1) AND BY(M)=BY(1).
C      TOP, BASE= THE Z COORDINATE OF THE TOP AND BASE OF THE PRISM.
C      H = THE DEPTH TO THE BASE OF THE FIRST CONDUCTIVITY
C      LAYER.  IF L = 1 H IS NOT USED.
C      HPC= THE HEAT PRODUCTION CONTRAST BETWEEN THE PRISM AND THE
C      SURROUNDING MEDIUM.
C      QSTAR= THE UNIFORM HEAT FLOW ENTERING THE BASE OF THE MODEL REGION.
C      K0= THE CONDUCTIVITY OF THE FIRST CONDUCTIVITY LAYER.
C      IF L = 1 K0 IS NOT USED.
C      K1= THE CONDUCTIVITY OF THE SECOND CONDUCTIVITY LAYER.
C      K2= THE CONDUCTIVITY OF THE PRISM.
C      NT= THE NUMBER OF TERMS TO BE KEPTED IN THE SERIES SOLUTION.
C      T= THE DOUBLE PRECISION ARRAY OF LENGTH N IN WHICH THE COMPUTED
C      TEMPERATURE VALUES ARE RETURNED TO THE MAIN PROGRAM.
C      RI= THE MAXIMUM SERIES TRUNCATION ERROR IN THE TEMPERATURE
C      VALUES RETURNED.
C      W1,W2,W3= DOUBLE PRECISION WORK ARRAYS OF DIMENSION N.
C
C
C      SUBROUTINES REQUIRED
C
C      SUBROUTINE CHI:  COMPUTES THE CHI FUNCTION FOR A POLYGONALY PRISM.
C
C      SUBROUTINE PSI:  CUMPUTES THE FUNCTION PSI FOR A POLYGONAL PRISM.
C
C
      DOUBLE PRECISION T(N),W1(N),W2(N),W3(N),PI,W1MAX,W2MAX,
     1A,B,C,C1,C3,CA,CK
      DIMENSION FX(N),FY(N),FZ(N),BX(M),BY(M)
      REAL K0,K1,K2
      PI=DATAN(1.0D0)*4.0D0
      CA=HPC/(PI*4.0D0)
      CK=3.0D0*QSTAR*DBLE(K2-K1)/(4.0D0*PI*DBLE(2.0*K1+K2))
      DO 1 I=1,N
    1 FZ(I)=ZOBS
C     COMPUTE THE EFFECT OF THE SOURCE POLYGON.
      CALL CHI(N,FX,FY,FZ,M,BX,BY,TOP,BASE,W1,W3)
      CALL PSI(N,FX,FY,FZ,M,BX,BY,TOP,BASE,W2,W3)
C     NOW ADDED THE EFFECT OF THE CORRECT SERIES OF IMAGES
C     TO THE EFFECT OF THE SOURCE, TO COMPLETE THE SOLUTION.
      IF(L.EQ.1) GO TO 100
      IF(K0.EQ.K1) GO TO 100
C     IF THIS LINE IS REACHED THE MODEL HAS TWO LAYERS.
      H2=H*2.0
      H2M=-H2
      B=DBLE(K0+K1)
      TEST=H-ZOBS
      IF(TEST.GT.0.0) GO TO 40
```

```
C       START OF THE SERIES FOR THE LOWER LAYER OF THE TWO LAYER CASE.
        A=DBLE(K0-K1)
        C=1.0D0/DBLE(K1)
        DO 10 I=1,N
   10   T(I)=C*(CA*W1(I)+CK*W2(I))
        CALL CHI(N,FX,FY,FZ,M,BX,BY,H2-TOP,H2-BASE,W1,W3)
        CALL PSI(N,FX,FY,FZ,M,BX,BY,H2-TOP,H2-BASE,W2,W3)
        C1=A/B
        C=-C*C1
        DO 20 I=1,N
   20   T(I)=T(I)+C*(CA*W1(I)-CK*W2(I))
        C=4.0D0*DBLE(K0)*C1/(A*A)
        C2=2.0D0/(A*A*DLOG(DABS(B/A)))
        C1=-C1
        DO 30 I=1,NT
        C2=C2*C1
        C=C*C1
        Z=H2M*(I-1)
        CALL CHI(N,FX,FY,FZ,M,BX,BY,Z-TOP,Z-BASE,W1,W3)
        CALL PSI(N,FX,FY,FZ,M,BX,BY,Z-TOP,Z-BASE,W2,W3)
        W1MAX=DABS(W1(1))
        W2MAX=DABS(W2(1))
        DO 30 J=1,N
        IF(W1MAX.LT.DABS(W1(J))) W1MAX=DABS(W1(J))
        IF(W2MAX.LT.DABS(W2(J))) W2MAX=DABS(W2(J))
   30   T(J)=T(J)+C*(CA*W1(J)-CK*W2(J))
        RI=C2*(DABS(CA*W1MAX)+DABS(CK*W2MAX))
        RETURN
   40   CONTINUE
C       START OF THE SERIES FOR THE UPPER LAYER IN THE TWO LAYER CASE.
        A=DBLE(K0-K1)
        C=2.0D0/B
        C1=A/B
        C2=2.0D0/(PI*B*DLOG(DABS(A/B)))
        DO 50 I=1,N
   50   T(I)=C*(CA*W1(I)+CK*W2(I))
        CALL CHI(N,FX,FY,FZ,M,BX,BY,-TOP,-BASE,W1,W3)
        CALL PSI(N,FX,FY,FZ,M,BX,BY,-TOP,-BASE,W2,W3)
        DO 60 I=1,N
   60   T(I)=T(I)+C*(CK*W2(I)-CA*W1(I))
        C=C1*C1*2.0/A
        DO 90 I=1,NT
        C2=C2*C1
        Z=H2M*FLOAT(I)
        CALL CHI(N,FX,FY,FZ,M,BX,BY,Z-TOP,Z-BASE,W1,W3)
        CALL PSI(N,FX,FY,FZ,M,BX,BY,Z-TOP,Z-BASE,W2,W3)
        W1MAX=DABS(W1(1))
        W2MAX=DABS(W2(1))
        DO 70 J=1,N
        IF(W1MAX.LT.DABS(W1(J))) W1MAX=DABS(W1(J))
```

```
      IF(W2MAX.LT.DABS(W2(J))) W2MAX=DABS(W2(J))
   70 T(J)=T(J)+C*(CA*W1(J)-CK*W2(J))
      C=-C
      Z=H2*FLOAT(I)
      CALL CHI(N,FX,FY,FZ,M,BX,BY,Z+TOP,Z+BASE,W1,W3)
      CALL PSI(N,FX,FY,FZ,M,BX,BY,Z+TOP,Z+BASE,W2,W3)
      DO 80 J=1,N
   80 T(J)=T(J)+C*(CA*W1(J)+CK*W2(J))
      RI=C2*(DABS(W1MAX)+DABS(W2MAX))
      C=C*C1
   90 CONTINUE
      RETURN
  100 CONTINUE
C     START OF THE ONE-LAYER CASE.
      C=1.0D0/DBLE(K1)
      DO 110 I=1,N
  110 T(I)=C*(CA*W1(I)+CK*W2(I))
      CALL CHI(N,FX,FY,FZ,M,BX,BY,-TOP,-BASE,W1,W3)
      CALL PSI(N,FX,FY,FZ,M,BX,BY,-TOP,-BASE,W2,W3)
      DO 120 I=1,N
  120 T(I)=T(I)+C*(CK*W2(I)-CA*W1(I))
      RETURN
      END
```

```
C-----------------------------------------------------------------------C
      SUBROUTINE QIMAGE(L,N,FX,FY,FZ,ZOBS,M,BX,BY,TOP,BASE,
     &H,HPC,QSTAR,KO,K1,K2,NT,RI,Q,W1,W2,W3)
C-----------------------------------------------------------------------C
C
C     SUBROUTINE TO COMPUTE THE HEAT-FLOW ANOMALY CAUSED
C     BY A POLYGONAL PRISM  OF CONTRASTING HEAT PRODUCTION
C     AND THERMAL CONDUCTIVITY IN A TWO-LAYERED HALF SPACE.
C     THE PROGRAM IS BASED ON EQUATIONS (21) AND (24).
C
C
C     COORDINATE SYSTEM
C
C     A LEFT HANDED COORDINATE SYSTEM IS USED WITH THE ORIGIN
C     AT THE SURFACE AND THE Z AXIS POSITIVE DOWN.
C
C                          *
C                        Y *
C                        *
C                      * * * * *
C                      *   X
C                    Z *
C                      *
C                      *
C
C
C     UNITS
C
C     THE UNITS OF ALL ARGUMENTS ARE ASSUMED TO BE CONSISTENT IN
C     THE DIMENSIONS OF ENERGY, LENGTH, TIME, AND TEMPERATURE.
C     FOR EXAMPLE IF ENERGY IS IN CALORIES, LENGTH IS IN KILOMETERS,
C     TIME IS IN SECONDS, AND TEMPERATURE IN DEGREES CENTIGRADE
C     THEN THERMAL CONDUCTIVITY MUST BE GIVEN IN
C     CAL/KM-SEC-DEGREE C.
C
C
C     ARGUMENTS
C
C     L=THE NUMBER OF CONDUCTIVITY LAYERS IN THE MODEL, (1 OR 2).
C     N= THE NUMBER OF FIELD POINTS AT WHICH THE HEAT FLOW WILL
C     BE COMPUTED.
C     FX,FY= ARRAYS OF LENGTH N CONTANING THE X,Y COORDINATES
C     OF THE FIELD POINTS.  ALL FIELD POINTS ARE ASSUMED TO BE
C     AT A COMMON DEPTH = ZOBS.
C     BX,BY= ARRAYS OF LENGHT M CONTAINING THE X,Y COORDINATES
C     OF THE CORNER POINTS IN CLOCKWISE ORDER AROUND THE PRISM.
C     NOTE:  THE LAST CORNER POINT MUST COINCIDE WITH THE FIRST;
C     THAT IS, BX(M)=BX(1) AND BY(M)=BY(1).
C     TOP, BASE= THE Z COORDINATE OF THE TOP AND BASE OF THE PRISM.
C     H = THE DEPTH TO THE BASE OF THE FIRST CONDUCTIVITY
```

```
C      LAYER.  IF L = 1 H IS NOT USED.
C      HPC= THE HEAT PRODUCTION CONTRAST BETWEEN THE PRISM AND THE
C      SURROUNDING MEDIUM.
C      QSTAR= UNIFORM HEAT FLOW ENTERING THE BASE OF THE MODEL REGION.
C      KO= THE CONDUCTIVITY OF THE FIRST CONDUCTIVITY LAYER.
C      IF L = 1 KO IS NOT USED.
C      K1= THE CONDUCTIVITY OF THE SECOND CONDUCTIVITY LAYER.
C      K2= THE CONDUCTIVITY OF THE PRISM.
C      NT= THE NUMBER OF TERMS TO BE KEPTED IN THE SERIES SOLUTION.
C      Q= THE DOUBLE PRECISION ARRAY OF LENGTH N IN WHICH THE COMPUTED
C      HEAT-FLOW VALUES ARE RETURNED TO THE MAIN PROGRAM.
C      RI= THE MAXIMUM SERIES TRUNCATION ERROR IN THE HEAT FLOW
C      VALUES RETURNED.
C      W1,W2,W3= DOUBLE PRECISION WORK ARRAYS OF DIMENSION N.
C
C
C      SUBROUTINES REQUIRED
C
C      SUBROUTINE PSI:  COMPUTES THE PSI FUNCTION FOR A POLYGONALY PRISM.
C
C      SUBROUTINE OMEGA:  CUMPUTES THE FUNCTION OMEGA FOR A POLYGONAL PRISM.
C
C
      DOUBLE PRECISION Q(N),W1(N),W2(N),W3(N),PI,
     1A,B,C,C1,C3,CA,CK,W1MAX,W2MAX
      DIMENSION FX(N),FY(N),FZ(N),BX(M),BY(M)
      REAL KO,K1,K2
      PI=DATAN(1.0D0)*4.0D0
      CA=HPC/(PI*4.0D0)
      CK=3.0D0*QSTAR*DBLE(K1-K2)/(4.0D0*PI*DBLE(2.0*K1+K2))
      DO 1 I=1,N
    1 FZ(I)=ZOBS
C     COMPUTE THE EFFECT OF THE SOURCE POLYGON.
      CALL PSI(N,FX,FY,FZ,M,BX,BY,TOP,BASE,W1,W3)
      CALL OMEGA(N,FX,FY,FZ,M,BX,BY,TOP,BASE,W2,W3)
C     NOW ADDED THE EFFECT OF THE CORRECT SERIES OF IMAGES
C     TO THE EFFECT OF THE SOURCE, TO COMPLETE THE SOLUTION.
      IF(L.EQ.1) GO TO 100
      IF(KO.EQ.K1) GO TO 100
C     IF THIS LINE IS REACHED THE MODEL HAS TWO LAYERS.
      H2=H*2.0
      H2M=-H2
      B=DBLE(KO+K1)
      TEST=H-ZOBS
      IF(TEST.GT.0.0) GO TO 40
C     START OF THE SERIES FOR THE LOWER LAYER OF THE TWO LAYER CASE.
      A=DBLE(KO-K1)
      CA=CA*DBLE(K1)
      CK=CK*DBLE(K1)
      C=1.0D0/DBLE(K1)
```

```
      DO 10 I=1,N
   10 Q(I)=C*(CA*W1(I)+CK*W2(I))
      CALL PSI(N,FX,FY,FZ,M,BX,BY,H2-TOP,H2-BASE,W1,W3)
      CALL OMEGA(N,FX,FY,FZ,M,BX,BY,H2-TOP,H2-BASE,W2,W3)
      C1=A/B
      C=-C*C1
      DO 20 I=1,N
   20 Q(I)=Q(I)+C*(CA*W1(I)-CK*W2(I))
      C=4.0D0*DBLE(K0)*C1/(A*A)
      C2=2.0D0/(A*A*DLOG(DABS(B/A)))
      C1=-C1
      DO 30 I=1,NT
      C2=C2*C1
      C=C*C1
      Z=H2M*(I-1)
      CALL PSI(N,FX,FY,FZ,M,BX,BY,Z-TOP,Z-BASE,W1,W3)
      CALL OMEGA(N,FX,FY,FZ,M,BX,BY,Z-TOP,Z-BASE,W2,W3)
      W1MAX=DABS(W1(1))
      W2MAX=DABS(W2(1))
      DO 30 J=1,N
      IF(W1MAX.LT.DABS(W1(J))) W1MAX=DABS(W1(J))
      IF(W2MAX.LT.DABS(W2(J))) W2MAX=DABS(W2(J))
   30 Q(J)=Q(J)+C*(CA*W1(J)-CK*W2(J))
      RI=C2*(DABS(CA*W1MAX)+DABS(CK*W2MAX))
      RETURN
   40 CONTINUE
C     START OF THE SERIES FOR THE UPPER LAYER IN THE TWO LAYER CASE.
      A=DBLE(K0-K1)
      CA=CA*DBLE(K0)
      CK=CK*DBLE(K0)
      C=2.0D0/B
      C1=A/B
      C2=2.0D0/(PI*B*DLOG(DABS(A/B)))
      DO 50 I=1,N
   50 Q(I)=C*(CA*W1(I)+CK*W2(I))
      CALL PSI(N,FX,FY,FZ,M,BX,BY,-TOP,-BASE,W1,W3)
      CALL OMEGA(N,FX,FY,FZ,M,BX,BY,-TOP,-BASE,W2,W3)
      DO 60 I=1,N
   60 Q(I)=Q(I)+C*(CK*W2(I)-CA*W1(I))
      C=C1*C1*2.0/A
      DO 90 I=1,NT
      C2=C2*C1
      Z=H2M*FLOAT(I)
      CALL PSI(N,FX,FY,FZ,M,BX,BY,Z-TOP,Z-BASE,W1,W3)
      CALL OMEGA(N,FX,FY,FZ,M,BX,BY,Z-TOP,Z-BASE,W2,W3)
      W1MAX=DABS(W1(1))
      W2MAX=DABS(W2(1))
      DO 70 J=1,N
      IF(W1MAX.LT.DABS(W1(J))) W1MAX=DABS(W1(J))
      IF(W2MAX.LT.DABS(W2(J))) W2MAX=DABS(W2(J))
```

```
   70 Q(J)=Q(J)+C*(CA*W1(J)-CK*W2(J))
      C=-C
      Z=H2*FLOAT(I)
      CALL PSI(N,FX,FY,FZ,M,BX,BY,Z+TOP,Z+BASE,W1,W3)
      CALL OMEGA(N,FX,FY,FZ,M,BX,BY,Z+TOP,Z+BASE,W2,W3)
      DO 80 J=1,N
   80 Q(J)=Q(J)+C*(CA*W1(J)+CK*W2(J))
      RI=C2*(DABS(W1MAX)+DABS(W2MAX))
      C=C*C1
   90 CONTINUE
      RETURN
  100 CONTINUE
C     START OF THE ONE-LAYER CASE.
      CA=CA*DBLE(K1)
      CK=CK*DBLE(K1)
      C=1.0D0/DBLE(K1)
      DO 110 I=1,N
  110 Q(I)=C*(CA*W1(I)+CK*W2(I))
      CALL PSI(N,FX,FY,FZ,M,BX,BY,-TOP,-BASE,W1,W3)
      CALL OMEGA(N,FX,FY,FZ,M,BX,BY,-TOP,-BASE,W2,W3)
      DO 120 I=1,N
  120 Q(I)=Q(I)+C*(CK*W2(I)-CA*W1(I))
      RETURN
      END
```

```
C-----------------------------------------------------------------------C
      FUNCTION TNORM(H,K0,K1,T0,Q0,A0,LA,A,D,Z)
C-----------------------------------------------------------------------C
C
C
C     SUBROUTINE WHICH COMPUTES TEMPERATURE AT A DEPTH Z IN A
C     ONE-DIMENSIONAL HEAT CONDUCTION OF THE EARTH CONSISTING
C     OF UP TO TWO UNIFORM CONDUCTIVITY LAYERS AND AN ARBITRARY
C     NUMBER OF UNIFORM HEAT PRODUCTION LAYERS.
C
C
C     COORDINATE SYSTEM
C
C     THE ORIGIN IS AT THE SURFACE AND Z IS POSITIVE DOWN.
C
C
C     UNITS
C
C     THE UNITS OF ALL ARGUMENTS ARE ASSUMED TO BE CONSISTENT IN
C     THE DIMENSIONS ENERGY, LENGTH, TIME AND TEMPERATURE.
C
C
C     ARGUMENTS
C
C     H= THE THICKNESS OF THE FIRST CONDUCTIVITY LAYER. H=0.0
C     CORRESPONDS TO THE ONE CONDUCTIVITY LAYER CASE.
C     K0, K1= THE THERMAL CODUCTIVITY OF THE TWO CONDUCTIVITY LAYERS.
C     IF H=0.0 K0 IS NOT USED.
C     T0= THE MEAN ANNUAL SURFACE TEMPERATURE IN THE MODEL REGION.
C     Q0= THE SURFACE HEAT FLOW IN THE MODEL REGION.
C     A0= THE HEAT PRODUCTION OF THE FIRST CONDUCTIVITY LAYER.
C     IF H=0.0 A0 IS NOT USED.
C     LA= THE NUMBER OF UNIFORM HEAT PRODUCING LAYERS IN THE
C     SECOND CONDUCTIVITY LAYER.
C     A= ARRAY OF LENGTH LA CONTAINING THE HEAT PRODUCTIONS OF THE
C     LA HEAT PRODUCING LAYERS IN THE SECOND CONDUCTIVITY LAYER.
C     D= ARRAY OF LENGTH LA CONTAINING THE Z COORDINATE OF THE BASE
C     OF EACH HEAT PRODUCTION LAYER.
C     Z= THE Z COORDINATE OF THE FIELD POINT AT WHICH TEMPERATURE IS
C     TO BE COMPUTED.
C
C
C
C
      DIMENSION A(LA),D(LA)
      REAL K0,K1
      IF(H.GT.0.0) GO TO 10
      T1=T0
      Q1=Q0
      GO TO 30
```

```
10 DZ=Z-H
   IF(DZ.GT.0.0) GO TO 20
   TNORM=(Q0*Z-0.5*A0*Z*Z)/K0+T0
   GO TO 80
20 Q1=Q0-A0*H
   T1=(Q0*H-0.5*A0*H*H)/K0+T0
30 M=0
   DO 40 I=1,LA
40 IF(Z.GT.D(I)) M=I
   IF(M.EQ.0) GO TO 70
   DT=0.5*A(1)*(D(1)-H)*(D(1)-H)
   IF(LA.EQ.1) GO TO 60
   DO 50 I=2,M
50 DT=DT+0.5*A(I)*(D(I)-D(I-1))*(D(I)-D(I-1))
   IF(M.EQ.LA) GO TO 60
   TNORM=T1+(Z-H)*Q1-DT-0.5*A(M+1)*(Z-D(M))*(Z-D(M))
   GO TO 80
60 TNORM=T1+(Z-H)*Q1-DT
   GO TO 80
70 TNORM=T1+(Z-H)*Q1-0.5*A(1)*(Z-H)*(Z-H)
80 CONTINUE
   RETURN
   END
```

```
C-----------------------------------------------------------------C
      SUBROUTINE CHI(N,FX,FY,FZ,M,BX,BY,TOP,BASE,U,DS)
C-----------------------------------------------------------------C
C
C
C     SUBROUTINE TO CUMPUTE THE FUNCTION CHI FOR A POLYGONAL PRISM.
C     THE PROGRAM IS BASED ON EQUATION (8).
C
C
C     ARGUMENTS
C
C     N=  THE NUMBER OF FIELD POINTS AT WHICH THE FUNCTION IS TO BE
C     COMPUTED.
C     FX,FY,FZ= ARRAYS CONTAINING THE N COORDINATES OF THE FIELD POINTS.
C     M= ONE PLUS THE NUMBER OF CORNER POINTS OF THE POLYGONAL PRISM.
C     BX,BY= ARRAYS CONTAINING THE X,Y COORDINATES OF THE CORNER
C     CORNER POINTS IN CLOCKWISE ORDER AROUND THE POLYGONAL PRISM.
C          NOTE:  THE LAST CORNER POINT MUST COINCIDE WITH THE FIRST;
C          THAT IS, BX(M)=BX(1) AND BY(M)=BY(1).
C     TOP, BASE= THE Z COORDINATE OF THE TOP AND BASE OF THE
C     POLYGONAL PRISM.
C     U= THE DOUBLE PRECISION ARRAY OF THE LENGTH N IN WHICH THE
C     VALUES OF TH CHI FUNCTION ARE RETURNED TO THE CALLING PROGRAM.
C     DS= A DOUBLE PRECISION WORK ARRAY.
C
C
C     SUBROUTINE REQUIRED
C
C     DOUBLE PRECISION FUNCTION ANGLE
C
C
      DIMENSION FX(N),FY(N),FZ(N),BX(M),BY(M)
      DOUBLE PRECISION U(N),DS(M)
      REAL K
      DOUBLE PRECISION X1,X2,Y1,Y2,R1Z1,R2Z1,R2Z2,R1Z2,R1SQ,R2SQ,
     1T1,T2,T3,T4,T5,T6,DX,DY,DZ,ZERO,EPS,TWO,Z1,Z2,DZSQ,Z1SQ,
     2Z2SQ,A1,A2,A3,A4,P,S,SSQ,SC,C,CSQ,D1,D2,DTEST,F1,F2,Q1,Q2,W11,W12,
     3W22,W21,X1SQ,X2SQ,Y1SQ,Y2SQ,HALF,AZ1,AZ2,ANGLE,
     4A,SIGN,X1Y1,X2Y2,ABSP,V(400)
      DATA ZERO/0.0D0/,EPS/1.0D-5/,HALF/0.5D0/,TWO/2.0D0/
C     COMPUTE THE LENGTH OF EACH SIDE AND STORE IN ARRAY DS
      MM=M-1
      DO 10 I=1,MM
      J=I+1
      DX=DBLE(BX(J)-BX(I))
      DY=DBLE(BY(J)-BY(I))
   10 DS(I)=DSQRT(DX*DX+DY*DY)
C     START THE LOOP FOR EACH FIELD POINT
      DO 110 LF=1,N
      U(LF)=ZERO
```

```
      Z1=DBLE(TOP-FZ(LF))
      Z2=DBLE(BASE-FZ(LF))
      AZ1=DABS(Z1)
      AZ2=DABS(Z2)
      IF(AZ1.GT.Z1.AND.AZ2.GT.Z2) GO TO 30
      IF(AZ1.NE.Z1.OR.AZ2.NE.Z2) GO TO 20
      IF(AZ1.LT.AZ2) GO TO 15
      Z1=AZ2
      Z2=AZ1
   15 CONTINUE
      NPOLY=1
      GO TO 40
   20 CONTINUE
C     IF THIS LINE IS REACHED THE POLYGON IS SPLIT INTO TWO
C     POLYGONS ALONG THE Z=FZ(LF) PLANE AND THE EFFECTS ARE
C     COMPUTED SEPERATELY AND ADDED.
      NPOLY=2
      Z1=ZERO
      Z2=AZ2
      GO TO 40
   30 NPOLY=1
      IF(AZ2.LT.AZ1) GO TO 35
      Z1=AZ1
      Z2=AZ2
      GO TO 40
   35 Z1=AZ2
      Z2=AZ1
   40 DO 110 IPOLY=1,NPOLY
      T1=ZERO
      T2=ZERO
      T3=ZERO
      T4=ZERO
      T5=ZERO
      T6=ZERO
      IF(IPOLY.EQ.2) Z2=AZ1
      DZ=Z2-Z1
      DZSQ=DZ*DZ
      Z1SQ=Z1*Z1
      Z2SQ=Z2*Z2
C     INITALISE R TERMS
      X2=DBLE(BX(1)-FX(LF))
      Y2=DBLE(BY(1)-FY(LF))
      R2SQ=X2*X2+Y2*Y2
      R2Z1=DSQRT(R2SQ+Z1SQ)
      R2Z2=DSQRT(R2SQ+Z2SQ)
      A1=R2Z2+Z2
      A4=R2Z1+Z1
C     START THE LOOP FOR EACH SIDE
   50 DO 100 LB=1,MM
      J=LB+1
```

```
C       MAKE THE SECOND POINT OF THE LAST SIDE THE FIRST POINT
C       OF THE CURRENT SIDE
        X1=X2
        Y1=Y2
        R1Z1=R2Z1
        R1Z2=R2Z2
        X2=DBLE(BX(J)-FX(LF))
        Y2=DBLE(BY(J)-FY(LF))
        DX=X2-X1
        DY=Y2-Y1
        X1SQ=X1*X1
        X2SQ=X2*X2
        Y1SQ=Y1*Y1
        Y2SQ=Y2*Y2
        X1Y1=X1*Y1
        X2Y2=X2*Y2
        P=(X1*Y2-X2*Y1)/DS(LB)
        ABSP=DABS(P)
        S=DX/DS(LB)
        SSQ=S*S
        C=DY/DS(LB)
        CSQ=C*C
        SC=S*C
        D1=X1*S+Y1*C
        D2=X2*S+Y2*C
        R2SQ=X2SQ+Y2SQ
        R2Z1=DSQRT(R2SQ+Z1SQ)
        R2Z2=DSQRT(R2SQ+Z2SQ)
C       DTEST, THE SMALLEST DISTANCE THAT CAN BE RESOLVED FOR THIS
C       SIDE IS DEFINED AS THE LENGTH OF THE SIDE TIMES 1.0E-N
C       WHERE N IS THE NUMBER OF SIGNIFICANT DIGITS REQUIRED
        DTEST=EPS*DS(LB)
C
C       NOW READY TO COMPUTE PRINCIPAL TERMS
C
C       COMPUTE THE LOG(R+Z) TERM
C       THIS TERM IS UNSTABLE WHEN THE FIELD POINT IS NEARLY
C       UNDER A CORNER POINT OF THE POLYGON
        A1=R1Z1+Z1
        A2=R1Z2+Z2
        A3=R2Z2+Z2
        A4=R2Z1+Z1
        IF(A1.LT.DTEST) A1=DTEST
        IF(A2.LT.DTEST) A2=DTEST
        IF(A3.LT.DTEST) A3=DTEST
        IF(A4.LT.DTEST) A4=DTEST
   60   F1=DLOG(A2/A1)
        F2=DLOG(A3/A4)
C       COMPUTE THE LOG(R+D) TERM
C       THIS TERM IS UNSTABLE WHEN THE FIELD POINT IS NEAR AN
```

```
C       EDGE OF THE POLYGON
        A1=R1Z1+D1
        A2=R1Z2+D1
        A3=R2Z2+D2
        A4=R2Z1+D2
        IF(A1.LT.DTEST) A1=DTEST
        IF(A2.LT.DTEST) A2=DTEST
        IF(A3.LT.DTEST) A3=DTEST
        IF(A4.LT.DTEST) A4=DTEST
   80   Q1=Z2*DLOG(A2)-Z1*DLOG(A1)
        Q2=Z2*DLOG(A3)-Z1*DLOG(A4)
C       COMPUTE THE ARCTANGENT TERM
C       THIS TERM GOES TO ZERO FOR P (THE PERPENDICULAR DISTANCE
C       BETWEEN THE FIELD POINT AND A LINE ALONG THE VERTICAL
C       PROJECTION OF THE EDGE) NEAR ZERO
        W11=ZERO
        W12=ZERO
        W22=ZERO
        W21=ZERO
        IF(ABSP.LE.DTEST) GO TO 90
        W11=DATAN(Z1*D1/(P*R1Z1))
        W12=DATAN(Z2*D1/(P*R1Z2))
        W22=DATAN(Z2*D2/(P*R2Z2))
        W21=DATAN(Z1*D2/(P*R2Z1))
C       FINISHED COMPUTING THE PRINCIPAL TERMS
C       NOW COMBINE THEM TO FORM THE 6 ELEMENTS OF THE POTENTIAL
   90   T1=T1+SC*((Y2SQ-X2SQ)*F2-(Y1SQ-X1SQ)*F1)
        T2=T2+(SSQ-CSQ)*(X2Y2*F2-X1Y1*F1)
        T3=T3+(X2SQ*CSQ-TWO*X2Y2*SC+Y2SQ*SSQ)*(W22-W21)
        T4=T4-(X1SQ*CSQ-TWO*X1Y1*SC+Y1SQ*SSQ)*(W12-W11)
        T5=T5+TWO*((Y2*S-X2*C)*Q2-(Y1*S-X1*C)*Q1)
  100   T6=T6-Z2SQ*(W22-W12)+Z1SQ*(W21-W11)
        T6=T6-ANGLE(BX,BY,M,FX(LF),FY(LF))*(Z2SQ-Z1SQ)
C       END OF LOOP FOR EACH SIDE
C       ACCOMULATE THE POTENTIAL
  110   U(LF)=U(LF)+HALF*(T1+T2+T3+T4+T5+T6)
C       END OF LOOP FOR EACH FIELD POINT
        RETURN
        END
```

```
C-----------------------------------------------------------------------C
      SUBROUTINE PSI(N,FX,FY,FZ,M,BX,BY,TOP,BASE,U,WORK)
C-----------------------------------------------------------------------C
C
C
C     SUBROUTINE WHICH COMPUTES THE PSI FUNCTION FOR A POLYGONAL PRISM.
C     THE PROGRAM IS BASED ON A GRAVITY MODELING PROGRAM "PSI"
C     PREPARED BY A. H. COGBILL AT VPI&US.  EQUATIONS PRESENTED BY
C     PLOUFF (1976), GEOPHYSICS, VOL. 41 (4) PAGES 727-741, ARE USED.
C
C
C     ARGUMENTS
C
C     N= THE NUMBER OF FIELD POINTS AT WHICH THE PSI FUNCTION IS TO BE
C     COMPUTED.
C     FX, FY, FZ= ARRAYS OF LENGTH N CONTAINING THE COORDINATES OF THE
C     FIELD POINTS.
C     M= THE NUMBER OF CORNER POINTS IN THE POLYGONAL PRISM PLUS ONE.
C     BX, BY= ARRAYS OF LENGTH M CONTAINING THE X,Y COORDINATES OF THE
C     CORNER POINTS IN CLOCKWISE ORDER AROUND THE PRISM.
C          NOTE:  THE LAST CORNER MUST COINCIDE WITH THE FIRST; THAT IS
C          BX(M)=BX(1) AND BY(M)=BY(1).
C     TOP, BASE= THE Z COORDINATES OF THE TOP AND BASE OF THE PRISM.
C     U= THE DOUBLE PRECISION ARRAY OF LENGTH N IN WHICH THE COMPUTED
C     VALUES OF PSI WILL BE RETURNED TO THE CALLING PROGRAM.
C     WORK= DOUBLE PRECISION WORK ARRAY OF LENGTH N.
C
C
C     SUBROUTINE REQUIRED
C
C     DOUBLE PRECISION FUNCTION ANGLE
C
C
      REAL FX(N),FY(N),FZ(N),BX(M),BY(M)
      REAL SUM,SNGL
      LOGICAL FLAG
      DOUBLE PRECISION U(N),WORK(N)
      DOUBLE PRECISION DSUM,DBLE,DABS,DMIN1,DMAX1,DSQRT,DLOG,DATAN2
      DOUBLE PRECISION ONE,HALF,FOURTH,DZERO,DTOLER,EPS,ARG,ANGLE
      DOUBLE PRECISION DX,DY,DS,PTEST,DTEST,ZTEST,ZT
      DOUBLE PRECISION X0,Y0,Z0,X1,Y1,Z1,X2,Y2,Z2,Z1SQ,Z2SQ,R1,R2,
     *                 RDZ1,RDZ2,R11,R12,R22,R21,D1,D2,DD1,DD2,
     *                 A,B,C,S,P,PH,GL,T1,T2,T3,DTOP,DBASE
      EQUIVALENCE (SUM,EPSS),(DSUM,ZT)
      DATA ONE/1.0D0/, HALF/0.5D0/, FOURTH/0.25D0/
      DATA DZERO/0.0D0/
C     LUN= THE LOCAL UNIT NUMBER ON WHICH ERROR STATEMENTS ARE WRITTEN
      DATA LUN/8/
C
C               "EPS" IS USED PRINCIPALLY TO CALCULATE THE
```

```
C                LOGARITHMS OF SUMS OF DIFFERENT SIGNS AND
C                VERY DIFFERENT MAGNITUDES (THE LOG TERMS MAY
C                HAVE NEGATIVE ARGUMENTS WITHOUT THIS PRECAUTION).
C
      FLAG=.FALSE.
C
C
C
C    ZERO THE VECTOR U(I) BEFORE PERFORMING ANY COMPUTATIONS.
C
      IF (N.LE.0) GO TO 200
   10 DO 20 I=1,N
   20 U(I)=0.0D0
C
C                COMPUTE MACHINE DOUBLE PRECISION -
C
      DTOLER=HALF
   30 DTOLER=HALF*DTOLER
      EPS=ONE+DTOLER
      IF (EPS.GT.ONE) GO TO 30
      DTOLER=DTOLER+DTOLER
      EPS=DSQRT(DTOLER)
      EPS=HALF*DSQRT(EPS)
C
C                USE "DSQRT" TWICE TO AVOID LOADING "X**Y"
C                NOW COMPUTE MACHINE SINGLE PRECISION -
C
      TOLER=0.5
   35 TOLER=0.5*TOLER
      EPSS=1.0+TOLER
      IF (EPSS.GT.1.0) GO TO 35
      TOLER=TOLER+TOLER
      IF (M.LT.4) GO TO 210
   40 M1=M-1
      IF (ABS(TOP-BASE).LT.TOLER*(ABS(TOP)+ABS(BASE))) GO TO 240
      IF (ABS(BX(M)-BX(1)).GT.TOLER*ABS(BX(M)+BX(1))) GO TO 220
      IF (ABS(BY(M)-BY(1)).GT.TOLER*ABS(BY(M)+BY(1))) GO TO 220
      IF (FLAG) GO TO 260
      DTOP=DBLE(TOP)
      DBASE=DBLE(BASE)
C
C                DETERMINE THE SHORTEST POLYGONAL SIDE.
C                TAKE SPECIAL CARE TO ACCOUNT FOR THE
C                POSSIBILITY THAT ALL VERTICES ARE COINCIDENT
C
      PTEST=DZERO
      L=0
   60 L=L+1
         IF (L.GT.M1) GO TO 90
         DX=DBLE(BX(L+1)-BX(L))
```

```
      DY=DBLE(BY(L+1)-BY(L))
      DS=DX*DX+DY*DY
      IF (DS.GT.DZERO) GO TO 70
      WORK(L)=DZERO
      WRITE (LUN,1030) L,BX(L),BY(L)
      GO TO 60
   70 DS=DSQRT(DS)
      WORK(L)=DS
      IF (L.GT.1) GO TO 80
      PTEST=DS
      GO TO 60
   80 IF (PTEST.EQ.DZERO) GO TO 60
      PTEST=DMIN1(PTEST,DS)
      GO TO 60
   90 IF (PTEST.EQ.DZERO) GO TO 250
C
C          "PTEST" WILL BE THE VALUE BELOW WHICH
C          ALL HORIZONTAL DISTANCES ARE CONSIDERED ZERO.
C
      PTEST=DTOLER*PTEST
      ZTEST=DSQRT(DTOLER)*DBLE((ABS(TOP)+ABS(BASE)))
      CM=0.5*(TOP+BASE)
C
C              BEGIN MAIN LOOP FOR ALL FIELD POINTS -
C
      DO 180 L=1,N
         X0=DBLE(FX(L))
         Y0=DBLE(FY(L))
         Z0=DBLE(FZ(L))
         Z1=DABS(DTOP-Z0)
         Z2=DABS(DBASE-Z0)
         IF (Z1.LT.Z2) GO TO 100
         ZT=Z1
         Z1=Z2
         Z2=ZT
  100    IF (Z1.GT.ZTEST) GO TO 110
         Z1=ZTEST
  110    Z1SQ=Z1*Z1
         Z2SQ=Z2*Z2
         X2=DBLE(BX(1))-X0
         Y2=DBLE(BY(1))-Y0
         R2=X2*X2+Y2*Y2
         R21=DSQRT(R2+Z1SQ)
         R22=DSQRT(R2+Z2SQ)
         DSUM=DZERO
C
C            PROCEED AROUND THE POLYGONAL PRISM,
C            SUMMING THE CONTRIBUTION FROM EACH SIDE.
C
         DO 170 K=1,M1
```

```
            X1=X2
            Y1=Y2
            R1=R2
            R11=R21
            R12=R22
            X2=DBLE(BX(K+1))-X0
            Y2=DBLE(BY(K+1))-Y0
            R2=X2*X2+Y2*Y2
            R21=DSQRT(R2+Z1SQ)
            R22=DSQRT(R2+Z2SQ)
            DX=X2-X1
            DY=Y2-Y1
            DS=WORK(K)
            IF (DS.LT.PTEST) GO TO 170
            P=(X1*Y2-X2*Y1)/DS
            IF (P.EQ.DZERO) GO TO 170
            C=DY/DS
            S=DX/DS
            D1=X1*S+Y1*C
            D2=X2*S+Y2*C
C
C                 CALCULATE THE LOG (R+D) TERMS -
C
  120       PH=P*P+Z1SQ
            RDZ1=R11+D1
            IF (D1.GE.DZERO) GO TO 140
            IF (D2.GT.DZERO) GO TO 130
            GL=(R21-D2)/(R11-D1)
            GO TO 160
  130       DTEST=PH/(D1*D1)
            DD1=DABS(D1)
            IF (DTEST.LT.EPS) RDZ1=HALF*DD1*DTEST*(ONE-FOURTH*DTEST)
  140       RDZ2=R21+D2
            IF (D2.GE.DZERO) GO TO 150
            DTEST=PH/(D2*D2)
            DD2=DABS(D2)
            IF (DTEST.LT.EPS) RDZ2=HALF*DD2*DTEST*(ONE-FOURTH*DTEST)
  150       GL=RDZ1/RDZ2
  160       T3=-P*DLOG(GL*(R22+D2)/(R12+D1))
C
C              COMPUTE THE ARCTANGENT TERMS -
C
            A=Z2*D1/(P*R12)
            B=-Z2*D2/(P*R22)
            C=ONE-A*B
            T1=Z2*DATAN2((A+B),C)
            A=Z1*D1/(P*R11)
            B=-Z1*D2/(P*R21)
            C=ONE-A*B
            T2=-Z1*DATAN2((A+B),C)
```

```
C
C              FINISHED WITH THE LOOP OF THE POLYGONAL SIDES -
C
C             T1,T2 = ARCTANGENT TERMS, T3 = LOG TERM.
C
             DSUM=DSUM+T1+T2+T3
  170     CONTINUE
          DSUM=DABS(DSUM)
          ARG=ANGLE(BX,BY,M,FX(L),FY(L))
          IF (ARG.EQ.DZERO) GO TO 180
          DSUM=ARG*(Z2-Z1)-DSUM
C
C               "ANGLE" COMPUTES THE SUM OF THE
C               INTERIOR ANGLES OF THE POLYGONAL
C               PRISM: IT USES A WINDING NUMBER ALGORITHM.
C
  180 U(L)=DSUM*DBLE(SIGN(1.0,CM-FZ(L)))
C
      GO TO 270
C    INITIATE ERROR PROCESSING HERE -
C
  200 WRITE (LUN,1000) N
      FLAG=.TRUE.
      GO TO 10
  210 WRITE (LUN,1010) M
      FLAG=.TRUE.
      GO TO 40
  220 WRITE (LUN,*) BX(1),BX(M),BY(1),BY(M)
  230 WRITE (LUN,1050)
      GO TO 260
  240 WRITE (LUN,1060) TOP,BASE
      GO TO 270
  250 WRITE (LUN,1040)
      GO TO 270
  260 WRITE (LUN,1100)
  270 RETURN
 1000 FORMAT (47H0*****     NUMBER OF FIELD POINTS IS § 1:  N = ,
     1   I4,1H.)
 1010 FORMAT (46H0*****     NUMBER OF BODY POINTS IS § 4:  M = ,I4,1H.)
 1030 FORMAT (17H0***   WARNING:  ,
     1        47HDUPLICATE BODY POINTS AT INDICES "L" AND "L+1.",/,
     2        7X,4HL = ,I3,1H.,/,7X,8HBX(L) = ,G16.7,/,7X,
     3        8HBY(L) = ,G16.7)
 1040 FORMAT (49H0***   WARNING:  POLYGONAL VERTICES ALL COINCIDE.,/,
     1        7X,27HFIELD OF PRISM SET TO ZERO.,/,
     2        7X,29HWARNING ISSUED FROM "PSI.")
 1050 FORMAT ('  ERROR FIRST AND LAST CORNER POINTS DO NOT COINSIDE')
 1060 FORMAT (45H0***   WARNING:  POLYGONAL PRISM IS TOO THIN.,/,
     1        7X,14HTOP OF BODY = ,G16.7,/,
     2        7X,15HBASE OF BODY = ,G16.7,/,
```

```
     3        7X,27HFIELD OF PRISM SET TO ZERO.,/,
     4        7X,29HWARNING ISSUED FROM "PSI.")
1100 FORMAT (11X,29HERROR(S) DETECTED IN "PSI")
     END
```

```
C-----------------------------------------------------------------------C
      SUBROUTINE OMEGA(N,FX,FY,FZ,M,BX,BY,TOP,BASE,U,DIST)
C-----------------------------------------------------------------------C
C
C
C     SUBROUTINE TO CUMPUTE THE FUNCTION OMEGA FOR A POLYGONAL PRISM.
C     THE PROGRAM IS BASED ON EQUATION (8).
C
C
C     ARGUMENTS
C
C     N=  THE NUMBER OF FIELD POINTS AT WHICH THE FUNCTION IS TO BE
C     COMPUTED.
C     FX,FY,FZ= ARRAYS CONTAINING THE N COORDINATES OF THE FIELD POINTS.
C     M= ONE PLUS THE NUMBER OF CORNER POINTS OF THE POLYGONAL PRISM.
C     BX,BY= ARRAYS CONTAINING THE X,Y COORDINATES OF THE CORNER
C     CORNER POINTS IN CLOCKWISE ORDER AROUND THE POLYGONAL PRISM.
C          NOTE:  THE LAST CORNER POINT MUST COINCIDE WITH THE FIRST;
C          THAT IS, BX(M)=BX(1) AND BY(M)=BY(1).
C     TOP, BASE= THE Z COORDINATE OF THE TOP AND BASE OF THE
C     POLYGONAL PRISM.
C     U= THE DOUBLE PRECISION ARRAY OF THE LENGTH N IN WHICH THE
C     VALUES OF TH OMEGA FUNCTION ARE RETURNED TO THE CALLING PROGRAM.
C     DS= A DOUBLE PRECISION WORK ARRAY.
C
C
C     SUBROUTINE REQUIRED
C
C     DOUBLE PRECISION FUNCTION ANGLE
C
C
      REAL FX(N),FY(N),FZ(N),BX(M),BY(M),U(N)
      REAL ABS,SNGL
      DIMENSION DIST(M)
      LOGICAL WARN,FATAL
      DOUBLE PRECISION A,B,C,C2,P,S,W,CI,CM,DS,DX,DY,D1,D2,D12,
     1                 SC,SD,SI,T1,T2,
     2                 X0,X1,X2,Y0,Y1,Y2,
     3                 ZT,Z1,Z2,CSQ,DD1,DD2,EPS,
     4                 DIST,EPS1,RDZ1,RDZ2,R1SQ,R2SQ,R1Z1,R2Z1,
     5                 R1Z2,R2Z2,Z1SQ,Z2SQ,DTEST,PTEST,SMALL,ZSMALL
      DOUBLE PRECISION DZERO,HALF,ONE,TEN
      DOUBLE PRECISION DCOS,DSIN,DLOG,DATAN,DATAN2,DSQRT,DABS,DBLE
      EQUIVALENCE (EPS1,ZT)
      DATA HALF/5.0D-1/, ONE/1.0D0/,  TEN/1.0D+1/
      DATA LUN/9/
      DATA ZERO/0.0/, DZERO/0.0D0/
      WARN=.FALSE.
      FATAL=.FALSE.
      DO 1 LF=1,N
```

```
    1 U(LF)=ZERO
      IF (N.LT.1) GO TO 170
   10 IF (M.LT.4) GO TO 180
   20 M1=M-1
C
C            CALCULATE DOUBLE-PRECISION MACHINE TOLERANCE
C
      EPS=HALF
   30 EPS=EPS*HALF
      EPS1=ONE+EPS
      IF (EPS1.GT.ONE) GO TO 30
      EPS1=DSQRT(EPS)
      SMALL=HALF*DSQRT(EPS1)
      EPS1=EPS1+EPS1
C
C          SET "ZSMALL" TO SMALL*ABS(TOP-BASE)
C
      ZSMALL=TEN*SMALL*DABS(DBLE(TOP-BASE))
      L=0
C
C       MAKE CERTAIN THAT THE THICKNESS OF THE SLAB IS NON-ZERO.
C       IF THE PRISM IS EXTREMELY THIN, SET OMEGA
C       TO ZERO AND WRITE A WARNING MESSAGE.
C
      IF (ABS(TOP-BASE).GT.SNGL(ZSMALL)) GO TO 40
      GO TO 200
C
C          DETERMINE THE LENGTH (†0) OF THE SHORTEST
C          POLYGONAL SEGMENT.
C
   40 L=L+1
         IF (L.GT.M1) GO TO 70
         X1=DBLE(BX(L))
         X2=DBLE(BX(L+1))
         Y1=DBLE(BY(L))
         Y2=DBLE(BY(L+1))
         DX=DABS(X2-X1)
         DY=DABS(Y2-Y1)
         IF (DX.GT.EPS*DABS(X1+X2)) GO TO 50
         IF (DY.GT.EPS*DABS(Y1+Y2)) GO TO 50
         DTEST=DZERO
         DIST(L)=DZERO
         GO TO 40
   50    DS=DSQRT(DX*DX+DY*DY)
         DIST(L)=DS
         IF (L.GT.1) GO TO 60
         DTEST=DS
         GO TO 40
   60    DTEST=DMIN1(DS,DTEST)
         GO TO 40
```

```
   70 IF (DTEST.EQ.DZERO) GO TO 200
      IF (FATAL) GO TO 190
      PTEST=EPS1*DTEST
C
C          "PTEST" = THE LENGTH BELOW WHICH HORIZONTAL
C          DISTANCES ARE ASSUMED TO BE ZERO.
C
C
C
C              START MAIN LOOP FOR EACH FIELD POINT -
C
      DO 160 LF=1,N
         Z1=DBLE(TOP-FZ(LF))
         Z2=DBLE(BASE-FZ(LF))
         CM=HALF*(Z1+Z2)
         Z1=DABS(Z1)
         Z2=DABS(Z2)
   90    Z1SQ=Z1*Z1
         Z2SQ=Z2*Z2
         X0=DBLE(FX(LF))
         Y0=DBLE(FY(LF))
         X2=DBLE(BX(2))-X0
         Y2=DBLE(BY(2))-Y0
         X1=DBLE(BX(1))-X0
         Y1=DBLE(BY(1))-Y0
         R1SQ=X1*X1+Y1*Y1
         R2SQ=X2*X2+Y2*Y2
         R1Z1=DSQRT(R1SQ+Z1SQ)
         R2Z1=DSQRT(R2SQ+Z1SQ)
         R1Z2=DSQRT(R1SQ+Z2SQ)
         R2Z2=DSQRT(R2SQ+Z2SQ)
C
C              START LOOP TO CALCULATE THE CONTRIBUTION FROM
C              EACH POLYGONAL SIDE: THERE ARE (M-1) SIDES.
C
         LB=1
  100       DX=X2-X1
            DY=Y2-Y1
C
C             IF THE LENGTH OF A SIDE IS § "PTEST",
C             NEGLECT THE CONTRIBUTION FROM THAT SIDE.
C
            DS=DIST(LB)
            IF (DS.LT.PTEST) GO TO 150
            C=DY/DS
            S=DX/DS
            SC=S*C
            CSQ=C*C
C
C           CALCULATE PERPENDICULAR DISTANCE "P" OF FIELD POINT
```

```
C           TO THE POLYGONAL LINE SEGMENT (OR ITS EXTENSION).
C           IF "P" IS VERY SMALL, SET "P" TO ZERO.
C
            P=(X1*Y2-X2*Y1)/DS
            IF (DABS(P).GT.PTEST) GO TO 110
            P=DZERO
  110       D1=X1*S+Y1*C
            D2=X2*S+Y2*C
            DD1=DABS(D1)
            DD2=DABS(D2)
            IF (DD1.GT.PTEST) GO TO 120
            D1=DZERO
  120       IF (DD2.GT.PTEST) GO TO 130
            D2=DZERO
  130       D12=D1*D2
C       P = 0, Z1 §= ZSMALL, AND D12 §= 0:  MOVE THE FIELD
C       POINT AWAY FROM THE FACE OF THE PRISM.
C
            Z1=ZSMALL
            Z1SQ=Z1*Z1
            R1Z1=DSQRT(R1SQ+Z1SQ)
            R2Z1=DSQRT(R2SQ+Z1SQ)
C           CALCULATE THE ARCTANGENT TERMS -
C
            W=DZERO
            IF (P.EQ.DZERO) GO TO 140
            A=Z2*D2/(P*R2Z2)
            B=-Z2*D1/(P*R1Z2)
            C2=ONE-A*B
            T1=DATAN2((A+B),C2)
            A=Z1*D1/(P*R1Z1)
            B=-Z1*D2/(P*R2Z1)
            C2=ONE-A*B
            T2=DATAN2((A+B),C2)
C
C            FINISHED WITH THE ARCTANGENT TERMS -
C            NOW SUM THE CONTRIBUTIONS.
C
            W=T1+T2
  140       U(LF)=U(LF)+W
C
C               PREPARE FOR THE NEXT POLYGONAL SEGMENT -
C
  150       LB=LB+1
            IF (LB.GT.M1) GO TO 160
            X1=X2
            Y1=Y2
            R1Z1=R2Z1
            R1Z2=R2Z2
            R1SQ=R2SQ
```

```
            X2=DBLE(BX(LB+1))-XO
            Y2=DBLE(BY(LB+1))-YO
            R2SQ=X2*X2+Y2*Y2
            R2Z1=DSQRT(R2SQ+Z1SQ)
            R2Z2=DSQRT(R2SQ+Z2SQ)
            GO TO 100
C
C                   END LOOP OF POLYGONAL SEGMENTS -
C
  160    CONTINUE
         GO TO 200
  170 WRITE (LUN,1000) N
         FATAL=.TRUE.
         GO TO 10
  180 WRITE (LUN,1010) M
         FATAL=.TRUE.
         GO TO 20
  190 WRITE (LUN,1030)
  200 IF (WARN.AND..NOT.FATAL) WRITE (LUN,1060)
         RETURN
 1000 FORMAT (47H0*****     NUMBER OF FIELD POINTS IS § 1:  N = ,
     1   I4,1H.)
 1010 FORMAT ('*****     NUMBER OF BODY POINTS IS § 4:  NBODY = ',
     1    I4,1H.)
 1030 FORMAT (11X,'ERROR(S) DETECTED IN "OMEGA"')
C 1040 FORMAT (48H0***   WARNING:  DUPLICATE BODY POINTS AT INDEX ,
C     1        I3,1H.,/,7X,15HX-COORDINATE = ,G16.7,/,
C     2                  7X,15HY-COORDINATE = ,G16.7)
C 1050 FORMAT (38H0***   WARNING:  FIELD POINT TOO CLOSE,
C     1        29H TO THE TOP OR BASE OF PRISM.,/,7X,
C     2        42HFIELD POINT WILL BE MOVED AWAY FROM PRISM.,/,7X,
C     3        24HDISTANCE TO PRISM NOW = ,D16.7,/,7X,
C     4        24HNEW DISTANCE TO PRISM = ,D16.7,//,7X,
C     5        32H---  FIELD POINT PARAMETERS  ---,/,12X,8HINDEX = ,
C     6        I4,1H.,/,12X,10HX-COORD = ,G16.7,/,12X,10HY-COORD = ,
C     7        G16.7,/,12X,10HZ-COORD = ,G16.7)
 1060 FORMAT (7X,'---  WARNING MESSAGES ISSUED FROM "OMEGA"  ---')
      END
```

```
C-----------------------------------------------------------------------C
      DOUBLE PRECISION FUNCTION ANGLE (X,Y,M,XO,YO)
C-----------------------------------------------------------------------C
      INTEGER S,T,UP
      REAL X(M),Y(M),XO,YO,DET,FLOAT,SQRT
      DOUBLE PRECISION DZERO,DBLE,PI,TWOPI
C
C           INPUT PARAMETERS -
C
C                 X,Y - REAL ARRAYS OF LENGTH "M" CONTAINING
C                       THE POLYGONAL VERTICES: THE LAST POINT
C                       (X(M),Y(M)) MUST COINCIDE THE FIRST POINT,
C                       (X(1),Y(1)).
C
C                 M   - LENGTH OF THE ARRAYS X,Y.
C
C                 XO  - X-COORDINATE OF POINT FOR WHICH THE INTERIOR
C                       ANGLE IS DESIRED.
C
C                 YO  - Y-COORDINATE OF POINT FOR WHICH THE INTERIOR
C                       ANGLE IS DESIRED.
C
C           PURPOSE - "ANGLE" CALCULATES THE SUM OF THE INTERIOR
C                     ANGLES OF A POLYGON DEFINED BY THE VERTICES
C                     (X(L),Y(L), L=1,M) WITH RESPECT TO THE POINT
C                     (XO,YO).  THIS ANGLE IS DEFINED AS FOLLOWS:
C
C                      (1) "ANGLE" = TWOPI IF (XO,YO) IS OVER POLYGON,
C                      (2) "ANGLE" = 0 IF (XO,YO) IS NOT
C                          OVER POLYGON OR ITS EDGE,
C                      (3) "ANGLE" = PI IF (XO,YO) IS OVER EDGE OF
C                          POLYGON BUT NOT OVER A VERTEX,
C                      (4) "ANGLE" = THE INTERIOR ANGLE SUBTENDED
C                          BY THE ADJACENT SIDES IF OVER A VERTEX.
C
C
C       CODE BASED UPON THE WINDING NUMBER ALGORITHM OF
C
C            LELEND, KENNETH O. (1975) AN ALGORITHM FOR WINDING
C                NUMBERS FOR CLOSED POLYGONAL PATHS,
C                MATHEMATICS OF COMPUTATION, VOL. 29(130),554-558.
C                ========================
C                CODE PREPARED BY A. H. COGBILL.
C
      DATA PI/3.141592653589793D0/, TWOPI/6.283185307179586D0/
      DATA DZERO/0.0D0/, ZERO/0.0/, HALF/0.5/, ONE/1.0/
C     DATA PI/3.1415926535898/, TWOPI/6.2831853071796/
C
C        MACHINE DEPENDENT CONSTANTS ARE "PI" AND "TWOPI".
C
```

```
      S=0
      M1=M-1
      X2=X(1)-XO
      Y2=Y(1)-YO
      K=0
   10 K=K+1
         IF (K.GT.M1) GO TO 60
         UP=0
         T=0
         X1=X2
         Y1=Y2
         X2=X(K+1)-XO
         Y2=Y(K+1)-YO
         IF (X1.EQ.ZERO  .AND.   Y1.EQ.ZERO) GO TO 90
         IF (Y2.EQ.ZERO) GO TO 15
         IF (Y2.GT.ZERO) GO TO 20
C                  Y2 § 0
         IF (Y1.LT.ZERO) GO TO 30
C                     Y1 †= 0, Y2 § 0.
         UP=1
         GO TO 40
   15    IF (X2.EQ.ZERO) GO TO 10
   20    IF (Y1.GE.ZERO) GO TO 30
C                      Y2 † = 0, Y1 § 0.
         UP=-1
         GO TO 40
C                 END STEP 1; BEGIN STEP 2.
   30    IF (Y1.NE.ZERO) GO TO 10
         IF (Y2.NE.ZERO) GO TO 10
         IF (X2.EQ.ZERO) GO TO 10
         IF (SIGN(ONE,X1).NE.SIGN(ONE,X2)) GO TO 80
         GO TO 10
C                  END STEP 2; BEGIN STEP 3.
   40    DET=X2*Y1-X1*Y2
         IF (DET.EQ.ZERO) GO TO 80
         IF (FLOAT(UP)*DET.GT.ZERO) GO TO 50
         T=-UP
   50    S=S+T
      GO TO 10
   60 IF (S.EQ.0) GO TO 70
      ANGLE=TWOPI
      RETURN
   70 ANGLE=DZERO
      RETURN
   80 ANGLE=PI
      RETURN
C
C           AT A VERTEX:  "ANGLE" = THE ANGLE SUBTENDED
C           BY ( (X(K-1),Y(K-1)), (X(K),Y(K)), (X(K+1),Y(K+1)) ).
C           BRANCH TO THIS CODE OCCURS ONLY WHEN X1=Y1=0.
```

```
C
   90 IF (K.GT.1) GO TO 100
      X1=X(M1)-XO
      Y1=Y(M1)-YO
      GO TO 110
  100 X1=X(K-1)-XO
      Y1=Y(K-1)-YO
  110 R1SQ=X1*X1+Y1*Y1
      R2SQ=X2*X2+Y2*Y2
      R3SQ=(X2-X1)**2 + (Y2-Y1)**2
      CTHETA=HALF*(R1SQ+R2SQ-R3SQ)/SQRT(R1SQ*R2SQ)
      ANGLE=DBLE(ARCOS(CTHETA))
C     ANGLE=ACOS(CTHETA)
      RETURN
      END
```

The vita has been removed from the scanned document

TEMPERATURE AND HEAT FLOW MODELING OF THREE-DIMENSIONAL BODIES IN A TWO-LAYERED HALF SPACE

by

John A. Dunbar, Jr.

(ABSTRACT)

A theoretical analysis was made of steady-state temperature and heat flow anomalies in the earth's crust caused by contrasts in heat production and thermal conductivity. Exact expressions were derived for the temperature and heat flow anomalies caused by polygonal prism heat sources in a half space overlain by a layer of contrasting conductivity. Expressions were also developed for the approximate thermal effects of polygonal prisms of contrasting conductivity. A comparison was made between the exact and apprroximate heat flow over an infinite semi-circular cylinder of contrasting conductivity. The two heat flow fields agree to within 5% for conductivity radios (the ratio of the conductivity of the medium and the conductivity of the cylinder) which are between 0.25 and 1.5. Comparisons were also made between polygonal prism and finite differnce models, three-dimensional and one-

dimensional models, and half space and two-layered half space models.

To illustrate the interpretation of heat flow anomalies a heat flow model was prepared for the Rolesville batholith and Castalia pluton, in Nash and Franklin Counties, North Carolina. It was shown that the observed variation in surface heat flow over these two granitic intrusions can be explained by variations in the thickness of the granite from 1 km to 30 km.